

Dear Mr. Schumann,

We thank a lot for your valuable comments and suggestions. We followed them as explained below.

The reviewers comments are repeated in **bold letters**, our replies are given in *italic*, and text modified or added to the manuscript is given in **blue**.

This is a nice model study of contrail and contrail cirrus formation on a regional scale. The approach is straightforward in extending a two-moment cloud microphysics scheme by including a separate contrail ice class. The scale jump from young contrails at aircraft wake vortex scales to grid scales is approximated by assuming that the contrail ice spreads immediately over a grid scale (vertically and horizontally). Part of the effects of this strong simplification is corrected by using an ice-crystal loss parametrization derived from LES results.

Of course this simple approach is possible only because the model study is restricted to regional scales, with just one day of simulation (actually only 8 h of contrail formation). The model is indeed useful to study regional effects of contrail cirrus on shortwave surface radiation and possibly on weather prediction. If applied for climate studies at global scales and for long simulation periods (years), the present approach would suffer from the same problems as other global models. For example, a regional model would require contrail cirrus boundary conditions if run for longer time periods, which are nontrivial if contrail effects outside the region impact the meteorology at inflow.

Any climate simulation would also require coupling to oceans etc. Nevertheless, the approach is useful for regional studies and interesting.

Of course, finally, the study should be published, though several minor and some major text issues need to be considered, as listed below, before the paper is acceptable.

The authors present a new contrail cirrus parameterization within the COSMO-ART model and study the impact of contrail cirrus on the SW radiation. The work is different to existing studies since they implemented their parameterization in a weather forecasting model. This would actually enable the authors to compare their results to observations but they do not do that. Instead they discuss the development of a contrail field in simulations only. Nevertheless, I find the model itself and the impact on the SW radiation interesting. There are a couple of major issues that need clarification and/or sorting out. The paper needs to be expanded regarding a more detailed evaluation with observations and a better comparison with earlier work.

*Dear Mr. Schumann,*

*Thanks a lot for your interest in our work and your detailed review. The issues raised in this review as well as the many questions and explanations clearly help to improve this manuscript. We hope to have addressed them to a satisfactory extent.*

**1. Page 1, line 11: insert "and humid" after "hot".**

*Done*

**2. Page 1, line 13: Note that the threshold temperature is pressure dependent; hence, -45°C is perhaps even too rough. More relevant is the fact that below a temperature near -38°C to -40°C, contrail particles, which are formed in liquid phase initially, freeze homogeneously and quickly to form ice particles which then persist in air with relative humidity below liquid saturation (but above ice saturation).**

We change in page 1, line 13:

Following the Schmidt-Appleman-Criterion (Schmidt, 1941; Appleman, 1953; Schumann, 1996), contrails form only when the ambient temperature is below a threshold temperature of roughly -45°C. With a favorable state of the atmosphere, i.e. characterized by supersaturation with respect to ice, the originally line-shaped contrails undergo various physical processes at the micro scale...

to:

Contrails form in case, the Schmidt-Appleman-Criterion (Schmidt, 1941; Appleman, 1953; Schumann, 1996) is fulfilled, i.e. the ambient temperature is below a threshold of around  $-45^{\circ}\text{C}$ . With plume temperatures near  $-38^{\circ}\text{C}$  to  $-40^{\circ}\text{C}$ , contrail particles, which are formed in the liquid phase initially, freeze homogeneously and quickly to form ice crystals. Those ice crystals grow in air with relative humidity above ice saturation and contrails persist. With such a favorable state of the atmosphere, the originally line-shaped contrails undergo various physical processes at the micro scale ...

**3. Page 1, line 17: There are other long-life-time contrail observations, but I agree, the one described by Minnis et al. (1998) is an early example. Others were summarized in Schumann and Heymsfield (2017), who also review the definition of contrail cirrus and other related knowledge.**

*We add in page 1, line 17:*

Other examples of long-lifetime contrail observation are summarized by Schumann and Heymsfield (2017).

**4. Page 1, line 20: It is not clear whenever important properties are “sufficiently investigated”, and there are many more observation (see Iwabuchi et al., 2012; Vazquez-Navarro et al., 2015; Schumann et al., 2017) and model studies than those covered in the IPCC report (Boucher et al., 2013).**

*Even taking into account the newer observations you mention we still believe that our statement is reasonable.*

**5. Page 2, line 17-18: “whether this study is the first of its kind” is at least debatable. In particular since the authors do not discuss earlier attempts like those of Duda et al. (2004) at this place. But I agree that the simplicity of the present approach including a balanced microphysics model (similar to recent approaches in global models) is attractive and the authors can claim a fresh approach.**

*We weaken the statement and mention the study of Duda later in the manuscript as it also uses real flight data. However, we do not consider the contrail advection tool of Duda to be a “full” contrail model, in the sense that ice microphysics is included. Hence, our aforementioned claim is not invalidated by disregarding the Duda work.*

*We add in page 2, line 18:*

Another approach using commercial flight data to study contrails on a regional scale is described in Duda et al. (2004). Here, a combination of commercial flight data and coincident meteorological satellite remote sensing data was used to perform a case study of a widespread contrail cluster.

Reference:

Duda, D. P., Minnis, P., Nguyen, L., and Palikonda, R.: A case study of the development of contrail clusters over the Great Lakes, *J. Atmos. Sci.*, 61, 1132 – 1146, 2004.

**6. Page 3, line 1-3: The method developed by Schumann (2012) and Schumann et al. (2015) (added reference, see below), though certainly with limitations, is still likely the only one covering the scale transition from thousands of single contrails to multi-year global climate cases. This method is not represented fairly in this citation (and in this introduction) which correctly mentions a problem but misses to mention the advantages of that approach. In fact, the mixed Lagrangian-Eulerian approach could be listed as a basic alternative to the Eulerian grid scale models. This approach has also been used by Caiazzo et al. (2017).**

*We changed the text accordingly:*

There, a mixed Lagrangian-Eulerian approach is used instead of the usual Eulerian treatment. This approach allows covering the scale ranging from thousands of single contrails to multi-year global climate simulations (Schumann (2012); Schumann et al. (2015); Caiazzo et al. (2017)).

7. Page 3, lines 13-15: The paper seems to make a big deal out of using 8 h of traffic movements. There were earlier studies doing far more in that direction (e.g., Schumann, 2012; Voigt et al., 2017).

The authors did not consider a case for which in situ- and satellite observations and other model studies are available, such as the ML-CIRRUS observations of 10 April 2014 over Germany (Voigt et al., 2017), for which the waypoint-traffic data (partly also from flightradar24.com) are available for about 4 weeks and for nearly the whole of Europe. See, e. g., Fig. 4 in Voigt et al. (2017). The existence of such data for future studies should be mentioned.

Perhaps, the introduction should mention the use of satellite data. But it should mention that there were many studies of satellite data in the past (from polar orbiting and geostationary satellites) and also a large variety of in-situ observations is available. So far, I feel that the discussion in this paper is too much biased to LES results instead.

*We now cite several more studies of contrail observations.*

*We do not think that the presentation or plausibility issues are overly biased towards LES, but it is clear that LES results build an integral part of the contrail initialisation used in our model.*

*At the time the manuscript was prepared, ML-Cirrus results were not published yet and it is not clear whether we would have been granted access at that phase to all the data needed to make conclusive comparisons.*

*We add the following after page 3, line 15:*

*In the future, further case studies should be performed for which in-situ observations of natural ice clouds and especially contrails are available.*

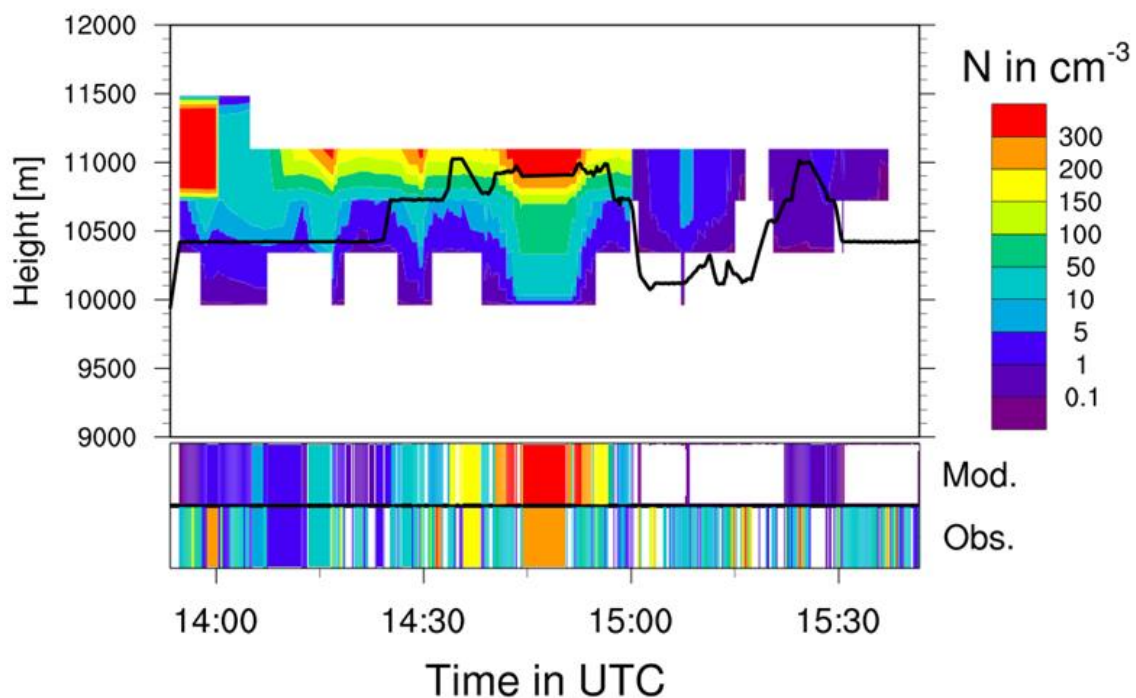


Fig. 1: 2014/04/10: Comparison of COSMO-ART ice crystal number concentration (contour) to SID3 measurements (ML-CIRRUS).

*We also performed a case study for 10 April, 2014 to compare with ML-CIRRUS data (Fig.1). In the future, we want to extend this work and present it in a separate study.*

8. Page 4, lines 20 to next page: The text explaining the parameters used in Eq. (2) appears a bit lengthy. I assume it can be reordered and shortened.

*We agree that the mentioned section is more technical than others. We condensed this part and moved the technical issues to the appendix.*

**9. Page 5, line 23: reorder “several input” -> “input several”**

Done

**10. Page 5, line 28: Is there any physical argument for using this maximum mixing ratio limit value? If not, say that this is arbitrarily taken. How sensitive are the results to this threshold?**

*In fact, this threshold is used for grid-scale ice clouds in the radiation scheme. For reasons of consistency (and as we find no other suitable study to justify another number) we leave it as it is. Indeed, the results do not seem to depend strongly on this threshold, unless it is changed to very large values ( $> 1.0e-6$ ). Then, the contrail ice becomes mostly “invisible” to the radiation scheme. Thus, only modification in the natural ice class is present.*

*We follow your suggestion and add after page 5, line 28:*

The same threshold value is used in Seifert and Beheng (2006) for grid-scale natural ice clouds.

**11. Page 5, lines 30 ff. The team around Ping Yang has developed an ice particle parameterization including smaller ice particles in recent years (see Bi and Yang, 2017, e.g.). The existence of such parameterizations should be mentioned and such new parameterizations could be used at least in future studies.**

*We are aware of this work and other (e. g. Fu et al. (2007)). Implementing a new description of cloud optical properties is a rather large effort, as much of the tuning of the COSMO model depends on the results of this part of the code. Currently, we are working on the cloud optical properties but this work will not be finished and ready to use in the near future.*

*We add the following after page 7, line 5:*

Other parameterizations exist that can compute reliable values for optical properties of small ice crystals with sizes down to  $0.2 \mu\text{m}$  (Bi and Yang, 2017). For future studies, using such an approach clearly could overcome the necessity of the threshold described above.

**12. Page 9, line 2: The introduction to this section, with “In contrast to previously mentioned global modeling studies, ...” and with “globally averaged fuel consumption ...” is no longer true if you mention CoCiP properly.**

We change:

“In contrast to previously mentioned global modeling studies...”

to

In contrast to most of the previously mentioned global modeling studies

**13. Page 7, line 4: replace “a potential function” by “a power law” or similar.**

We change:

“a potential function”

to

power law

**14. Page 7, line 13: “Microphysical properties” – this is a very vague term. What do you mean? If you mean optical extinction, I am not sure that your statement is correct (I expect that extinction and optical depth are equally sensitive to number and mass).**

*At a given time, certainly both, mass and number control optical properties. What we wanted to say is that optical properties of AGED contrails depend on the initial ice crystal number and not much on the initial ice mass. We expand the description to avoid misunderstandings.*

*We change:*

“Microphysical properties of contrails depend a lot more on the number of ice crystals than on the ice mass after the vortex phase (Unterstrasser and Gierens, 2010b).”

to:

Microphysical properties of aged contrails depend a lot more on the number of ice crystals than on the ice mass after the vortex phase (Unterstrasser and Gierens, 2010b). The initial ice mass is of minor importance, as the later growth of contrail ice crystals and the related ice mass evolution in a persistent contrail is mainly controlled by the ambient water vapor supply. On the other hand, the ice crystal number changes only slowly in a long-living contrail. Hence, its initial value determines the typical ice crystal sizes in the evolving contrail-cirrus (for a given environmentally controlled ice mass), which affects the radiative properties and the sedimentation-related life cycle.

**15. Page 8, line 19: 600 m is a large upper bound which is reached very rarely. To be fair, the lower bound should be correspondingly small (100 m; even smaller values occur for small business jets). We change the limits to 100 m and 500 m.**

**16. Page 9, line 2 (“In contrast to...”): Note that some previous global model studies used similar data for the whole year of 2006 (“ACCRI” waypoint data). Hence, this is not really a big step forward.**

**The word “exact” does not fit well to this description. When are data exact? Also “real time-based” data is not really the right term. I would simply say you use traffic waypoint data from transponder data (not radar).**

*We change:*

*Rather than statistical calculations for globally averaged fuel consumption, the basic data consist of exact flight trajectories over a limited area that are recorded from real time-based data (flightradar24.com, 2015).*

*To:*

*Rather than statistical calculations for globally averaged fuel consumption, or radar data, the basic data consist of traffic waypoint information over a limited area recorded from transponders on the plane (flightradar24.com, 2015).*

**17. Page 11, line 3: Here and at several later places you could also cite observation results. Here, e.g., Petzold et al. (1997) and Heymsfield et al. (1999) found strongest growth at the edges of contrails from in-situ measurements.**

**The discussion of observability of contrail cirrus is not needed in this paper. Otherwise, the statements are controversial and would require more in-depth discussion for completeness. For example, observations discriminate contrails and cirrus also based on the concentration of exhaust trace gases and aerosols and use trajectory analysis, partly in correlation with air traffic and meteorological situation history (Voigt et al., 2017). I suggest reducing this discussion in this paper. It is not needed for this paper.**

*We now mention the studies by Petzold and Heymsfield, additionally we included Poellot et al 1999 and Voigt et al 2017 at a later occasion.*

*We change page 11, line 10:*

*“Consistently, large-eddy simulation studies indicate the strongest growth at the edges of a contrail (Unterstrasser and Gierens, 2010a; Lewellen et al., 2014).”*

*to:*

*Consistently, large-eddy simulation studies (Unterstrasser and Gierens, 2010a; Lewellen et al., 2014) and in-situ measurements (Petzold et al., 1997; Heymsfield et al., 1998) indicate the strongest growth at the edges of a contrail.*

*We change page 13, line 1:*

*“The effective radii in the aviation simulation are typically one order of magnitude smaller than in natural cirrus clouds and do not exceed 10  $\mu\text{m}$ . These results are in reasonable agreement with large-eddy studies (Unterstrasser and Gierens, 2010a; Lewellen et al., 2014).”*

*to:*

The effective radii in the aviation simulation are typically one order of magnitude smaller than in natural cirrus clouds and do not exceed 10  $\mu\text{m}$ . These results are in agreement with large-eddy studies (Unterstrasser and Gierens, 2010a; Lewellen et al., 2014) and in situ observations (Poellot et al., 1999).

*For comparison with Voigt et al. (2017), see answer to Comment 20.*

*We think that the paragraph on observability gives useful indications on how to interpret the COSMO results and hence we leave this section as is. The given reference (Unterstrasser et al, 2017) discusses this issue in more detail and the interested reader can read it.*

*A few thoughts on observability and your mentioned examples:*

*Lewellen et al (2014) contrast the spatial distribution of a passive chemical tracer and contrail-cirrus. Clearly, contrail area and plume area evolve differently over time, as ice crystals sediment as opposed to a passive tracer. Hence, exhaust trace gas measurements cannot be used to identify the complete contrail-cirrus. This method only allows tracking the contrail regions around the formation altitude where small ice crystals reside which have not yet fallen out of the aircraft plume.*

#### References:

Heymssfield, A. J., Lawson, R. P., and Sachse, G. W.: Growth of ice crystals in a precipitating contrail, *Geophys. Res. Lett.*, 25, 114 013, 1998.  
doi:10.1029/98GL00189

Lewellen, D., Meza, O., and Huebsch, W.; Persistent Contrails and Contrail Cirrus. Part I: Large-Eddy Simulations from Inception to Demise, *J. Atmos. Sci.*, 71, 4399 – 4419, 2014.  
doi: 10.1175/JAS-D-13-0316.1

Petzold, A., Busen, R., Schröder, F. P., Baumann, R., Kuhn, M., Ström, J., Hagen, D. E., Whitefield, P. D., Baumgardner, D., Arnold, F., Borrmann, S., and Schumann, U.: Near-field measurements on contrail properties from fuels with different sulfur content, *J. Geophys. Res.*, 102, 114 013 1997.  
doi:10.1029/97JD02209

Poellot, M. R., Arnott, W. P., and Hallett, J.: In situ observations of contrail microphysics and implications for their radiative impact, *J. Geophys. Res.*, 104, 12 077–12 084, 1999.  
doi:10.1029/1999JD900109, <http://dx.doi.org/10.1029/1999JD900109>

**18. Page 14, line 1 etc.:** I agree that Fig. 5 exhibits a remarkably thick layer with apparently strong supersaturation (what is the maximum RH<sub>i</sub> value in this figure?). I wonder how this layer developed. Is this the results of initial conditions or the result so vertical lifting or radiative cooling? How realistic is the model result in this respect? As far as I understand, the high humidity coincides with some thin cirrus. How can the humidity persist so long in the presence of cirrus? If there is no cirrus yet then I would have expected some homogeneous ice nucleation at such high humidity values. Therefore: How realistic are the high RH<sub>i</sub> values? Please explain.

*We changed the color coding as well as the scale in Fig. 5 . The upper bound is now 1.4 instead of 1.8. The maximum value for RH<sub>i</sub> is 1.34.*

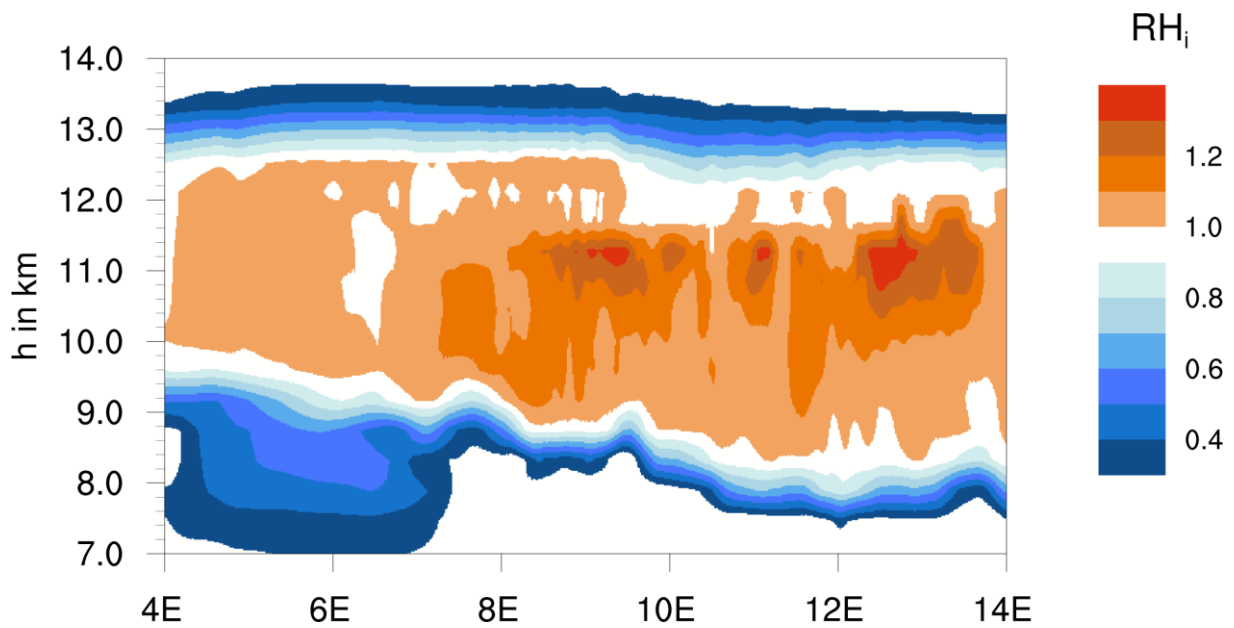


Fig 2. Updated version of Figure 5 in the manuscript.

Furthermore, we extend the discussion about  $RH_i$ , adding the following figure:

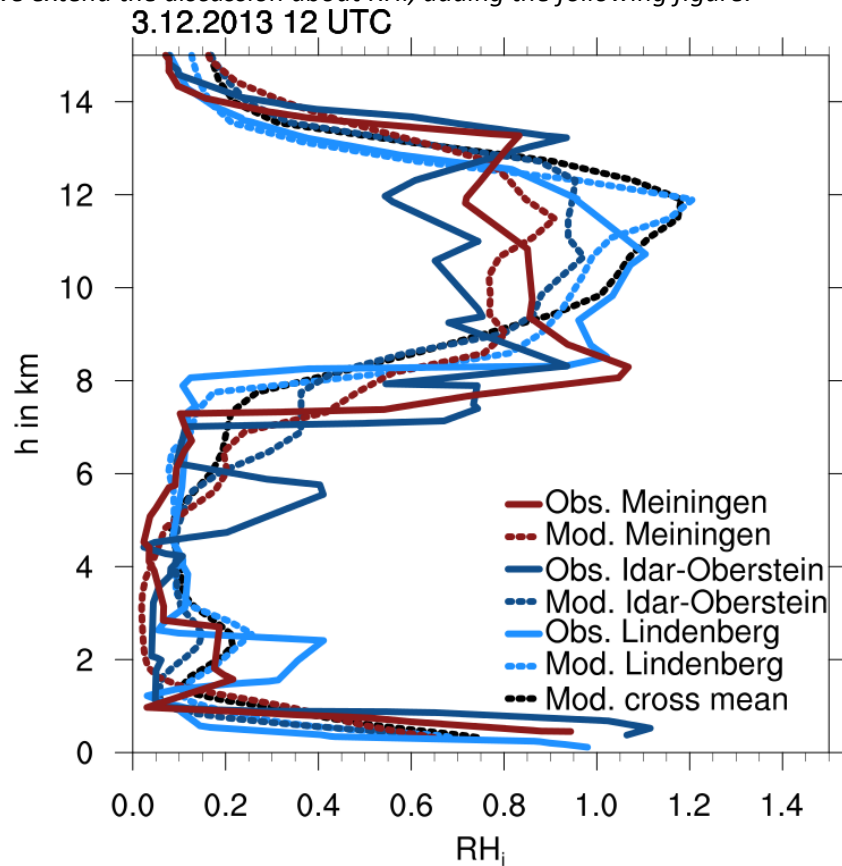


Figure 6. Radio soundings for several locations (solid lines) (UWYO, 2018) and corresponding profiles from aviation simulation (dotted lines) of relative humidity  $RH_i$ . The black dotted line are mean values along the black line in Fig. 4.

The fidelity of such high values of  $RH_i$  is corroborated by a comparison with observations. Here, vertical profiles obtained from radio soundings (UWYO, 2018) and simulated data evaluated at radiosonde stations are depicted in Fig. 6. In general, high values of  $RH_i$  are observed by radio soundings, even supersaturation occurs over Lindenberg and Meiningen. The model clearly

overestimates RHi for Idar-Oberstein, however Meiningen and Lindenberg agree quite well. Additionally, the black curve shows the mean vertical profile of the cross section displayed in Fig. 5. From this it becomes apparent that the relative humidity in the displayed cross section is remarkably high compared to the radiosonde locations. The large layer of supersaturation is caused by lifting and radiative cooling. It can persist, as natural cirrus clouds are located mostly below this layer (Fig. 7b). Also, the cirrus clouds present in the layer are too thin, i. e. occurring number concentrations are too low (Fig. 7e) to effectively reduce supersaturation.

Reference:

UWYO: <http://weather.uwyo.edu/upperair/sounding.html>, 01.02.2018.

Acknowledgements:

We acknowledge the use of the radio sounding data provided by the University of Wyoming, Department of Atmospheric Science.

**19. Page 14, line 11-12: Why did contrails form only between 11 km and 13 km altitude? Is this because there was no traffic below and above, or because of drier and warmer air above and below?**

*We add in page 17, line 6:*

This is caused by the absence of air traffic below this layer.

**20. Page 15, line 2-4: Again you compare to LES only. You could as well compare to observations. Such data are readily available from Schumann et al. (2017). If you would have plotted the ice particle concentration per volume along a line through the contrail cirrus clouds, you could have compared to the findings in, e.g., Voigt et al. (2017), Fig. 6.**

*We follow your suggestion and add the following figure and description:*

In Fig. 8, the relative occurrence of ice crystal number concentrations and temperature for the cross section shown in Fig. 7 is depicted. The relative occurrence is normalized with the sum over all values. Both, reference simulation (Fig. 8a) and aviation simulation (Fig. 8b) are similar for higher temperatures (i. e. lower heights) up to 220 K. For lower temperatures, high number concentrations up to  $7 \text{ cm}^{-3}$  occur in the aviation simulation, whereas number concentrations clearly decrease strongly with temperature in the reference simulation. Here, a rough comparison to measurement data can be made. In Voigt et al. (2017), mid-latitude cirrus clouds and contrails were probed in-situ during an aircraft measurement campaign. Comparing their Fig. 6(b) to Fig. 8, a similar increase in  $n$  below temperatures of about 220 K is found. Therefore, most likely, the high values occurring in the aviation simulation and not in the reference simulation, are due to aviation induced clouds.

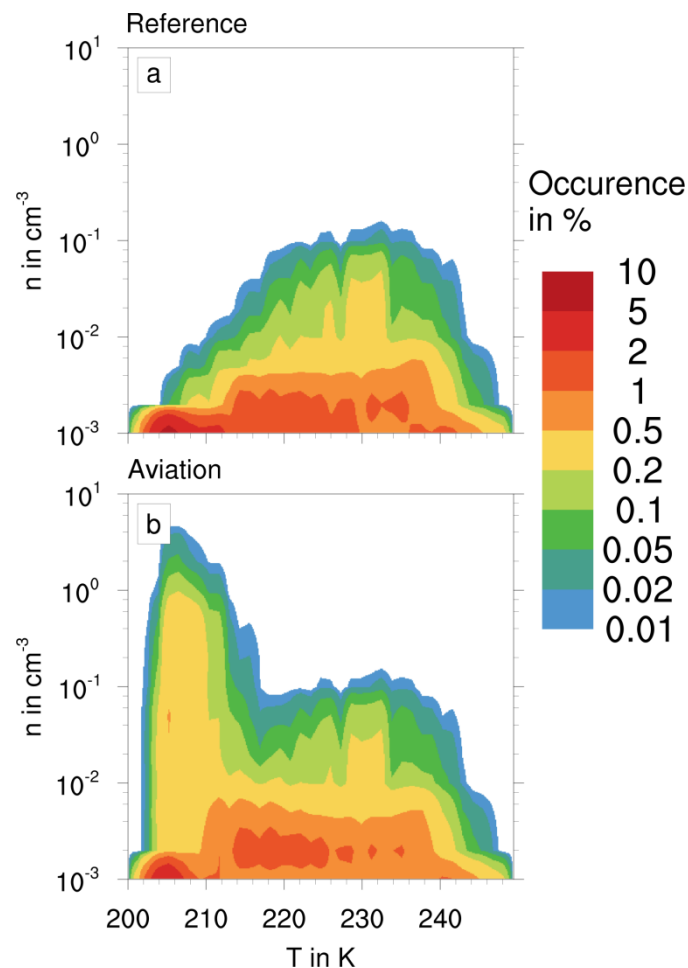


Figure 8. Relative occurrence of ice crystal number concentration versus temperature for natural cirrus, contrail and contrail cirrus at 12 UTC for the cross section along the black line in Fig. 4; a) reference simulation; b) aviation simulation.

#### Reference:

Voigt, C., Schumann, U., Minikin, A., Abdelmonem, A., Afchine, A., Borrmann, S., Boettcher, M., Buchholz, B., Bugliaro, L., Costa, A., Curtius, J., Dollner, M., Dörnbrack, A., Dreiling, V., Ebert, V., Ehrlich, A., Fix, A., Forster, L., Frank, F., Fütterer, D., Giez, A., Graf, K., Groß, J., Groß, S., Heimerl, K., Heinold, B., Hüneke, T., Järvinen, E., Jurkat, T., Kaufmann, S., Kenntner, M., Klingebiel, M., Klimach, T., Kohl, R., Krämer, M., Krisna, T., Luebke, A., Mayer, B., Mertes, S., Molleker, S., Petzold, A., Pfeilsticker, K., Port, M., Rapp, M., Reutter, P., Rolf, C., Rose, D., Sauer, D., Schäfler, A., Schlage, R., Schnaiter, M., Schneider, J., Spelten, N., Spichtinger, P., Stock, P., Walser, A., Weigel, R., Weinzierl, B., Wendisch, M., Werner, F., Wernli, H., Wirth, M., Zahn, A., Ziereis, H., and Zöger, M.: ML-CIRRUS: The Airborne Experiment on Natural Cirrus and Contrail Cirrus with the High-Altitude Long-Range Research Aircraft HALO, *Bull. Amer. Meteor. Soc.*, 98, 271 – 288, 2017. doi:10.1175/BAMS-D-15-00213.1

**21. Page 15, line 16: The last sentence of section 4.2 appears trivial. If there is no traffic, there is no chance to affect cirrus that moves in from upstream. That would be different if you could show that a cirrus parcel which you follow in a Lagrangian manner and that did contain contrails for some time recovered and approached the properties of natural cirrus in a short time after the period with traffic. I think, you cannot show this from this study. So, this sentence should probably be eliminated.**

*We delete the corresponding sentence.*

22. Section 4.3 is on low technical level. It is not even clear from which satellite and sensor the data are taken. What is spatial and temporal resolution of the data? Which spectral channels are used? How sensitive are the observation results to the processing methods used? This needs improvements.

We rewrite section 4.3 and use other satellite images with much better resolution and more precise information about the algorithm.

We replace Fig 8 (now Fig. 10) with the following:

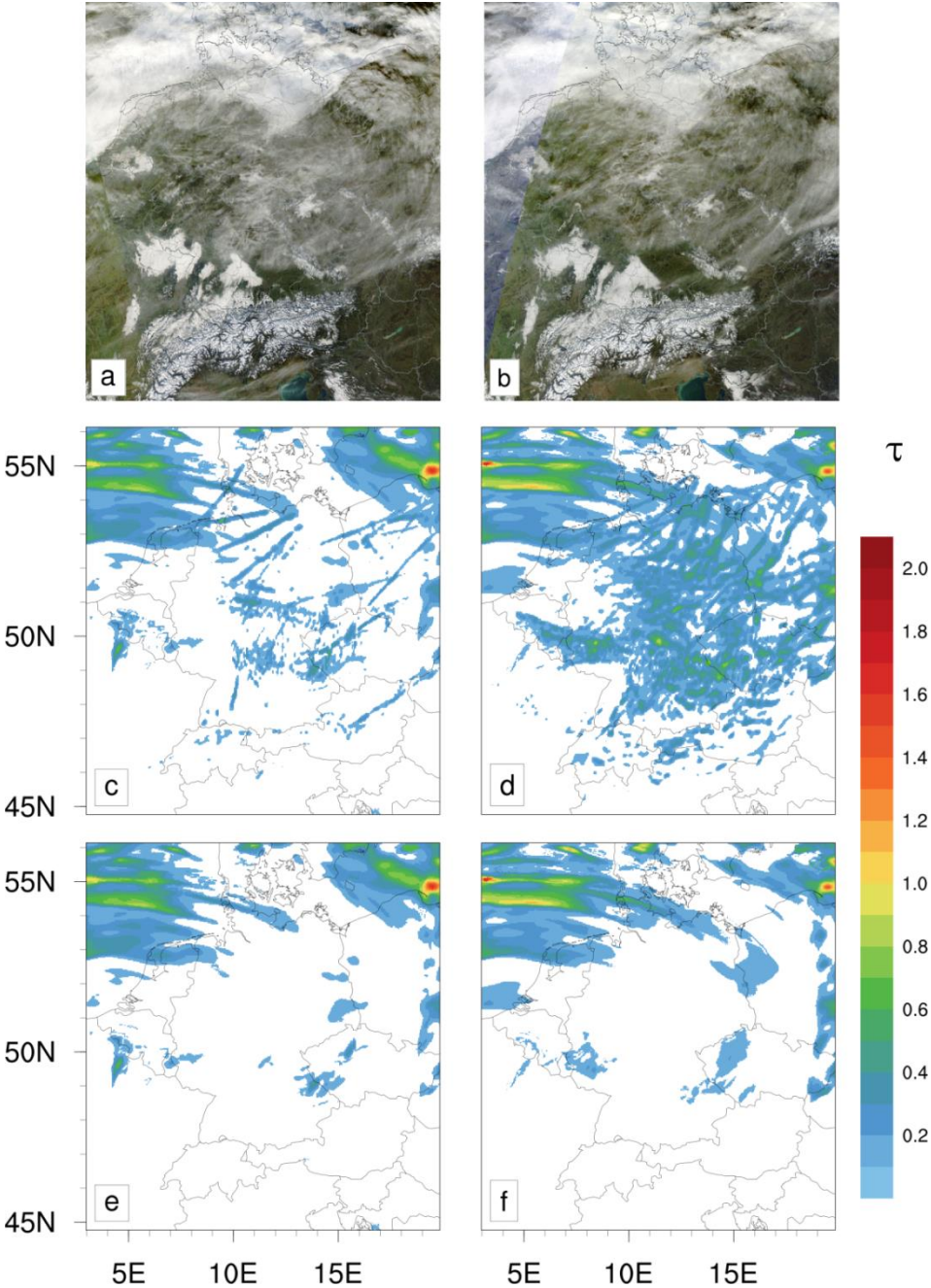


Figure 10. Top row: satellite image (MODIS True Color - Corrected Reflectance) (NASA/GSFC/ESDIS, 2018); center row: optical depth at 1.115  $\mu\text{m}$  of all ice clouds for the aviation simulation; bottom row: optical depth of all ice clouds for the reference simulation; left column: 10 UTC; right column: 12 UTC.

In the following, satellite images (created with Global Imagery Browse Services (GIBS) NASA/GSFC/ESDIS, 2018) are shown in Fig. 10 for a qualitative assessment of the simulations. The panels a and b show the "MODIS Terra Corrected Reflectance True Color" at 10 UTC and 12 UTC for the simulated day, respectively, both with a resolution of 250 m. The "True Color" composition consists of MODIS bands 1, 4 and 3 (NASA/GSFC/ESDIS, 2018). Beside a cloud bank over the North and Baltic Seas and fog over Southern and Western Germany, a considerable number of line-shaped contrails and diffuse cirrus clouds are present across both satellite images. Main contrail clusters are found over Central Germany for both situations. Contrails can also be identified over the Netherlands and Belgium, over the Czech Republic, and south of the Alps. At 12 UTC, the rather widespread high-level cloud cover seems to have decreased compared to 10 UTC.

Comparing Fig. 10a and Fig. 10e, obviously, the reference simulation underestimates the coverage of high clouds in the center of the domain, which, in large parts, consists of contrails and contrail cirrus Fig. 10c. Clearly, the amount of cloud cover seems to be underestimated also in the aviation simulation at 10 UTC. This discrepancy is probably due to the fact that air traffic was switched on at 08 UTC and earlier flight movements are disregarded in our simulation. Hence, the simulation evaluation at 10 UTC neglects all contrails older than 2 hours. The comparison at 12 UTC is more favorable and observations match much better with the aviation simulation than with the reference simulation.

...

#### Acknowledgements:

We acknowledge the use of imagery from the Land Atmosphere Near real-time Capability for EOS (LANCE) system and services from the Global Imagery Browse Services (GIBS), both operated by the NASA/GSFC/Earth Science Data and Information System (ESDIS, [\url{http://earthdata.nasa.gov}](http://earthdata.nasa.gov)) with funding provided by NASA/HQ.

**23. Page 19, Fig. 11: It took me some time to find the red circle. Please add the coordinates (12°E, 53°N) in the figure caption.**

*Done*

**24. Page 22, line 11: What is a "nominal capacity"?**

*The nominal capacity (or nominal power) is the power that an electrical device can produce (or handle) when operating in a reasonable manner as proposed by the manufacturer.*

*We change the paragraph from:*

*A nominal capacity is assumed, consisting of a specific PV module and PV inverter combination. The tilt and orientation of the PV module as well as the technical specifications are taken from Rieger et al. (2017).*

*to:*

*For a specific combination of a PV module and a PV inverter combination, a nominal power and a reasonable tilt is assumed. These technical specifications are taken from Rieger et al. (2017).*

**25. Page 22: Section 4.5: This section depends on the accuracy of the model used (with about 2 km horizontal and 300 m (or 400 m at the tropopause?) vertical resolution) since the early contrail ice crystal loss certainly depends on the time scale of plume mixing. This should be mentioned.**

*The early contrail ice crystal loss is part of the initialization in COMSO-ART which is based on LES results. By setting  $\lambda_{Ns} = 1$  we simply disregard any losses that appear in a young contrail. This sensitivity test is not affected by COSMO grid resolution and plume mixing within COSMO.*

**26. Page 23 line 10-12. The numbers given depend on temperature. See Fig. 5 in Schumann et al. (2017) and Fig. 6 in Voigt et al. (2017), and many other related studies. In fact, this should have been discussed earlier in the text. In the conclusion, it should be said that the numbers for IWC and other contrail-cirrus properties are valid for the specific meteorological situation considered.**

*We add in page 23, line 10:*

For a single case study, it was shown, ...

**Additional references:**

**Bi, L., and P. Yang: Improved ice particle optical property simulations in the ultraviolet to far-infrared regime, J. Quant. Spectrosc. Radiat. Transf., 189, 228-237, doi:10.1016/j.jqsrt.2016.12.007, 2017.**

**Caiazza, F., Agarwal, A., Speth, R. L., and Barrett, S. R. H.: Impact of biofuels on contrail warming, Environ. Res. Lett., 12, , doi:10.1088/1748-9326/aa893b, 2017.**

**Duda, D. P., Minnis, P., Nyuyen, L., and Palikonda, R.: A case study of the development of contrail clusters over the Great Lakes, J. Atmos. Sci., 61, 1132-1146, 2004.**

**Heymsfield, A. J., Lawson, R. P., and Sachse, G. W.: Growth of ice crystals in a precipitating contrail, Geophys. Res. Lett., 25, 1335-1338, doi: 10.1029/98GL00189, 1998.**

**Iwabuchi, H., Yang, P., Liou, K. N., and Minnis, P.: Physical and optical properties of persistent contrails: Climatology and interpretation, J. Geophys. Res., 117, D06215, doi:10.1029/2011JD017020, 2012.**

**Petzold, A., Busen, R., Schröder, F. P., Baumann, R., Kuhn, M., Ström, J., Hagen, D. E., Whitefield, P. D., Baumgardner, D., Arnold, F., Borrmann, S., and Schumann, U.: Near-field measurements on contrail properties from fuels with different sulfur content, J. Geophys. Res., 102, 29867-29880, doi: 10.1029/97JD02209, 1997.**

**Schumann, U., Penner, J. E., Chen, Y., Zhou, C., and Graf, K.: Dehydration effects from contrails in a coupled contrail-climate model, Atmos. Chem. Phys., 15, 11179-11199, doi:10.5194/acp-15-11179-2015, 2015.**

**Schumann, U., Baumann, R., Baumgardner, D., Bedka, S. T., Duda, D. P., Freudenthaler, V., Gayet, J.-F., Heymsfield, A. J., Minnis, P., Quante, M., Raschke, E., Schlager, H., Vázquez-Navarro, M., Voigt, C., and Wang, Z.: Properties of individual contrails: A compilation of observations and some comparisons, Atmos. Chem. Phys., 17, 403-438, doi:10.5194/acp-17-403-2017, 2017.**

**Schumann, U., and Heymsfield, A.: On the lifecycle of individual contrails and contrail cirrus, Meteor. Monogr., 58, 3.1-3.24, doi: 10.1175/AMSMONOGRAPHS-D-16-0005.1, 2017.**

**Vázquez-Navarro, M., Mannstein, H., and Kox, S.: Contrail life cycle and properties from 1 year of MSG/SEVIRI rapid-scan images, Atmos. Chem. Phys., 15, 8739-8749, doi:10.5194/acp-15-8739-2015, 2015.**

Dear Referee 2,

We thank a lot for your valuable comments and suggestions. We followed them as explained below.

The reviewers comments are repeated in **bold letters**, our replies are given in *italic*, and text modified or added to the manuscript is given in blue.

**The authors use a regional scale model and contrail parameterization to simulate contrails and cirrus clouds occurring over central Europe during a single day – December 3rd, 2013. The simulated cloud cover and ice crystal mass mixing ratios are used in an online radiation scheme to understand the impact of aviation on direct and diffuse shortwave radiation reaching the surface, which in turn, affect the production of photovoltaic power. Overall, it is reported that aviation-induced cloudiness reduces PV power production by up to 10%. Assumptions related to the emissions index of ice crystals and crystal loss during the contrail vortex phase significantly alter this estimate. This is an interesting case study, which should be worth publishing in ACP; however, the limited time and spatial coverage of the reported model simulations limit the usefulness of authors' conclusions for broader understanding the relevance of aviation contrail cirrus to solar energy production. It certainly would be nice to see more data points for other spatial locations or time periods (e.g., summer). The following comments must be adequately addressed before I can recommend that this paper be acceptable for publication.**

*Thanks a lot for your review and your interest in our work. We see (and share) your opinion of the problem concerning the limited time and spatial coverage. However, this study should be seen only as a first step: developing the model, doing some comparison with observations and LES. Future studies with longer simulation time and other (larger) domains can follow this work.*

*A certain problem, at least with the presented setup is the following: The regional model needs lateral boundary data. From global models, we can get those information for the meteorology (partly also for gas phase and aerosols). However, neither data on contrails or contrail cirrus nor on aviation-modified cirrus clouds is available currently. Those would be needed to drive a model producing realistic results for longer time. Currently, several efforts to implement contrails into the ICON model are undertaken. Using this will overcome this issue.*

*Indeed, one day of simulation is not enough for providing a significant and statistically robust signal. We improved the figure that shows the time series of radiation related quantities by adding standard deviations as error bars. Furthermore, we additionally compare values for the mean for the entire simulation domain to the ones obtained for the selected area.*

*Further studies will follow, applying the model to other days, time of year, regions etc. to further investigate and enhance the significance (and relevance) of the influence of aviation on PV production.*

**1. Pg. 2, Line 16-17: This sentence is confusing. What is being claimed here – that this is the first time a regional scale model has been applied to study contrails and contrail cirrus? I don't think a statement like this is really necessary, but in any case, please be specific with what is being claimed as novel.**

*We delete the sentence in page 2, line 16-17:*

*"In this respect, the presented study is complementary to the aforementioned approaches and is, to our knowledge, the first study of its kind."*

*Instead, we add at the end of the corresponding paragraph:*

*Especially with respect to the spatial scale used in the regional scale COSMO-ART model, the presented study is complementary to the aforementioned approaches and is, to our knowledge, the first study of its kind.*

**2. Pg. 3, Line 12: What is the state of the art with respect to PV forecasts? There does appear to be some literature on this topic using both NWP and statistical models (e.g., Wan et al., 2015). Please expand this section to discuss current methods and considerations.**

*We change in page 3, line 9:*

*The presented model configuration serves to study microphysical evolution of contrails and contrail cirrus, their influence on natural high-level cloudiness, and their impact on the radiative fluxes on a regional scale and short time periods. This gains importance, e.g., in predicting the energy yield from photovoltaic (PV) systems, because additional cloud cover due to contrails is not represented in operational weather forecasting.*

*to:*

The presented model configuration serves to study microphysical evolution of contrails and contrail cirrus, their influence on natural high-level cloudiness, and their impact on the radiative fluxes on a regional scale and short time periods. This gains importance, e.g., in predicting the energy yield from photovoltaic (PV) systems.

During the past decades, the development of alternative, clean energy production was enhanced to counteract global warming and reduce air pollution. Within the scope of methods, one of the most promising sources is solar energy, gained by PV cells.

To assure a sustainable supply, the demand of precise prediction of the energy yield from PV systems is desired (Lew and Richard, 2010). Several approaches exist to forecast PV power, such as statistical models, neural networks, remote sensing models and numerical weather prediction models (Inman et al., 2013). Especially PV forecast using numerical weather prediction models is challenged by special weather situations or phenomena that are poorly represented in the models (Köhler et al., 2017). E. g. Rieger et al. (2017) found a large impact of mineral dust due to Saharan dust outbreaks on the solar radiation over Germany. This becomes important, as mineral dust is currently not considered adequately in operational weather forecast.

Another phenomenon that is not represented at all in numerical weather prediction, is the influence of aviation.

References:

Lew, D. and Richard, P.: Western wind and solar integration study, Tech. rep., National Renewable Energy Laboratories, 2010.

Inman, R. H., Pedro, H. T., and Coimbra, C. F.: Solar forecasting methods for renewable energy integration, Prog. Energy Combust. Sci., 39, 535 – 576, 2013  
doi: 10.1016/j.pecs.2013.06.002.

Köhler, C., Steiner, A., Saint-Drenan, Y.-M., Ernst, D., Bergmann-Dick, A., Zirkelbach, M., Ben Bouallègue, Z., Metzinger, I., and Ritter, B.: Critical weather situations for renewable energies – Part B: Low stratus risk for solar power, Renew. Energ., 101, 794–803, 2017  
doi: 10.1016/j.renene.2016.09.002.

**3. Pg. 3, Line 14-15 and Pg. 9, Lines 2-5: How are the flight radar data obtained and input into the model? How do these flight tracks compare/interface with the ADS-B data presented in Figure 2? Are these data publicly available, and if so, how can the reader obtain the data?**

*We change page 3, line 14-15:*

*“Another feature of this study is the new and recently developed data set of real time flight tracks. Rather than statistical calculations for globally averaged fuel consumption, the basic data consist of real time-based flight trajectories (flightradar24.com, 2015)”*

*to:*

Another feature of this study is the new and recently compiled data set of flight trajectories. Rather than statistical calculations for globally averaged fuel consumption, the basic data consist of real commercial aircraft waypoint data (flightradar24.com, 2015).

In Sec. 3.2 (Determination of Flight Tracks) we explain in more detail.

We change page 9, lines 2 - 5:

*“In addition to time, height and geographical position of the aircraft, information on aircraft type and current velocity is also available. In this study, besides position and time, we only use the wing span bspan as a proxy for the aircraft emission parameters (see section 3.1). “*

to:

Rather than statistical calculations for globally averaged fuel consumption, or radar data, the basic data consist of traffic waypoint information over a limited area recorded from ADS-B<sup>4</sup> transponders on the plane (flightradar24.com, 2015). The ADS-B data is obtained mainly from flightradar24.com (2015). The DLR holds a historic data file that can be purchased from flightradar24.com (2015). This data is cleaned and combined with the input of the Official Airline Guide Database that is also hold by DLR.

From this information, a dataset is compiled, containing spatially and temporally resolved information on geographical position, height, current velocity and type of aircrafts. For reasons of efficiency, the information on geographical position is interpolated to fit onto the grid of the model. As a proxy for the aircraft emission parameters (see section 3.1), the wing span bspan is used.

<sup>4</sup>Automatic Dependent Surveillance - Broadcast

**4. Pg. 3, Line 20: In the following what? This sentence is confusing.**

We change in page 3, line 20:

*“In the following, ...”*

to:

In this section, ...

**5. Pg. 4, Line 21: How often and under what conditions are these limits actually reached in the simulations?**

*In general, critical processes are sedimentation and melting / sublimation of hydrometeors. To assure numerical stability, the limits are introduced within a clipping routine at the end of the microphysics. As mass and number concentrations are treated separately, it may occur, that at the end of a time step, e. g. due to sedimentation, a rather large value for the number concentration remains with a small amount of mass present or vice versa. This would result in unphysically small or large crystals. The same may occur during melting / sublimation. Here, in the first place, only the mass concentration is changed resulting in very small mean masses for the ice crystals.*

*Apart from this, the microphysical scheme is designed in a way to avoid reaching these limits. E. g. ice gets converted to snow via accretion or graupel starts melting when getting too large by simply sedimenting in lower and warmer layers.*

*About the “how often”:*

Tab.1 Occurrence of limits violated for both classes and simulations, each for simulation hour 12

	aviation		reference
	cirrus class	contrail class	cirrus class
$m < m_{MIN}$	0.002 %	0.005 %	0.001 %
$m > m_{MAX}$	0.03 %	-	0.03 %

*In Tab.1, the relative occurrence of violated limits is shown for cloudy grid boxes both simulations and the classes considered for the 12th hour simulated. Note that only cloudy grid boxes (i. e. mass concentration > 0) are considered. Apparently, the limits for both classes are reached only rarely, also when including contrail ice.*

*For the case study shown, also the plots for effective radii (in Fig. 3, 4, 6, 7) may give a hint:*

*Limiting the number concentration of ice crystals to assure a fixed mean mass ( $m$ ) would result in a constant value for the effective radius ( $r_e = r_e(m)$ ). As the respective plots show in large parts at least some variability over most areas for values of  $r_e$ , the limits most likely are not reached.*

**6. Pg. 5, Line 26-28: How are contrail and contrail cirrus ice distinguished from cirrus ice given the statement on Pg. 5, Line 5 that the cirrus and contrail cirrus ice classes are lumped together?**

*As mentioned in page 5, line 5, we cannot distinguish directly between contrail cirrus and natural cirrus directly, as soon as the contrail cirrus gets transferred to the “natural” cirrus class.*

*The statement in page 5, line 26 – 28 actually refers only to the fact, that the contrail ice class is represented in the radiation algorithm with its own cloud cover and optical properties.*

*The contribution to the natural cirrus class can only be seen comparing to the reference simulation.*

*We change:*

*“To include contrails and contrail cirrus into the radiative algorithm, we include a contrail ice cloud cover determined from the contrail and contrail cirrus ice mass mixing ratio.”*

*to:*

To include contrails and contrail cirrus in the radiative algorithm, we include a contrail ice cloud cover determined from the contrail ice class mass mixing ratio.

...

As mentioned before, the aviation contribution to the natural cirrus ice class can only be determined by comparison with the reference simulation.

**7. Pg. 7, Line 26: Is there a citation for the assumed EI\_iceno?**

*We add in page 7, line 26:*

... following Unterstrasser, 2014.

**8. Pg. 8, Line 18: What is the vertical resolution of the model?**

*We change in page 8, line 18:*

*“In the vertical direction, it is reasonable to assume that ice crystals are distributed over the whole grid layer.”*

*to:*

In the vertical direction, it is assumed that ice crystals are distributed over the whole grid layer. Close to the ground, the vertical grid size is about 10 m and increases to 300 m at the tropopause.

**9. Pg. 10, Line 30: Is this sentence referring to Figure 3 instead of Figure 4?**

*This is true. We move it to the paragraph above.*

**10. Pg. 12, Line 3-4: What properties are being referred to here? I certainly wouldn't say that the number concentration in 4e and 4f are similar, and there are also large differences in IWC in 4b and 4c.**

*Changed:*

*“Again, the properties of the aged contrails and the natural cirrus around Germany are similar.”*

*to:*

Here, local enhancements in both IWC and  $n$  occur in the cirrus ice class, where aged contrails are transferred to (Fig. 4e), compared to the reference simulation ( Fig. 4f).

**11. Pg. 14, Lines 11-12: Why do contrails only form at altitudes between 11 km and 13 km? Is this because air traffic is restricted to these altitudes on this line or are there lower altitude flights but the Schmidt-Appleman criterion is only satisfied at these altitudes?**

*Taking into account the rather high values for RHi also below 11 km, the Schmidt-Appleman criterion likely would be fulfilled.*

*But the traffic data we use hardly contains flights taking place below 11 km except for climbing and descending. At least for the cross section selected, apparently none of these movements was taking place...*

This is caused by the absence of air traffic below this layer.

**12. Pg. 15, Line 6: Should the first word be “below”?**

Changed “beyond” to  
below

**13. Pg. 15, Line 10: Does the model account for downward subsidence of the aircraft vortices and plumes or is the vertical structure in the modeled contrails only due to gravitational settling of the larger ice crystals? The enhancements in ice number shown in Figure 6 appear to occur at flight level, but the enhancement in IWC is below flight level.**

Change paragraph starting in page 15, line 5:

*“In the aviation simulation, changes in the natural ice class can be found mainly at heights where contrails form and slightly beyond. Here, local increases in IWC and N occur. Keeping in mind the simple design of our model setup, those ice crystals represent both fall streaks of contrails as well as the transition into contrail cirrus.”*

to:

In the aviation simulation, changes in the natural ice class can be found mainly at heights where contrails form and slightly below of it. The enhancement of ice number concentrations occurs mostly at flight levels, whereas an increase in IWC is found below. During the initialization, contrail ice crystals are vertically distributed over the whole grid layer and this indirectly accounts for the initial wake vortex induced vertical expansion of a contrail. Within our simulation, the vertical structure of the contrails is determined only due to the gravitational settling of the larger ice crystals.

**14. I would like to see the satellite observations more directly integrated into the discussion surrounding Figures 3-4 rather than in its own section since I think that it can provide a lot of context and validation for the model results. Figures 8 and 9 as they stand now are kind of on their own and not particularly informative other than to denote that there are thin, high-level cirrus and no low clouds. The cirrus clouds shown in Figure 8a appear to be much more diffuse than the MODIS imagery for this time period, with the MODIS images showing a lot of contrail structure and providing a good snapshot of the time evolution of the scene during the two simulations. I suggest the authors strike Figures 8 and 9, and add MODIS satellite images at 1000Z and 1150Z either as part of Figures 3 and 4 or as a separate figure before them. Such an example figure created from [worldview.earthdata.nasa.gov](http://worldview.earthdata.nasa.gov) images is on the next page with detailed web references at the end of this review.**

*We have rewritten parts of section 4.3 (Comparison with Satellite Observation). We use the great source for images you suggest for both time steps considered. However, we refrain from including the discussion into the section before. There, we want to focus on the behavior of the model itself and consequences that arise thereof. A future study for situations where preferably in-situ measurements are available will then also include a more detailed verification and comparison with satellite data.*

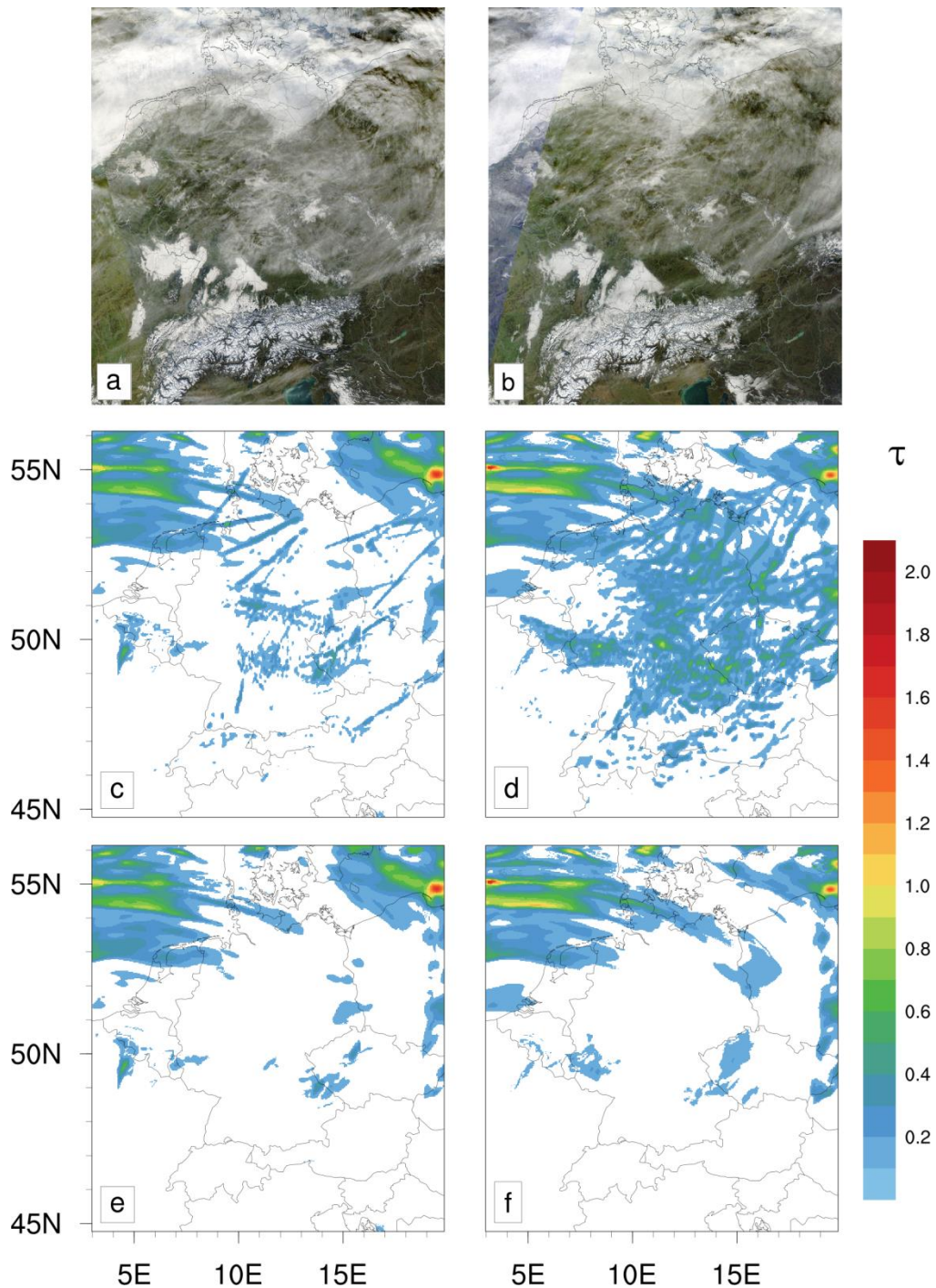


Figure 10. Top row: satellite image (MODIS True Color - Corrected Reflectance) (NASA/GSFC/ESDIS, 2018); center row: optical depth at  $1.115 \mu\text{m}$  of all ice clouds for the aviation simulation; bottom row: optical depth of all ice clouds for the reference simulation; left column: 10 UTC; right column: 12 UTC.

In the following, satellite images (created with Global Imagery Browse Services (GIBS) NASA/GSFC/ESDIS, 2018) are shown in Fig. 10 for a qualitative assessment of the simulations. The panels a and b show the "MODIS Terra Corrected Reflectance True Color" at 10 UTC and 12 UTC for the simulated day, respectively, both with a resolution of 250 m. The "True Color" composition consists of MODIS bands 1, 4 and 3 (NASA/GSFC/ESDIS, 2018). Beside a cloud bank over the North and Baltic Seas and fog over Southern and Western Germany, a considerable number of line-shaped contrails and diffuse cirrus clouds are present across both satellite images. Main contrail clusters are found over Central Germany for both situations. Contrails can also be identified over the Netherlands

and Belgium, over the Czech Republic, and south of the Alps. At 12 UTC, the rather widespread high-level cloud cover seems to have decreased compared to 10 UTC.

Comparing Fig. 10a and Fig. 10e, obviously, the reference simulation underestimates the coverage of high clouds in the center of the domain, which, in large parts, consists of contrails and contrail cirrus Fig. 10c. Clearly, the amount of cloud cover seems to be underestimated also in the aviation simulation at 10 UTC. This discrepancy is probably due to the fact that air traffic was switched on at 08 UTC and earlier flight movements are disregarded in our simulation. Hence, the simulation evaluation at 10 UTC neglects all contrails older than 2 hours. The comparison at 12 UTC is more favorable and observations match much better with the aviation simulation than with the reference simulation.

...

Acknowledgements:

We acknowledge the use of imagery from the Land Atmosphere Near real-time Capability for EOS (LANCE) system and services from the Global Imagery Browse Services (GIBS), both operated by the NASA/GSFC/Earth Science Data and Information System (ESDIS, [\url{http://earthdata.nasa.gov}](http://earthdata.nasa.gov)) with funding provided by NASA/HQ.

**15. What is the coordinate chosen for the red circle in Figure 11 and related time series analysis in Figure 12? Why was this coordinate chosen? Do the results change if a set of coordinates in the  $\Delta SW < -5\%$  band is chosen?**

*The red circle (53°N, 12°E) marks the center of an area of 140 km x 140 km. The curves in Fig. 12 thus represent an average over this area. But of course, the results slightly change, when looking at another location. Nevertheless, the overall patterns are similar there.*

*We add to the description of Fig. 12.:*

The red circle (53°N, 12°E) marks the location evaluated.

*To draw more robust conclusions, we modify the evaluation of SW and PV reduction, by replacing Fig. 12 (now Fig. 13) with the following figure and text:*

Fig. 13 shows the temporal evolution of incoming SW radiation and normalized PV power. Panels a to d represent mean values for the entire simulation domain, panel e additionally represents mean values for an area of approximately 50 km x 50 km centered at a spot in the north-eastern part of the simulated domain, indicated by the red circle (53°N, 12°E) in Fig. 12. This is the location of one of the largest solar parks in Germany (Solarpark Brandenburg-Briest). Also several other major solar parks are located around this area. For enhanced clearness, values for the sensitivity study (see Sec. 4.5) are depicted only as difference to the reference simulation. The differences between the aviation simulation and the reference simulation are in general more pronounced for the selected location than on average over the entire simulation domain.

During the whole time of daylight, contrails and contrail cirrus reduce up to  $15 \text{ Wm}^2$  (about 7 %) of the total incoming SW radiation in the entire domain (Fig. 13a). The effect is largest during noon and ceases during the day. This corresponds to the size of contrail ice crystals. As in our simulation, contrails start to form at 08 UTC, the average contrail ice crystal size grows during the day. Accordingly, contrail ice effective radii also increase with time and lead to smaller values of the extinction coefficient.

Separating the total SW radiation into its direct (Fig. 13b) and diffuse (Fig. 13c) fraction, it is clear that especially the direct incoming SW radiation is strongly reduced by more than  $20 \text{ Wm}^2$  due to the presence of additional ice crystals in the atmosphere.

In contrast, the diffuse incoming SW radiation is increased by up to  $10 \text{ Wm}^2$ . Enhanced scattering of SW radiation caused by the contrail ice crystals increases the diffuse SW radiation at the ground.

Notably, the peak in reduction of diffuse SW radiation occurs in the afternoon, around 13 UTC.

Between 08 UTC and about 11 UTC, the amount of diffuse SW radiation reaching the ground is larger in the aviation simulation. During this time, as mentioned before, contrail ice crystals are smallest on

average and forward scattering is less pronounced than for larger crystals, whereas contrail ice crystals grow on average during the day resulting in enhanced forward scattering.

In the aviation simulation, young and aged contrails generally reduce the incoming SW radiation at the surface. This effect is currently neglected in operational weather forecast models. However, this effect is of relevance for the production of solar energy. The temporal evolution of the normalized PV power is depicted in Fig. 13d) and Fig. 13e. The normalized PV is calculated using the open source PV modeling environment PV\_LIB for python (Andrews et al., 2014). For a specific combination of a PV module and a PV inverter combination, a nominal power and a reasonable tilt is assumed. These technical specifications are taken from Rieger et al. (2017). They assume panels consisting of a south-oriented PV module with a nominal power of 220 W and a size of 1.7 m<sup>2</sup>. Compared to the reference simulation, the normalized PV power is decreased in the aviation simulation most of the day. The largest losses of up to 10 % occur in the morning and diminish during the day, even an increase occurs for the selected location in the late afternoon (Fig. 13e). The normalized PV power is somewhat more strongly reduced than the total SW radiation. For production of PV power, the incoming direct radiation is of greater importance than the diffuse; of the two, the direct experiences the larger reduction from contrails and contrail cirrus.

The error bars in Fig. 13d and Fig. 13e represent the mean values +/- the standard deviation with respect to the entire simulation domain and the area of 50 km x 50 km around the selected location, respectively. The standard deviation in Fig. 13d reflects the large-scale variability of the impact of contrails and contrail cirrus on the incoming SW radiation, whereas Fig. 13e illustrates the small-scale variability.

Compared to the selected location, standard deviations are larger for the mean of the domain. Obviously, clouds modify the amount of SW radiation reaching the ground in a non-uniform manner. The magnitudes of the standard deviations for the aviation simulation are about the same magnitude like the ones for the reference simulation. Apparently, the impact of contrails and contrail cirrus on incoming SW radiation is as variable as the impact of natural clouds. E. g., even at 12 UTC, when the impact of contrails and contrail cirrus is largest, confined areas exist, which are unaffected by contrails and contrail cirrus (Fig. 11b).

However, the small-scale variability of the impact of contrails and contrail cirrus on SW radiation is rather small, reflected by much smaller standard deviations in Fig. 13e. One can therefore deduce that the exact location of contrails or contrail cirrus is not crucial for the strength of the impact on SW radiation.

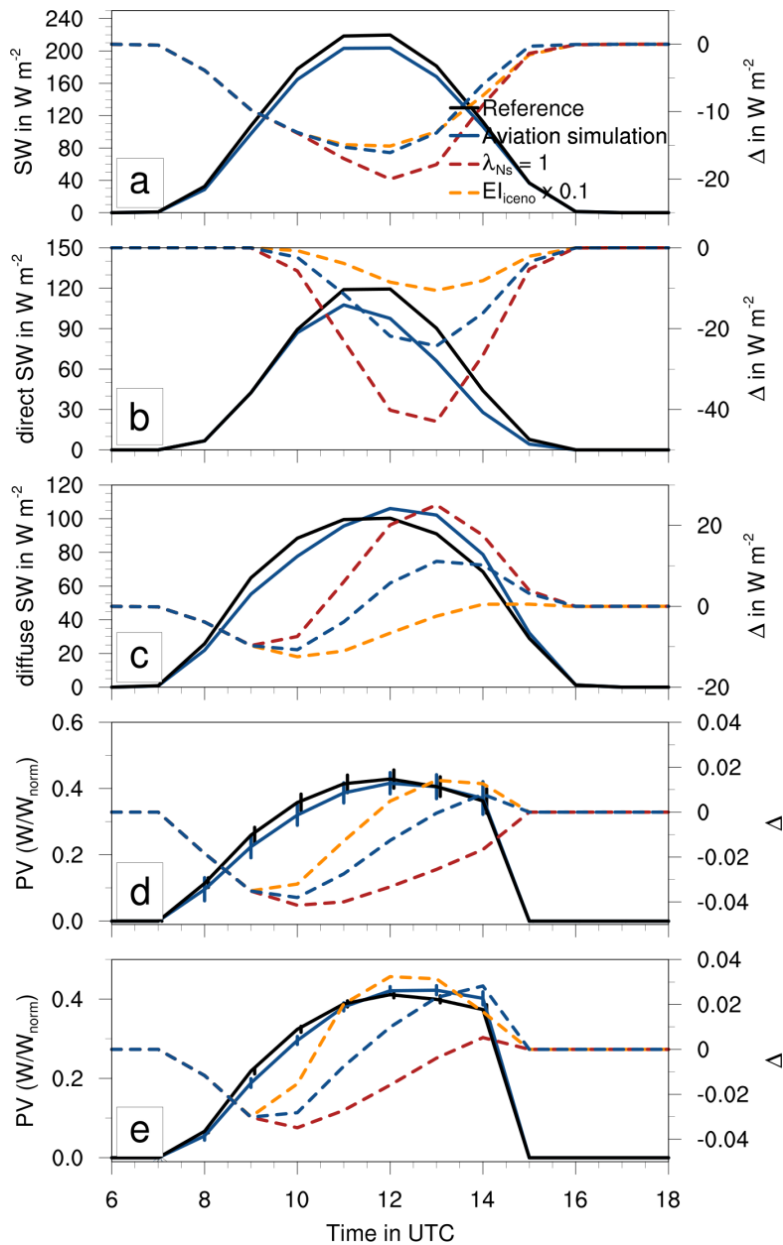


Figure 13. Temporal evolution for 3 December 2013 of incoming shortwave radiation: reference (black); aviation simulation as before (blue); "bio-fuel" scenario with  $EI_{iceno} \times 0.1$  (orange), omission of crystal loss during contrail vortex phase with  $\lambda_{Ns} = 1$  (red). Dashed lines (corresponding to right y-Axis) are difference to reference simulation. a) total SW; b) direct SW; c) diffuse SW; d),e) normalized PV-power. a) - d) over entire domain; e) mean for the location marked with the red circle in Fig. 12. Error bars represent mean values  $\pm$  standard deviation.

16. Pg. 22, Line 20-21: Suggest rewording, "In reality..." to "This scenario explores lower engine soot emissions caused by either improved engine combustor technologies or fuel composition changes from, e.g., biofuel adoption (Moore et al., 2017).

*We adopt your suggestion.*

17. Figure 2: Should this be COSMO-ART to be consistent with the text?

*Actually, the name of the domain is not important. COSMO-DE is the domain, used by the German Weather Service to run their high resolved forecast for Germany*

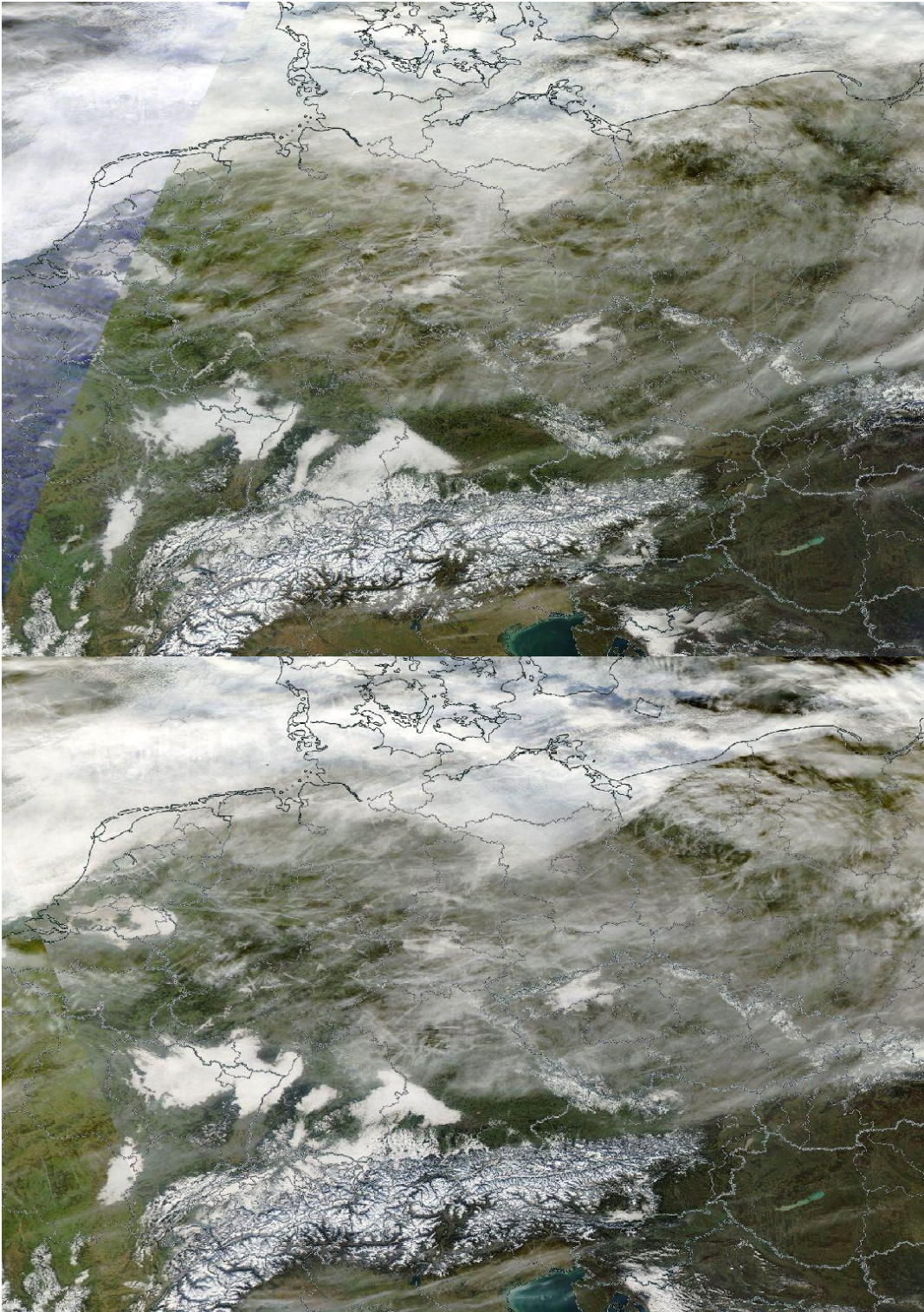
*We change the caption of Fig. 2 from "Flight trajectories for the COSMO-DE domain ..."*

*Flight trajectories for the simulated domain ...*

**18. Figure 12: Please use a more descriptive legend and spell out abbreviations.**

*We spell out the abbreviations.*

- Reference
- Aviation Simulation
- lambda\_Ns = 1
- El\_iceno x 0.1



**References Cited:**

**Wan et al. (2015) "Photovoltaic and Solar Power Forecasting for Smart Grid Energy Management", CSEE Journal of Power and Energy Systems, 1(4).  
doi:10.17775/CSEEJPES.2015.00046,  
<http://ieeexplore.ieee.org/document/7377167/>.**

**NASA Worldview Viewer with imagery and orbit tracks:**

[https://worldview.earthdata.nasa.gov/?p=geographic&l=VIIRS\\_SNPP\\_CorrectedReflectance\\_TrueColor\(hidden\),MODIS\\_Aqua\\_CorrectedReflectance\\_TrueColor,MODIS\\_Terra\\_CorrectedReflectance\\_TrueColor,Aqua\\_Orbit\\_Asc,Terra\\_Orbit\\_Dsc,Reference\\_Labels\(hidden\),Reference\\_Features\(hidden\),Coastlines&t=2013-12-03&z=3&v=-17.06324930328618,31.036661088764802,35.3750429177626,68.87135186462584](https://worldview.earthdata.nasa.gov/?p=geographic&l=VIIRS_SNPP_CorrectedReflectance_TrueColor(hidden),MODIS_Aqua_CorrectedReflectance_TrueColor,MODIS_Terra_CorrectedReflectance_TrueColor,Aqua_Orbit_Asc,Terra_Orbit_Dsc,Reference_Labels(hidden),Reference_Features(hidden),Coastlines&t=2013-12-03&z=3&v=-17.06324930328618,31.036661088764802,35.3750429177626,68.87135186462584)

**Time stamp information for the Terra and Aqua images is shown on the orbit tracks.**

**Editable Link to 1000Z Terra Image JPEG:**

[https://gibs.earthdata.nasa.gov/image-download?TIME=2013337&extent=3,45,20,56&epsg=4326&layers=MODIS\\_Terra\\_CorrectedReflectance\\_TrueColor,Coastlines,Reference\\_Features&opacities=1,1,1&worldfile=false&format=image/jpeg&width=1080&height=768](https://gibs.earthdata.nasa.gov/image-download?TIME=2013337&extent=3,45,20,56&epsg=4326&layers=MODIS_Terra_CorrectedReflectance_TrueColor,Coastlines,Reference_Features&opacities=1,1,1&worldfile=false&format=image/jpeg&width=1080&height=768)

**Similarly, for the 1150Z Aqua image JPEG:**

[https://gibs.earthdata.nasa.gov/image-download?TIME=2013337&extent=3,45,20,56&epsg=4326&layers=MODIS\\_Aqua\\_CorrectedReflectance\\_TrueColor,Coastlines,Reference\\_Features&opacities=1,1,1&worldfile=false&format=image/jpeg&width=1080&height=768](https://gibs.earthdata.nasa.gov/image-download?TIME=2013337&extent=3,45,20,56&epsg=4326&layers=MODIS_Aqua_CorrectedReflectance_TrueColor,Coastlines,Reference_Features&opacities=1,1,1&worldfile=false&format=image/jpeg&width=1080&height=768)

where coloring denotes: **Year and Julian Day**, **Bounding Coordinates**, **Layer**, **Image Dimensions in Pixels (controls resolution, aspect ratio)**

Dear Referee 3,

We thank a lot for your valuable comments and suggestions. We followed them as explained below.

The reviewers comments are repeated in **bold letters**, our replies are given in *italic*, and text modified or added to the manuscript is given in **blue**.

**This paper describes a parametrization of contrails that is embedded in the two moment cloud microphysics of the COSMO regional atmospheric model. It is followed by a case study including the impact of contrails and contrails-cirrus on short wave radiation and on possible PV production. The paper presents interesting new results, but before being published the authors should address the following points.**

*Thanks a lot for your remarks. Most of your points address errors and mistakes that one does only recognize when having a very close look at the manuscript. Your review helped a lot improving our manuscript.*

**General remarks:**

**1. I was a bit surprised that the authors have chosen a model with a complete representation of atmospheric chemistry and aerosols (COSMO-ART) for this study. From the description of the parametrization in Section 2 it seems to me that changes by aircraft to atmospheric chemistry as well as soot emissions are not directly considered. Thus it seems that the usage of the COSMO model (without the computationally expensive ART modules) in conjunction with the 2-moment scheme of Seifert and Beheng (2006) are sufficient for the present study. If this is not the case it should be shown more clearly why the ART modules are needed.**

*Indeed, no interactions of aircraft emissions are considered in this study. Also, no soot emissions are taken into account explicitly.*

*But COSMO-ART comprises more than only parameterizations for aerosol dynamics and gas phase chemistry. For example, the infrastructure, e. g. the ART-tracer structure and modules to read emission data are used for the contrails parameterizations. Also the coupling of aerosol-dynamics and the microphysics is adapted to calculate contrail microphysics.*

*In the future, we want to extend the model to also consider aircraft emissions. Therefore, the entire COSMO-ART model is referred to.*

*We add in Sec. 2 (Model Description) after*

*“In this section, the parameterizations to calculate the microphysical properties of ice crystals and the modifications to represent contrails are presented.”*

*The model system COSMO-ART comprises a detailed treatment of aerosol dynamics and gas-phase chemistry (Vogel et al., 2009). However, most of these features are not used for the simulations shown in this study. Nevertheless, large parts of the infrastructure contained in COSMO-ART, e. g. the tracer structure and modules for reading emission data are adopted for the contrails parameterizations.*

**2. Whereas the case study in section 4 is well described, sections 2 and 3 are rather hard to read and understand and would profit from a rewrite. In section 2.1 it is very difficult to understand where the description of the standard cirrus class is ended and the description of the newly introduced contrail class starts. I would thus recommend separating by introducing a new section. Also this section would highly profit from a table explaining the differences between both classes as well as a schematics such as Fig 1 in Salzmann et al. (2010) to highlight the interactions of the newly introduced contrail ice class with the other ice classes. A Table is provided at the end of the paper explaining the differences, but is not referenced in the text. I would moreover suggest in Table 1 to distinguish more clearly between the cirrus and contrail ice class. Similarly in section 2.2 a Table would help to understand the differences between the interactions with radiation of both classes.**

*Refrain from presenting schematics, as very complex for SB06, also actually contrail – cirrus interaction not too complicated to understand.*

*We change Tab. 1 to more clearly distinguish between contrail ice class and natural ice class.*

*We change in section 2.1 The Contrail Ice Class, page 4, line 4:*

*“A longer description including various formulae is deferred to the appendix.”*

*to:*

*A longer description including various formulae as well as a table showing the different coefficients characterizing both the contrail and the cirrus ice class (Tab. 1) is deferred to the appendix.*

*Section 2.2: There are no differences in the interaction of contrail / natural ice with radiation.*

**3. It seems quite strange that a completely new scenario "bio fuels" is introduced in the last section of the paper, but referenced already in Fig 12. I would suggest to keep section 4.5 as sensitivity case study, and not introduce a new scenario here. As shown by Ferrone (2011) biofuels also have an impact on the Appleman-Schmidt criterion and this would need to be changed accordingly.**

*We do not aim at introducing a new “bio fuel” scenario where also effects on contrail formation had to be included (as you correctly mention). It is common practice in contrail studies to study the sensitivity to the initial ice crystal number. Various reasons (uncertainty and variability of  $EI_{iceno}$ -value, biofuels effect) to do so exist.*

**Specific remarks:**

**4. In the last line of page 2, the resolution of Global Circulation Models (GCMs, the abbreviation is not introduced) are given as 250km, however most recent models have a resolution of 50 km or higher (IPCC, 2015).**

*This is a fair point, but the argument is still valid comparing to 50 km resolution. We change in page 2, line 32:*

*“Compared to GCM parameterizations, this omission seems acceptable in a regional model, as the spatial resolution is much higher (horizontal grid size of 2.8 km versus 250 km in a GCM).”*

*to*

*Compared to GCM (Global Circulation Model) parameterizations, this omission seems acceptable in a regional model, as the spatial resolution is much higher (horizontal grid size of 2.8 km versus 50 km in a GCM).*

**5. Caption of Figure 2: The abbreviation COSMO-DE is not introduced**

*Actually, the name of the domain is not important. COSMO-DE is the domain, used by the German Weather Service to run their high resolved forecast for Germany*

*We change the caption of Fig. 2 from*

*“Flight trajectories for the COSMO-DE domain ...”*

*Flight trajectories for the simulated domain ...*

**6. Figures 3, 4, 6 and 7 would become more interesting and easy to interpret if a difference plot between the middle and right column would be added.**

*We avoid difference plots here, as their interpretation becomes problematic. Due to the design of our model, we cannot distinguish between contrail cirrus and natural cirrus in the cirrus ice class.*

*By formation of contrails in the aviation simulation, humidity changes and thus partly, no cirrus clouds form, where they do in the reference simulation. Also the properties of natural cirrus may change in the aviation simulation.*

**7. Figure 8 and 9: If I understood correctly, the black boxes should highlight the same areas but they are slightly shifted.**

*Indeed, the boxes were not covering the same areas, thanks for the remark. Due to restructuring the section, Fig. 9 (black boxes) are not shown anymore.*

**8. In the list of abbreviations given on page 31 and 32 some Units are erroneous. Units such as  $\text{kg}^{(-/\mu)}$ ,  $\text{m}^{(-/\mu)}$ ;  $\text{kg}^{(-b_{\text{vel}})}$ ;  $\text{kg}^k$  do not exist.**

*In case, one insists on SI units, this is a fair point, although the quantities are defined as such in Seifert and Beheng (2006).*

*We convert the equations, where the strange units occur (A6, A7) into numerical value equations and remove the units.*

*We add in Appendix A:*

*page 24, line 6:*

*Here, m is in units of kg.*

*page 25, line 5:*

*In Eqs. A6 and A7, m and  $\overline{m}$  are in kg; and v and  $\overline{v}_k$  are in in  $\text{m s}^{-1}$ .*

*page 25, line 20:*

*... with, L in units of m:*

*Also Tab 1 and the list of abbreviations is changed accordingly.*

#### **References:**

**Ferrone, A, (2011): Aviation and climate change in Europe: from regional climate modelling to policy-options.**

**<http://hdl.handle.net/2078.1/74779>**

**IPCC, 2013: Climate Change 2013: The Physical Science Basis. Contribution of Working Group I to the Fifth Assessment Report of the Intergovernmental Panel on Climate Change [Stocker, T.F., D. Qin, G.-K. Plattner, M. Tignor, S.K. Allen, J. Boschung, A. Nauels, Y. Xia, V. Bex and P.M. Midgley (eds.)]. Cambridge University Press, Cambridge, United Kingdom and New York, NY, USA, 1535 pp, doi:10.1017/CBO9781107415324.**

**Salzmann, M., Y. Ming, J. C. Golaz, P. A. Ginoux, H. Morrison, A. Gettelman, M. Krämer, and L. J. Donner, 2010: Two-moment bulk stratiform cloud microphysics in the GFDL AM3 GCM: Description, evaluation and sensitivity tests. Atmospheric Chemistry and Physics, 10, 8037-8064, doi:10.5194/acpd-10-6375-2010.**

**Seifert, A. and Beheng, K. D.: A two-moment cloud microphysics parameterization for mixed-phase clouds. Part 1: Model description, Meteorol. Atmos. Phys., 92, 45 – 66, doi:10.1007/s00703-005-0112-4, 2006.**

# Contrails and Their Impact on Shortwave Radiation and Photovoltaic Power Production - A Regional Model Study

Simon Gruber<sup>1</sup>, Simon Unterstrasser<sup>2</sup>, Jan Bechtold<sup>3</sup>, Heike Vogel<sup>1</sup>, Martin Jung<sup>3</sup>, Henry Pak<sup>3</sup>, and Bernhard Vogel<sup>1</sup>

<sup>1</sup>Karlsruhe Institute of Technology – Institute of Meteorology and Climate Research, Hermann-von-Helmholtz-Platz 1, 76344 Eggenstein-Leopoldshafen, Germany

<sup>2</sup>Deutsches Zentrum für Luft- und Raumfahrt (DLR) – Institut für Physik der Atmosphäre, Oberpfaffenhofen, 82234 Wessling, Germany

<sup>3</sup>Deutsches Zentrum für Luft- und Raumfahrt (DLR) – Institut für Flughafenwesen und Luftverkehr, 51147 Cologne, Germany

*Correspondence to:* S. Gruber (simon.gruber@kit.edu)

**Abstract.** A high resolution regional-scale numerical model was extended by a parameterization that allows for both the generation and the life cycle of contrails and contrail cirrus to be calculated. The life cycle of contrails and contrail cirrus is described by a two-moment cloud microphysical scheme that was extended by a separate contrail ice class for a better representation of the high concentration of small ice crystals that occur in contrails. The basic input data set contains the spatially and temporally highly resolved flight trajectories over Central Europe derived from real time data. The parameterization provides aircraft-dependent source terms for contrail ice mass and number. A case study was performed to investigate the influence of contrails and contrail cirrus on the [shortwave](#) radiative fluxes at the earth's surface. Accounting for contrails produced by aircraft enabled the model to simulate high clouds that were otherwise missing on this day. The effect of these extra clouds was to reduce the incoming shortwave radiation at the surface as well as the production of photovoltaic power by up to 10 %.

## 10 1 Introduction

Contrails consist of ice crystals formed in the exhaust plume of aircraft due to ~~a~~-mixing of the hot [and humid](#) exhaust with cold environmental air. ~~Following Contrails form in case,~~ the Schmidt-Appleman-Criterion (Schmidt, 1941; Appleman, 1953; Schumann, 1996) ~~;-contrails-form-only-when-is-fulfilled, i.e.~~ the ambient temperature is below a threshold ~~temperature-of~~ ~~roughly-of-around~~  $-45^{\circ}$  C. With ~~plume temperatures near  $-38^{\circ}$  C to  $-40^{\circ}$  C,~~ ~~contrail particles, which are formed in the liquid~~ ~~phase initially, freeze homogeneously and quickly to form ice crystals. Those ice crystals grow in air with relative humidity~~ ~~above ice saturation and contrails persist. With such~~ a favorable state of the atmosphere, ~~i.e.-characterized-by-supersaturation~~ ~~with-respect-to-ice,~~ the originally line-shaped contrails undergo various physical processes at the micro scale, spread by the influence of shear and sedimentation and change their structure and microphysical properties. At some point, contrails are no longer distinguishable from natural cirrus in observations. This type of anthropogenic cloud is then called contrail cirrus (Heymsfield et al., 2010) and can have lifetimes of several hours. In a particular case, an 18-hour old contrail-cirrus could be tracked in a satellite imagery (Minnis et al., 1998). [Other examples of long-lifetime contrail observations are summarized by](#)

Schumann and Heymsfield (2017).

Contrails influence the radiative budget of the atmosphere in a way that is comparable to that of thin natural cirrus clouds (Sausen et al., 2005). Important properties, such as the optical depth or the spatial and temporal extent of occurrence, have not been sufficiently investigated and are also not quantified to a satisfactory extent (Boucher et al., 2013). The radiative forcing of aged contrails and contrail cirrus is of greater importance than the one originating from young, line-shaped contrails (Stubenrauch and Schumann, 2005; Eleftheratos et al., 2007; Burkhardt and Kärcher, 2011).

Previous model studies primarily used global circulation models extended by parameterizations that are able to simulate line-shaped contrails. Here, the global radiative forcing due to contrails was quantified. The values ~~spread around  $0.4 \text{ mWm}^{-2}$  (Ponater et al., 2002) to  $3.5 \text{ mWm}^{-2}$  (Marquart et al., 2003)~~range from roughly  $5$  to  $20 \text{ mWm}^{-2}$  depending on the simulated year and assumed contrail properties (Marquart et al., 2003; Stuber and Forster, 2007; Kärcher et al., 2010) and are consistent with satellite-based estimates by Spangenberg et al. (2013). Taking the larger effect of contrail cirrus into account, a global mean radiative forcing of approximately  $38 \text{ mWm}^{-2}$  (Burkhardt and Kärcher, 2011) (recently updated to  $56 \text{ mWm}^{-2}$  by Bock and Burkhardt et al., 2016) to  $40$  to  $80 \text{ mWm}^{-2}$  (Schumann and Graf, 2013) is found. The major drawbacks of these methods are the coarse resolution of the models in both space and time.

Another class of studies simulates single contrails with high resolution LES<sup>1</sup> or RANS<sup>2</sup> models, hereby focusing on contrail formation (Paoli et al., 2013; Khou et al., 2015), young contrails with ages up to 5 minutes and their interaction with the descending wake vortices (Lewellen and Lewellen, 2001; Unterstrasser, 2014) and the transition into contrail-cirrus over time scales of hours (Unterstrasser and Gierens, 2010a; Lewellen, 2014). Usually, the contrail evolution is studied for a variety of environmental scenarios which helps to single out important process and ambient and aircraft parameters. Parameter studies allow for investigating the conditions under which contrails are persistent and the manner in which microphysical and optical properties change during transition and decay. Because this method is not applicable for a larger number of contrails and often limited to idealized environmental scenarios, it is not suited to quantify the impact of air traffic on the state of the atmosphere. The spatial scale applied in this study lies between those typically used for large-eddy simulations and global climate models.

~~In this respect, the presented study is complementary to the aforementioned approaches and is, to our knowledge, the first study of its kind.~~ We use the online coupled regional-scale model system COSMO-ART (Baldauf et al., 2011; Vogel et al., 2009).

In this context, online coupled means that meteorology, chemistry and contrail-related processes are simulated in one model at the same grid and one main time step for integration is used. For this study, the model is extended by introducing a new hydrometeor class for contrail ice crystals. The contrail initialization is based on a parametrization of early contrail properties by Unterstrasser (2016). The prognostic equations for contrail ice are similar to those of the natural cirrus ~~cloud-ice~~ class.

Despite their similar treatment in terms of model equations, the evolution of the two cloud types can be quite different, as their formation mechanisms are different. Especially with respect to the spatial scale used in the regional scale COSMO-ART model, the presented study is complementary to the aforementioned approaches and is, to our knowledge, the first study of its kind.

---

<sup>1</sup>Large-Eddy Simulation

<sup>2</sup>Reynolds-Averaged Navier Stokes

Ice crystals in young contrails are considerably smaller than the ones that form in natural cirrus clouds and occur with substantially higher ice crystal number concentrations (Febvre et al., 2009; Schröder et al., 2000; Voigt et al., 2010). Therefore, the original microphysical scheme was extended by a new hydrometeor class that allows for a separate treatment of the small contrail ice crystals separate from natural ice. This approach allows for the investigation of contrail microphysical properties and their changes during the various stages of development represented in a regional atmospheric model. In contrast to other studies using a two-moment microphysical scheme (Bock and Burkhardt, 2016a), the presented model configuration uses no fractional cloud coverage and no prognostic equations for contrail geometric properties like volume or area which describe the contrail spreading on the subgrid scale. Compared to GCM<sup>3</sup> parameterizations, this omission seems acceptable in a regional model, as the spatial resolution is much higher (horizontal grid size of 2.8 km versus ~~250 km~~ 50 km in a GCM).

Regarding the contrail microphysics and the interaction with the meteorological situation, the entire procedure is online coupled, thus allowing feedback processes between contrails and natural clouds in contrast to other models on a comparable grid scale (Schumann, 2012). There, a mixed Lagrangian-Eulerian approach is used instead of the usual Eulerian treatment. This approach allows covering the scale ranging from thousands of single contrails to multi-year global climate simulations (Schumann, 2012; Schumann et al., 2015; Caiazzo et al., 2017).

One of the key goals of this study is thus to quantify the influence of contrails and contrail cirrus on natural high-level cloudiness. Moreover, the radiative properties of contrails and their local influence on the shortwave radiative fluxes at the surface are examined.

The model uses a diagnostic radiation scheme (Ritter and Geleyn, 1992). Because the description of shortwave optical properties for ice clouds is optimized for ~~different~~ various naturally occurring crystal habits (Fu et al., 1998; Key et al., 2002), a separate treatment of contrail ice crystals is introduced here as well.

Another feature of this study is the new and recently compiled data set of flight trajectories. Rather than statistical calculations for globally averaged fuel consumption, the basic data consist of real commercial aircraft waypoint data (flightradar24.com, 2015). Another approach using commercial flight data, to study contrails on a regional scale is described in Duda et al. (2004). Here, a combination of commercial flight data and coincident meteorological satellite remote sensing data was used to perform a case study of a widespread contrail cluster. In the future, further case studies should be performed for which in-situ observations of natural ice clouds and especially contrails are available. Der letzte Satz passt hier nicht rein. Das klingt so als muesste duda die weiteren fall studien machen und nicht wir.

The presented model configuration serves to study microphysical evolution of contrails and contrail cirrus, their influence on natural high-level cloudiness, and their impact on the radiative fluxes on a regional scale and short time periods. This gains importance, e.g., in predicting the energy yield from photovoltaic (PV) systems, ~~because additional cloud cover due to contrails is not represented~~. During the past decades, the development of alternative, clean energy production was enhanced to counteract global warming and reduce air pollution. Within the scope of methods, one of the most promising sources is solar energy, gained by PV cells. To assure a sustainable supply, the demand of precise prediction of the energy yield from PV systems is desired (Lew and Richard, 2010). Several approaches exist to forecast PV power, such as statistical models, neural networks,

---

<sup>3</sup>Global Circulation Model

remote sensing models and numerical weather prediction models (Inman et al., 2013). Especially PV forecast using numerical weather prediction models is challenged by special weather situations or phenomena that are poorly represented in the models (Köhler et al., 2017). E. g. Rieger et al. (2017) found a large impact of mineral dust due to Saharan dust outbreaks on the solar radiation over Germany. This becomes important, as mineral dust is currently not considered adequately in operational weather forecasting. Another feature of this study is the new and recently developed data set of real-time flight tracks. Rather than statistical calculations for globally averaged fuel consumption, the basic data consist of real-time-based flight trajectories (flightradar24.com, 2015) forecast. Another phenomenon that is not represented at all in numerical weather prediction, is the influence of aviation.

In section 2, the modification of the microphysical scheme and the radiation scheme are described. Section 3 presents a description of the parameterization providing the source terms for contrail ice. In section 4, the results of a case study and comparison with satellite observations are presented.

## 2 Model Description

In the following this section, the parameterizations to calculate the microphysical properties of ice crystals and the modifications to represent contrails are presented.

The model system COSMO-ART comprises a detailed treatment of aerosol dynamics and gas-phase chemistry (Vogel et al., 2009). However, most of these features are not used for the simulations shown in this study. Nevertheless, large parts of the infrastructure contained in COSMO-ART, e. g. the tracer structure and modules for reading emission data are adopted for the contrails parameterizations.

In this study, the COSMO-ART model is coupled with a comprehensive two-moment microphysical scheme following Seifert and Beheng (2006). Until now, the scheme contained one cloud ice class (besides other hydrometeor types in warm and mixed-phase clouds) that describes ice crystals in high-level ice clouds. Because ice crystals in freshly formed contrails are considerably smaller than those in natural cirrus, the basic microphysical processes in young contrails are treated in a separate, newly introduced *contrail ice class*. From now on, the original ice cloud class is called *cirrus ice class*. The separate treatment allows simulating local bi-modal size spectra.

Consequently, also in the radiation scheme, contrails are treated separately from the cirrus ice using the new contrail ice class. The applied radiation scheme is described in section 2.2.

Unless otherwise indicated, the parameterized processes for the new contrail ice class are the same as those used for the cirrus ice class.

Similar approaches with a separate contrail ice class using climate models with coarser grid size are described by Burkhardt and Kärcher (2009) and Bock and Burkhardt (2016a).

## 2.1 The Contrail Ice Class

In this section, we first describe shortly the treatment of ice crystals in the cirrus ice class. Hereby, we mainly focus on those aspects that are relevant for understanding contrail-specific modifications in the contrail ice class explained later on. A longer description including various formulae as well as a table showing the different coefficients characterizing both the contrail and the cirrus ice class (Tab. 1) is deferred to the appendix.

In each grid box, the ice mass distribution is assumed to follow a generalized  $\Gamma$ -distribution  $f(m)$  (see Eq. A1). Prognostic equations are solved for the ice crystal number concentration  $n$  (zeroth moment of  $f(m)$ ) and the ice crystal mass concentration  $q_i$  (first moment of  $f(m)$ ). Written concisely, the prognostic equations for the moments  $M^k$  of order  $k = 0$  or 1 (see Eq. A2 for a definition) read as

$$10 \quad \frac{\partial M^k}{\partial t} + \nabla \cdot [\mathbf{u}M^k] - \nabla \cdot [K_h \nabla M^k] + \frac{\partial}{\partial z} [\bar{v}_{sed,k} M^k] = S^k, \quad (1)$$

where  $\mathbf{u}$  is the grid scale mean wind,  $K_h$  is the turbulent diffusion coefficient and  $\bar{v}_{sed,k}$  is the number or mass-weighted sedimentation velocity (see Eq. A7).  $S^k$  comprises all source and sink terms like nucleation, deposition/sublimation and aggregation.

The deposition source term is derived from the growth equation of a single ice crystal which is integrated over the whole ice crystal mass spectrum.

The ice crystals have a hexagonal shape and the mass  $m$  of a single ice crystal is related to its size  $L$  via the mass-size relation

$$m = a_{geo} L^{b_{geo}} \quad (2)$$

For  $m$  in kg and  $L$  in m, the parameter values are  $a_{geo,nat} = 1.59$  and  $b_{geo,nat} = 2.56$  (A. Seifert, personal communication, June, 01, 2017). ~~In order to avoid unreasonably small or large mean masses  $\bar{m} = q_i/n$ , a lower limit  $m_{min} = 10^{-12}$  kg and upper limit  $m_{max} = 10^{-6}$  kg are introduced. If  $\bar{m}$  lies outside the interval  $[m_{min}, m_{max}]$  in a grid box, the ice crystal number concentration is increased to  $q_i/m_{min}$  or reduced to  $q_i/m_{max}$ , respectively. The limits correspond to sizes  $L_{min} = 17.5 \mu\text{m}$  and  $L_{max} = 3800 \mu\text{m}$ . are valid in the size range  $[L_{min} = 17.5 \mu\text{m}, L_{max} = 3800 \mu\text{m}]$ .~~

The treatment of contrail ice is analogous to that of natural cirrus with only a few modifications. ~~For the contrail ice class, the nucleation~~ Nucleation is switched off in the contrail ice class. Instead, the generation of contrail ice depends on air traffic and the atmospheric state and is explained in section 3.1.

As mentioned before, most ice crystals in contrails are smaller than in natural cirrus. ~~We use a smaller lower limit  $m_{min} = 10^{-15}$  kg and employ a different mass-size relation which guarantees and different values for  $a_{geo}$  and  $b_{geo}$  (values are given in the appendix) assure~~ reasonable aspect ratios, also for small ice crystals. ~~For this, we use a piece-wise definition of  $a_{geo}$  and  $b_{geo}$  (Spichtinger and Gierens, 2009; Heymsfield and Iaquinta, 2000). For masses above  $m_{split} = 2.15 \times 10^{-13}$  kg (corresponds to  $L_{split} = 7.42 \mu\text{m}$ ),  $a_{geo,con} = 0.04142$  and  $b_{geo,con} = 2.2$  are used. For masses below  $m_{split}$ ,  $a_{geo,con} = 526.1$  and  $b_{geo,con} = 3.0$~~

is prescribed which defines quasi-spherical hexagonal columns with aspect ratio 1 (see derivation in Spichtinger and Gierens, 2009). The upper down to sizes of  $L_{\min} = 1.24 \mu\text{m}$ . The upper size limit is set to a relatively small value of  $m_{\max} = 2 \times 10^{-11} \text{ kg}$  and the treatment of grid boxes with too large mean masses is different compared to the cirrus ice class. Instead of bounding  $n$ ,  $L_{\max} = 58 \mu\text{m}$ . If the mean ice crystal size in a grid box exceeds  $L_{\max}$ , then the total ice crystal mass and number from such a grid box are transferred from the contrail ice class to the cirrus ice class. This is reasonable, as contrails show distinct bi-modal size spectra with many small ice crystals with sizes around  $10 \mu\text{m}$  and fewer large ice crystals in the fall streaks (Unterstrasser et al., 2016a; Lewellen et al., 2014)(Unterstrasser et al., 2017a; Lewellen et al., 2014). The contrail ice class contains predominantly small ice crystals and the cirrus ice class allows for larger ice crystals that may also stem from aged contrails or contrail fall streaks. Using the new mass-size relation, the limits for  $\bar{m}$  correspond to size  $L_{\min} = 1.24 \mu\text{m}$  and  $L_{\max} = 58 \mu\text{m}$ . One drawback of this approach is that the anthropogenic contribution in the cirrus ice class cannot be directly determined. Instead, we analyze the differences in the cirrus ice class between simulations with and without air traffic. This indirect quantification of the aged contrail contribution could be circumvented by introducing further contrail ice classes and may be implemented in the future.

The sedimentation parameterization and other components are as in the cirrus ice class.

The introduction of a second ice cloud class leads to a more complex behavior as both ice cloud classes are coupled and interact with each other in several ways. They are directly coupled via the collection process (see appendix) and the mass transfer of large contrail ice crystals as described above. Moreover, they interact indirectly via the competition for the available water vapor and possibly via dynamical changes through diabatic processes.

For a first illustration of our approach, Fig. 1 shows average size distributions (ASD) of a simulation with and without air traffic. Each ASD is a superposition of local  $\Gamma$ -distributions. In this example, the contrails are at most 4 hours old. More details on the simulation setup follow in section 4.1. The solid blue line shows the contrail ice class which has a peak at sizes around  $20 \mu\text{m}$ . A less pronounced maximum is located at about  $2 \mu\text{m}$ . The contribution of aged contrails becomes apparent by comparing the two dashed lines. Those show the cirrus ice class ASDs of a simulation with air traffic (blue) and without air traffic (green). Apparently, the anthropogenic contribution is substantial, in particular in terms of total number. The ice crystals in aged contrails are on average smaller than in natural cirrus and the peak size of the SD is shifted to a smaller value.

## 2.2 The Radiation Scheme

The atmospheric radiative fluxes in the COSMO-ART model are calculated using the GRAALS (General Radiative Algorithm Adapted to Linear-type Solutions) radiation scheme (Ritter and Geleyn, 1992). The algorithm needs as several input quantities such as temperature, pressure thickness of the model layers, trace gas concentrations, as well as the cloud cover and the mass mixing ratio for each hydrometeor class considered (Ritter and Geleyn, 1992).

To include contrails and contrail cirrus into the radiative algorithm, we include a contrail ice cloud cover determined from the contrail and contrail cirrus ice class mass mixing ratio. Grid cells, where their the ice mass mixing ratio exceeds  $10^{-8} \text{ kg kg}^{-1}$ – $10^{-8} \text{ kg kg}^{-1}$  are considered to be covered with contrails or contrail cirrus. The same threshold value is used in Seifert and Beheng (2006) for grid-scale natural ice clouds. As mentioned before, the aviation contribution to the natural cirrus

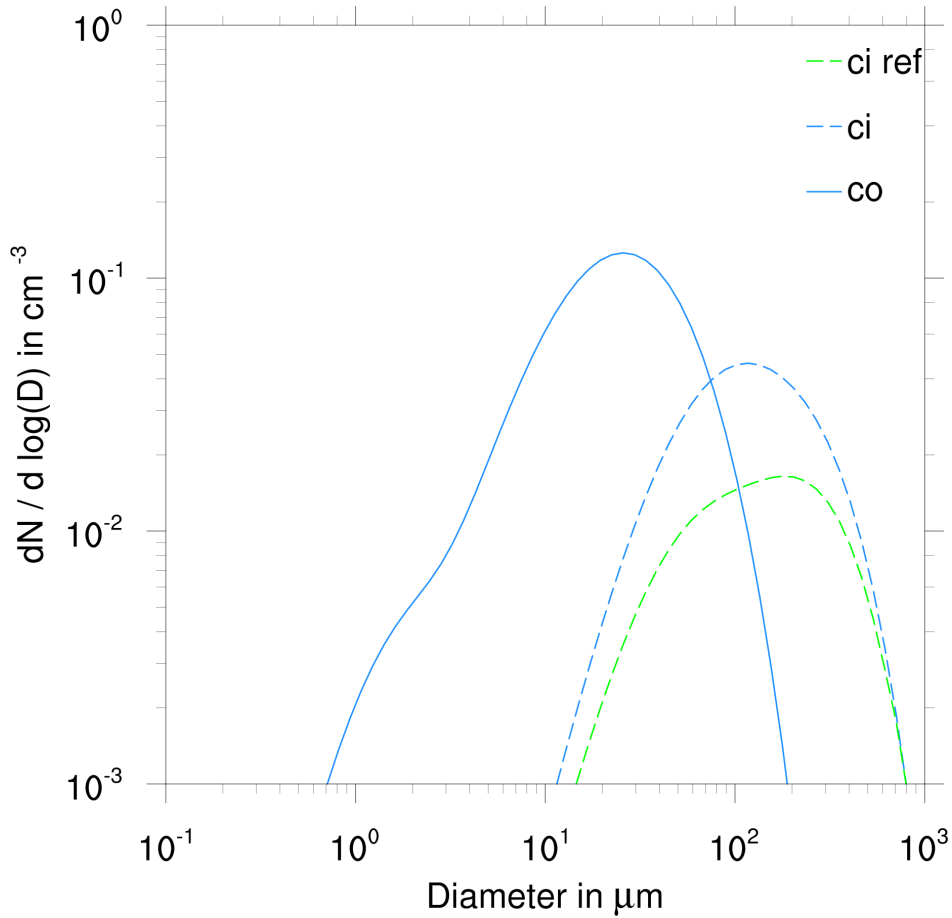


**Figure 1.** Ice crystal size distribution of the simulation with (blue) and without (green) aviation. For the simulation with aviation, separate ASDs of the contrail and cirrus ~~cloud~~-ice class are shown (solid and dotted line). 12 UTC.

ice class can only be determined by comparison with the reference simulation.

Within the radiative algorithm, optical properties of hydrometeors are calculated. These are the mass specific extinction coefficient, single scattering albedo, asymmetry factor and the forward peak of the phase function. For ice clouds, the parameterizations following Fu et al. (1998) and Key et al. (2002) are used. Because they are optimized for natural ice clouds, the scheme  
 5 computes reliable values for effective radii  $r_e$  between 5 and 60  $\mu\text{m}$  (Fu et al., 1998), whereas for ice crystal populations with radii smaller than 5  $\mu\text{m}$ , the parameterization is not well defined. Ice crystals in young contrails often have effective radii smaller than 5  $\mu\text{m}$ . To overcome this problem, we are using the parameterization of Fu et al. (1998) and Key et al. (2002), but we prescribe a lower limit of 5  $\mu\text{m}$  for the calculation of the optical properties. For  $q_i$ , no limit is prescribed; instead, the simulated  $q_i$  is used to calculate the optical properties of the ice crystals. As the radiation scheme uses  $q_i$  and  $r_e$  for determining  
 10 the radiative fluxes, implicitly fewer but larger crystals are assumed here. The extinction due to small ice crystals is expected

to be larger than that for larger ones. Therefore, in our study, the radiative effect of young contrails may be underestimated. The calculation of the contrail effective radii follows Fu et al. (1998). Here, the ice crystals are assumed to be randomly oriented, hexagonal columns.

$$r_e = \frac{1}{2} \left( \int_0^\infty D^2 L f_L(L) dL \right) \left( \int_0^\infty \left( DL + \frac{\sqrt{3}}{4} D^2 \right) f_L(L) dL \right)^{-1} \quad (3)$$

- 5  $D$  denotes the half width of an ice crystal which is implicitly given by the mass size relation (see Eq. B2). The size distribution  $f_L$  is related to the mass distribution  $f(m)$  via the transformation property  $f_L(L)dL = f(m(L))dm$ . One can show that  $f_L(L)$  (= number concentration per size range) follows a generalized  $\Gamma$ -distribution, if  $f(m)$  (= number concentration per mass range) does so and the mass size relation is a [potential function-power law](#) (see Eqs. B3 and B4).  
[Other parameterizations exist that can compute reliable values for optical properties of small ice crystals with sizes down to](#)  
10 [0.2  \$\mu\text{m}\$  \(Bi and Yang, 2017\). For future studies, using such an approach clearly could overcome the necessity of the threshold described above.](#)

### 3 Formation of Contrails

For the description of contrails, the first step is to check whether the environmental conditions are favorable for the formation of contrails. Here, the Schmidt-Appleman-Criterion (Schumann, 1996) is used which defines a threshold temperature below  
15 which contrail formation occurs.

In the second step, the source term of contrail ice mass and number has to be calculated. The parameterization used to calculate those source terms is described in detail in Unterstrasser (2016).

#### 3.1 Initial Values for Contrails

Microphysical properties of [aged](#) contrails depend a lot more on the number of ice crystals than on the ice mass after the  
20 vortex phase (Unterstrasser and Gierens, 2010b). [The initial ice mass is of minor importance, as the later growth of contrail ice crystals and the related ice mass evolution in a persistent contrail is mainly controlled by the ambient water vapor supply. On the other hand, the ice crystal number changes only slowly in a long-living contrail. Hence, its initial value determines the typical ice crystal sizes in the evolving contrail-cirrus \(for a given environmentally controlled ice mass\), which affects the radiative properties and the sedimentation-related life cycle.](#)

25 Therefore, it is appropriate to explicitly prescribe an initial ice crystal number concentration instead of an initial ice mass. The presented procedure is applied at each model time step and for each grid cell, given that both an aircraft is present and the Schmidt-Appleman-Criterion is simultaneously fulfilled.

The parameterization provides ice crystal numbers for contrails that are about 5 minutes old. As meteorological input parameters, it requires the temperature  $T$  at cruise altitude, the ambient relative humidity with respect to ice  $RH_i$  and the Brunt-Väisälä

frequency  $N_{BV}$ . Furthermore, aircraft properties are characterized by the water vapor emission  $I_0$ , an 'emission' index for ice crystals  $EI_{iceno}$  and the wing span  $b_{span}$ .

We determine  $I_0$  for medium fuel flow at cruise conditions as assumed in Unterstrasser and Görsch (2014). Here, a simple parabolic fit for  $I_0$  depending on the wing span  $b_{span}$  is used (Unterstrasser, 2016). Information on the wing span is available in  
 5 the flight track data (see section 3.2).

$$I_0 = c_1 \left( \frac{b_{span}}{c_2} \right)^2; \quad c_1 = 0.02 \text{ kg m}^{-1}; \quad c_2 = 80 \text{ m} \quad (4)$$

In this study only the most common JET-A fuel is assumed to be used; therefore  $EI_{iceno}$  is set to  $2.8 \times 10^{14} \text{ kg}^{-1}$  [following Unterstrasser \(2014\)](#).

The total number of ice crystals formed in the beginning,  $N_0$ , is calculated using the following equation:

$$10 \quad N_0 = \frac{I_0}{EI_{H2O}} EI_{iceno} \quad (5)$$

with water vapor emission index  $EI_{H2O} = 1.25$ . Note that  $EI_{iceno}$  is not reduced when the ambient temperature is only slightly below threshold temperature, even though in such situations fewer ice crystals would form (Kärcher et al., 2015).

The descending movement of the primary wake of an aircraft causes adiabatic heating within the plume. Due to this, sublimation and loss of ice crystals occurs, even in a supersaturated environment (e.g. Unterstrasser, 2016). As the spatial and  
 15 temporal resolution of the model is too coarse to simulate these processes, the fraction of ice crystals surviving the vortex phase is parameterized by a loss factor  $\lambda_{Ns}$ . Details can be found in Unterstrasser (2016). The total number of surviving ice crystals per flight path  $N_s$  is calculated with:

$$N_s = N_0 \lambda_{Ns} \quad (6)$$

For the initial ice mass produced, the water vapor emission  $I_0$  is used. The values for the produced ice mass and ice crystal  
 20 number per flight distance are distributed equally on all grid cells, the aircraft passes within a time step:

$$n_{init} = \frac{N_s d}{V_{cell}}; \quad q_{init} = \frac{I_0 d}{V_{cell}} \quad (7)$$

Here,  $V_{cell}$  denotes the volume of the grid cells,  $d$  is the flight distance within a grid box.

In global models, contrail parameterizations usually contain further prognostic equations that describe in some way the bulk contrail geometry (e.g. fractional cloud coverage or even some measure of contrail depth). In our approach, we assume that contrail ice crystals always populate the whole grid box as the horizontal scale is much smaller than in GCMs. In the vertical direction, it is ~~reasonable to assume~~ assumed that ice crystals are distributed over the whole grid layer. Close to the  
5 ground, the vertical grid size is about 10 m and increases to 300 m at the tropopause. In supersaturated conditions, contrail depth varies between ~~200 m and 600 m~~ 100 m and 500 m (mostly depending on aircraft type and stratification) and is similar to the depth of the grid layer. In the horizontal plane, the simplifications could have a larger effect. If few flight routes transect a grid box and the segments are in total  $d_{AT} = 10$  km long then this implicitly results in an hypothetical initial contrail width of  $\frac{2.8 \times 2.8}{10}$  km  $\approx 800$  m. This is larger than what is typically observed for 5 minute old contrails and better fits to 15 minute  
10 contrails (Freudenthaler et al., 1995). Hence, disregarding fractional coverage smears out the initialized contrails to some extent.

### 3.2 Determination of Flight Tracks

In contrast to most of the previously mentioned global modeling studies, this study uses a new and recently derived data set. Rather than statistical calculations for globally averaged fuel consumption, or radar data, the basic data consist of ~~exact flight~~  
15 ~~trajectories~~ traffic waypoint information over a limited area ~~that are recorded from real-time-based data (flightradar24.com, 2015)~~ ~~-In addition to time, height and geographical position of the aircraft, information on aircraft type and current velocity is also available.~~ ~~In this study, besides position and time, we only use the wing span  $b_{span}$  as recorded from ADS-B<sup>4</sup> transponders on the plane (flightradar24.com, 2015).~~ The ADS-B data is obtained mainly from flightradar24.com (2015). The DLR holds a historic data file that can be purchased from flightradar24.com (2015). This data is cleaned and combined with the input of the Official  
20 Airline Guide Database that is also hold by DLR. From this information, a dataset is compiled containing spatially and temporally resolved information on geographical position, height, current velocity and type of aircrafts. For reasons of efficiency, the information on geographical position is interpolated to fit onto the grid of the model. As a proxy for the aircraft emission parameters (see section 3.1) ~~-, the wing span  $b_{span}$  is used.~~  
25 2013. The trajectories of all flights during this period are displayed in Fig. 2.

## 4 Case Study

To test the methods described in the previous sections, a case study was performed. For this purpose, a situation over Germany with a high density of contrails in an otherwise cloud-free environment was chosen as the simulation period.

---

<sup>4</sup>Automatic Dependent Surveillance - Broadcast

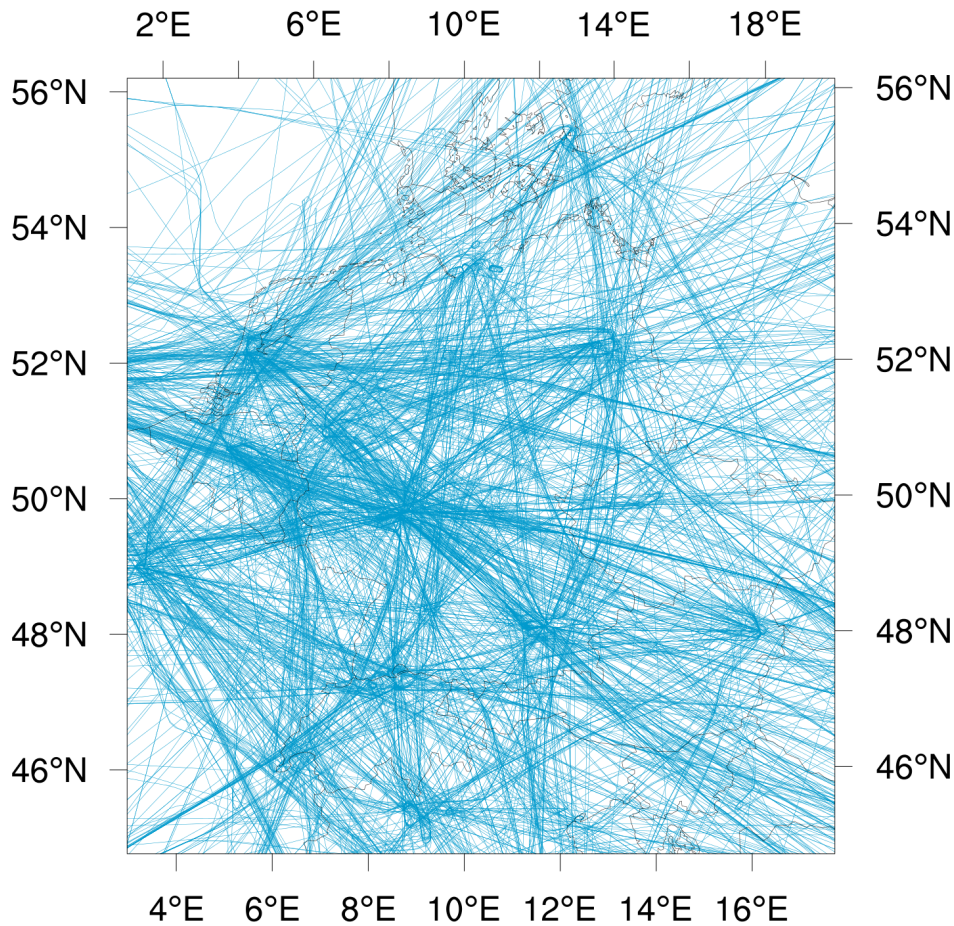


**Figure 2.** Flight trajectories for the [COSMO-DE-simulated](#) domain derived from ADS-B data (08 UTC - 16 UTC 3 December 2013). Each trajectory is plotted as a faint dashed line. Seemingly solid or thick lines are indicative of multiple overlaid trajectories.

#### 4.1 Model Setup

On 3 December 2013, the meteorological conditions over Central Europe were favorable for the formation of contrails. Additionally, the natural high-cloud coverage was relatively low, thus allowing for the identification of contrails on satellite images. For the case study, two simulations were conducted, both running for 24 hours, starting on 3 December 2013, 00 UTC. They use a horizontal  $2.8 \times 2.8$  km grid and 60 vertical levels, resulting in a mean distance between the model layers of 300 m in the upper troposphere and 15 m in the lowest model layer. For boundary data, hourly COSMO re-analyses were used. In the reference run, air traffic is turned off and the cirrus [cloud-ice](#) class is the only ice cloud class to be active. For the run with air traffic, which we call aviation simulation, the previously explained configuration with two ice cloud classes is employed. Air traffic is switched on at 08 UTC and the two simulations evolve identically up to this point. Practically, a spin up phase shorter

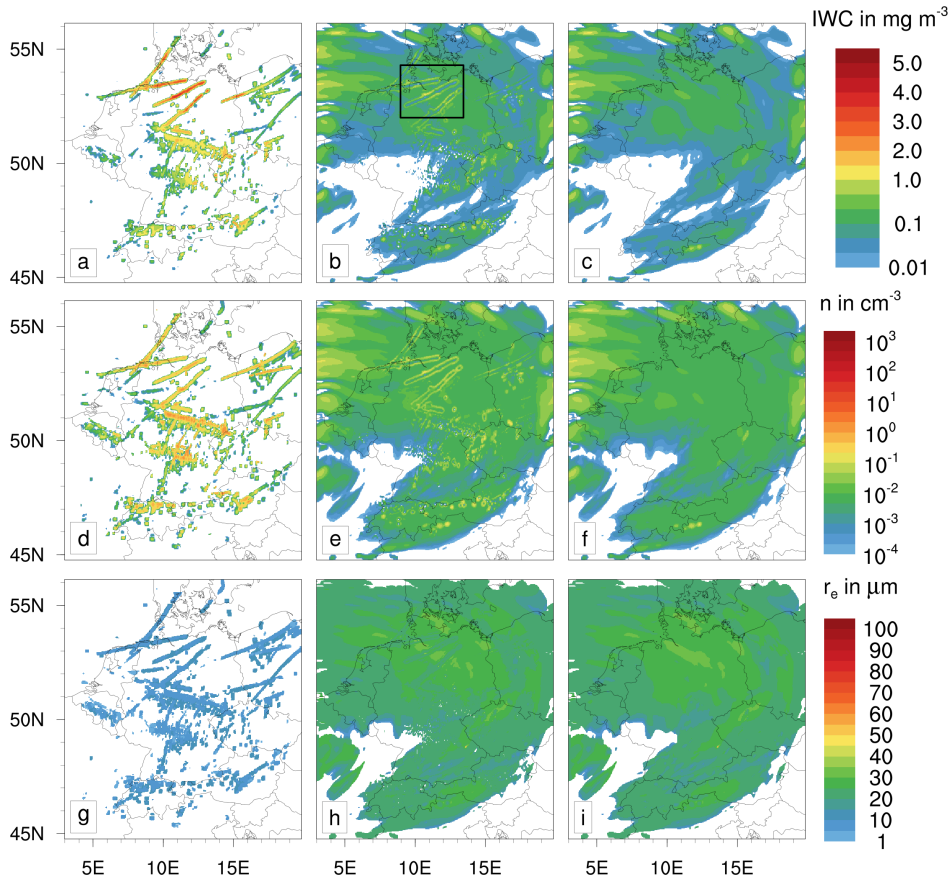


**Figure 3.** Various ice cloud properties are depicted for 10 UTC at an altitude of 11900 m (top row: ice water content; center row: ice crystal number concentration; bottom row: effective radii). Depicted are the simulation with aviation (left column: contrail `ice` class; middle column: cirrus `cloud-ice` class) and without aviation (right column).

than 8 h could have been used, but from an operational point of view it was simpler to start the simulations at 00 UTC. As the data set of flight trajectories contains no information about air traffic after 16 UTC, no new contrails form after this time.

## 4.2 Simulated Contrail Properties

The contrail treatment in the microphysics scheme is designed such that contrail-induced changes occur both in the newly introduced contrail `cloud-ice` class and in the existing cirrus `cloud-ice` class. The contribution of young contrails can be directly assessed by evaluating the contrail `cloud-ice` class. The contribution of aged contrails is found by comparing the cirrus `cloud-ice` class of the aviation simulation and of the reference simulation.

Figure 3 shows ice cloud properties over Central Europe in the model layer centered at  $z = 11900$  m, at 10 UTC. The various rows (from top to bottom) show the ice water content  $IWC$ , the ice crystal number concentration  $N_n$ , and the effective radius  $r_e$ . The left column shows the contrail `cloud-ice` class of the aviation simulation, whereas the middle and right columns show

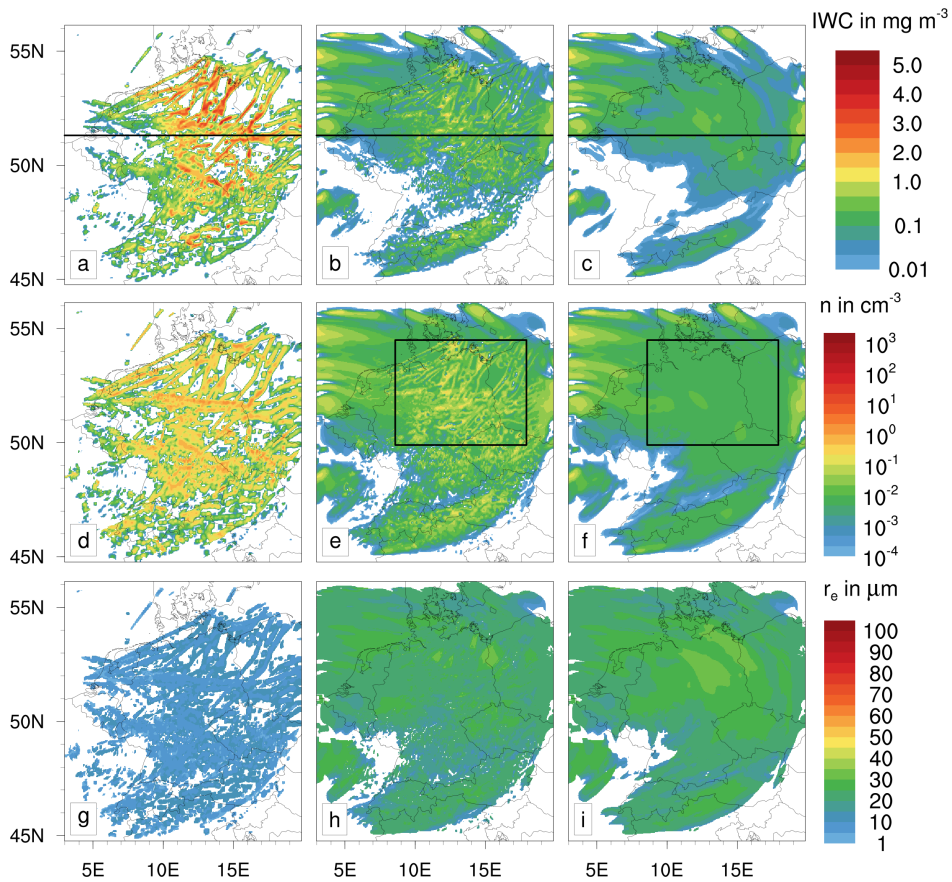


**Figure 4.** Analogous to Fig. 3, now for 12 UTC. The black horizontal lines indicate the location of the curtain displayed in Figs. 5 and 7; black boxes are discussed in the text.

the cirrus [cloud-ice](#) class of the aviation and the reference simulation. At this time, contrails are at most two hours old and mostly consist of numerous very small ice crystals.

Independent of the considered quantity, the contrail [cloud-ice](#) class features mostly line-shaped structures. The *IWC* reaches values up to  $5 \text{ mg m}^{-3}$ , which is larger than in the simulated natural cirrus. This hints at an accumulation of emitted water vapor additional to the ambient supersaturation. Furthermore, the absolute humidity at the heights considered is relatively low. Therefore, the *IWC* of natural cirrus is small and cirrus clouds are very thin and almost invisible. The ice crystal number concentrations often lie between  $1 \text{ cm}^{-3}$  and  $100 \text{ cm}^{-3}$  and can exceed those in natural cirrus by a factor of up to 1000. Consequently, the ice crystal effective radii in contrails are much smaller and lie below  $10 \text{ }\mu\text{m}$ .

The middle panel in Figure 4 shows that the most dense contrails over Northern Germany already leave a mark in the cirrus [cloud-ice](#) class (see black box in panel b)). Notably, each line-shaped structure in the left panel corresponds to a pair of lines in the middle panel. This indicates growth of ice crystals particularly at the margins where the contrail ice mass is soon transferred to the cirrus [cloud-ice](#) class. Consistently, large-eddy simulation studies ([Unterstrasser and Gierens, 2010a](#); [Lewellen et al., 2014](#))

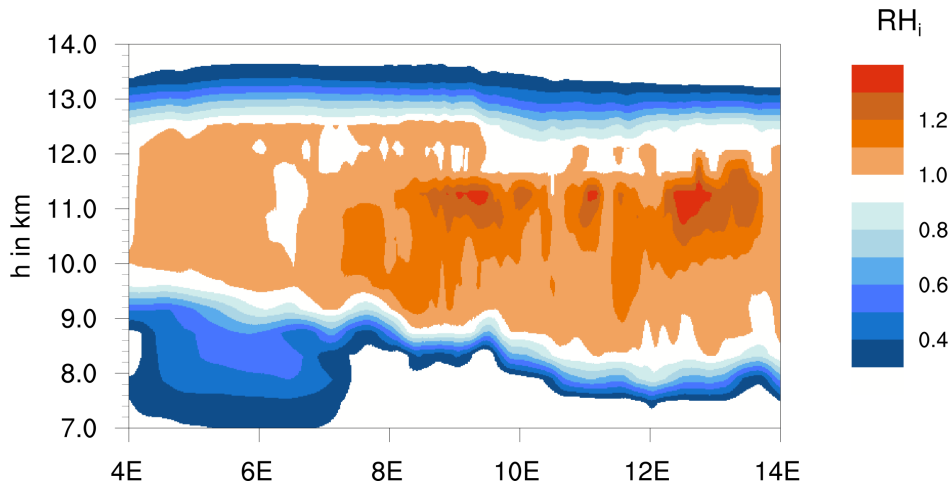


**Figure 5.** Vertical cross section of relative humidity  $RH_i$  at 12 UTC along the black line in Fig. 4.

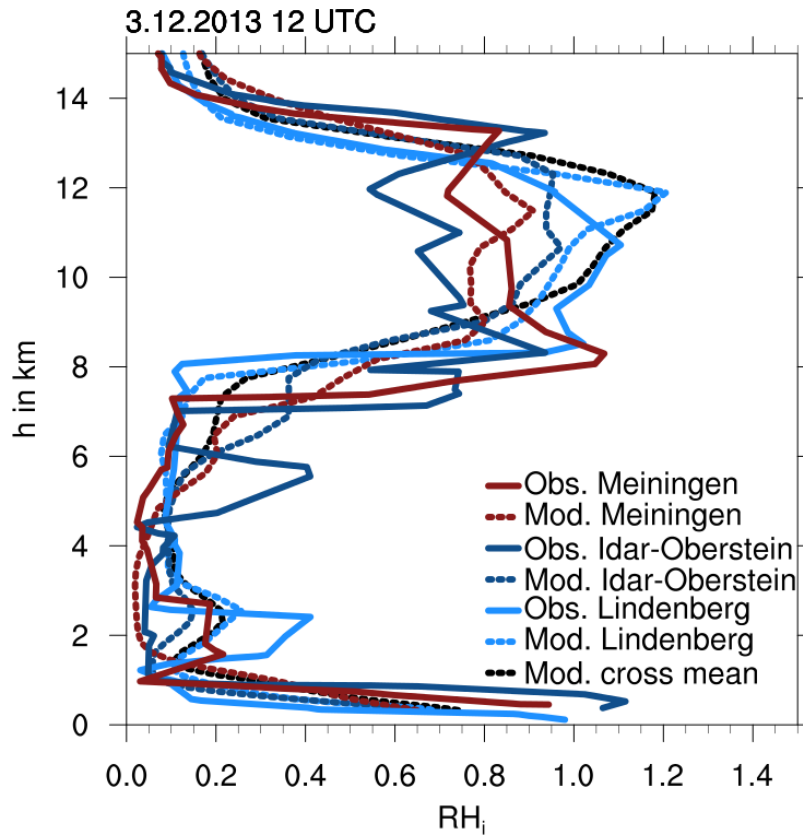


**Figure 6.** [Radio soundings for several locations \(solid lines\) \(UWYO, 2018\) and corresponding profiles from aviation simulation \(dotted lines\) of relative humidity  \$RH\_i\$ . The black dotted line are mean values along the black line in Fig. 4.](#)

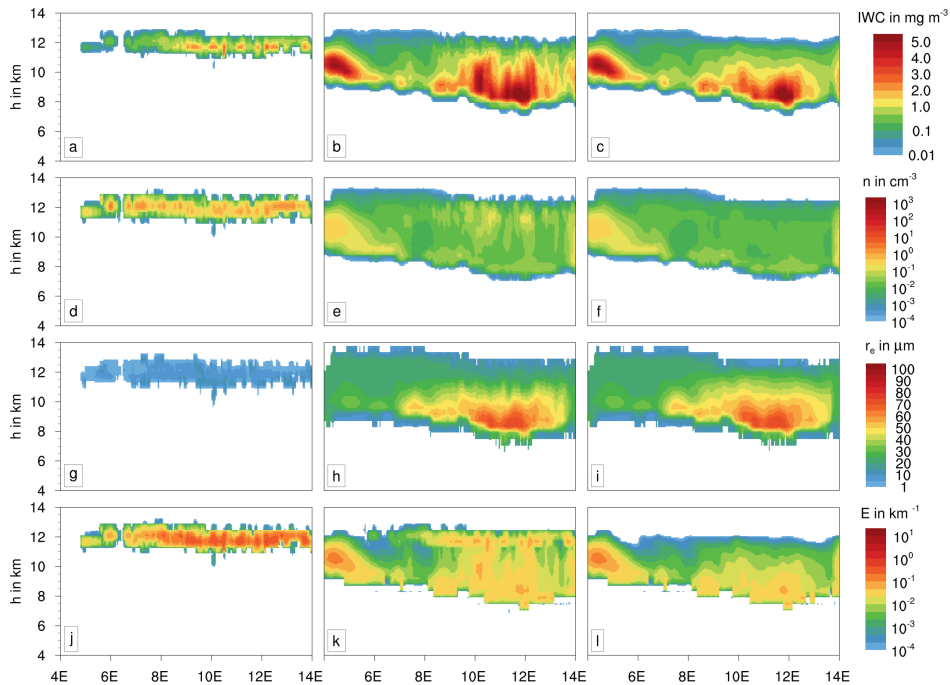


**Figure 7.** Vertical cross section of various contrail properties at 12 UTC along the black line in Fig. 4: ice water content, ice crystal number concentration, effective radius, and extinction coefficient (from top to bottom). Depicted are the simulation with aviation (left column: contrail ice class; middle column: cirrus cloud-ice class) and without aviation (right column).

and in-situ measurements (Petzold et al., 1997; Heymsfield et al., 1998) indicate the strongest growth at the edges of a contrail (Unterstrasser and Gierens, 2010a; Lewellen et al., 2014). A closer inspection (not shown) reveals that each line-shaped structure in the aforementioned box consists of several contrails. Those were produced by several aircraft that fly along the same route with short time separations.

- 5 Nevertheless, the  $IWC$ ,  $Nn$  and  $r_e$ -values of the aged contrails and the surrounding natural cirrus shown in Fig. 3 are similar. Figure 4 shows the situation at 12 UTC, analogous to Fig. 3 for 10 UTC. As time progresses, existing contrails continue to grow and further contrails are generated. Four hours after air traffic was activated in the model, a major part of the model layer is filled with contrails (left panel). Line-shaped patterns are still identifiable in some places, particularly over Northern Germany. South of  $52^\circ\text{N}$  many contrails overlap and represent a huge contrail cluster. Based on their visual appearance, no
- 10 clear distinction from natural cirrus would be possible.

Those contrail clusters still feature high  $IWC$ , high  $Nn$ , and low  $r_e$  values comparable to those two hours earlier and distinct to the surrounding natural cirrus. Moreover, we find lots of aged contrails over Germany (black box in middle panel), a region that is basically cirrus-free if there is no air traffic (black box in right panel). ~~Again, the properties of the aged contrails and the natural cirrus around Germany are similar.~~ Here, local enhancements in both  $IWC$  and  $n$  occur in the cirrus ice class, where

- 15 aged contrails are transferred to (Fig. 4e), compared to the reference simulation (Fig. 4f).

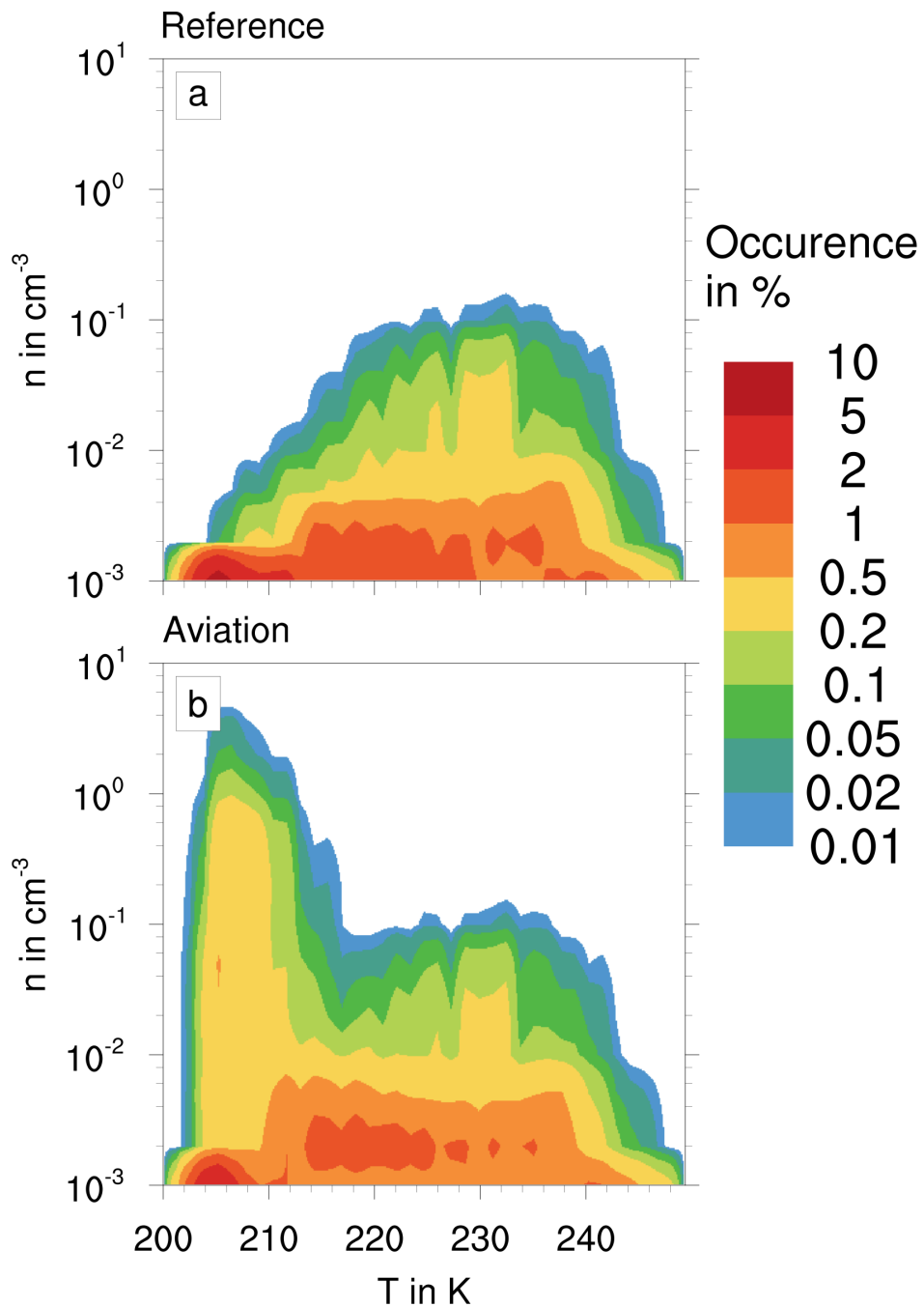


**Figure 8.** Relative occurrence of ice crystal number concentration versus temperature for natural cirrus, contrail and contrail cirrus at 12 UTC for the cross section along the black line in Fig. 4; a) reference simulation; b) aviation simulation.

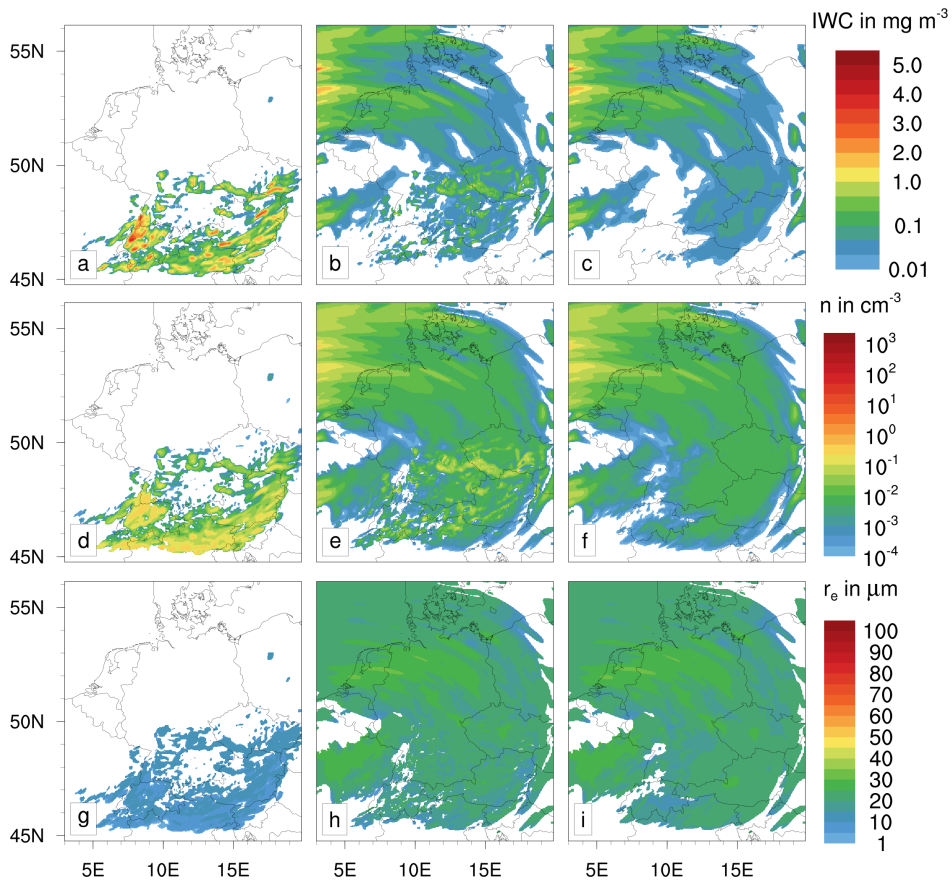


**Figure 9.** Analogous to Fig. 3, now for 20 UTC

The results indicate that, in observations, microphysical criteria may help to separate at least young contrails from natural cirrus. In general, contrail fall streaks and aged contrails ~~can not~~ cannot be identified as such once their linear shape is lost or masked. [Unterstrasser et al. \(2016b\)](#) [Unterstrasser et al. \(2017b\)](#) shows that natural cirrus that forms in high-updraft scenarios can have ice crystal numbers similar to those of young contrails, which renders even the separation between young contrails and natural cirrus impossible. Moreover, they show that contrails that become embedded in natural cirrus have large volumes where ice crystals of both ~~origin~~ origins co-exist. Hence, it is no longer meaningful to try to draw a strict separation line between natural cirrus and the anthropogenic cloud contribution.

Next, we analyze vertical distributions along the black line depicted in Fig. 4. Fig. 5 displays the relative humidity  $RH_i$  and reveals a remarkably thick layer with strong supersaturation ([maximum value: 1.34](#)) that extends over the complete east-west extent of the model domain. The layer depth increases from 2.5 km in the west to more than 4 km in the east. These are generally very favorable conditions for the persistence and spreading of contrails.

[The fidelity of such high values of  \$RH\_i\$  is corroborated by a comparison with observations. Here, vertical profiles obtained](#)

from radio soundings (UWYO, 2018) and simulated data evaluated at radiosonde stations are depicted in Fig. 6. In general, high values of  $RH_i$  are observed by radio soundings, even supersaturation occurs over Lindenberg and Meiningen. The model clearly overestimates  $RH_i$  for Idar-Oberstein, however Meiningen and Lindenberg agree quite well. Additionally, the black curve shows the mean vertical profile of the cross section displayed in Fig. 5. From this it becomes apparent that the relative humidity in the displayed cross section is remarkably high compared to the radiosonde locations. The large layer of supersaturation is caused by lifting and radiative cooling. It can persist, as natural cirrus clouds are located mostly below this layer (Fig. 7b). Also, the cirrus clouds present in the layer are too thin, i. e. occurring number concentrations are too low (Fig. 7e) to effectively reduce supersaturation.

Figure 7 shows the same ice cloud properties as Fig. 4 and additionally the extinction coefficient  $E$  at a wavelength of 1.115  $\mu\text{m}$ . Again, the left column shows the contrail ~~cloud-ice~~ class of the aviation simulation, whereas the middle and right column show the cirrus ~~cloud-ice~~ class of the aviation and the reference simulation.

In the reference simulation, natural ice is present over the entire supersaturated area. The number concentrations are mostly small, leading to optically thin cirrus clouds with extinction coefficients hardly exceeding  $10^{-2}$  to  $10^{-1}$   $\text{km}^{-1}$ . Rather large ice crystals are present throughout the supersaturated area, with the largest values of  $r_e$  found in the lower part of the cirrus around 10 to 14° E.

In the aviation simulation, it becomes obvious from the left column plots that contrails form only at altitudes between 11 km and 13 km. This is caused by the absence of air traffic below this layer. As already seen in Fig. 4a;b, the  $IWC$  is comparable to that of natural cirrus, whereas number ~~concentration-concentrations~~ reach much higher values. The effective radii in the aviation simulation are typically one order of magnitude smaller than in natural cirrus clouds and do not exceed 10  $\mu\text{m}$ . These results are in ~~reasonable~~-agreement with large-eddy studies (Unterstrasser and Gierens, 2010a; Lewellen et al., 2014) and in situ observations (Poellot et al., 1999). The numerous small crystals lead to high values for the extinction coefficient (up to 2  $\text{km}^{-1}$ ). Therefore, contrail ice is of great importance for the radiation budget.

~~In the aviation simulation,~~ In Fig. 8, the relative occurrence of ice crystal number concentrations and temperature for the cross section shown in Fig. 7 is depicted. The relative occurrence is normalized with the sum over all values. Both, reference simulation (Fig. 8a) and aviation simulation (Fig. 8b) are similar for higher temperatures (i. e. lower heights) up to 220 K. For lower temperatures, high number concentrations up to 7  $\text{cm}^{-3}$  occur in the aviation simulation, whereas number concentrations clearly decrease strongly with temperature in the reference simulation. Here, a rough comparison to measurement data can be made. In Voigt et al. (2017), mid-latitude cirrus clouds and contrails were probed in-situ during an aircraft measurement campaign. Comparing their Fig. 6(b) to Fig. 8, a similar increase in  $n$  below temperatures of about 220 K is found. Therefore, most likely, the high values occurring in the aviation simulation and not in the reference simulation, are due to aviation induced clouds.

In the aviation simulation, changes in the natural ice class can be found mainly at heights where contrails form and slightly ~~beyond. Here, local increases~~ below of it. The enhancement of ice number concentrations occurs mostly at flight levels, whereas an increase in  $IWC$  and  $N$  occur. ~~Keeping in mind the simple design of our model setup, those ice crystals represent both fall streaks of contrails as well as the transition into contrail cirrus. In both processes,~~ is found below. During the initialization,

contrail ice crystals are vertically distributed over the whole grid layer and this indirectly accounts for the initial wake vortex induced vertical expansion of a contrail. Within our simulation, the vertical structure of the contrails is determined only due to the gravitational settling of the larger ice crystals. During this process, ice crystals number concentrations tend to decrease. In contrast, only a slight increase in  $r_e$  is found. In areas where contrail ice enters the cirrus ice class, a large increase in extinction coefficient occurs. Values of the extinction coefficient are comparable to those for of the contrail ice class and reach up to can be as high as  $1 \text{ km}^{-1}$ .

After 16 UTC, no new contrails are formed-initialized in our simulation. Four hours after the end of new contrail formation, the remaining contrail ice has been advected to the southern part of domain (Fig. 9). Local patterns of increased number concentrations in the cirrus ice class are now limited to those regions, where contrail ice is still present. The line shaped structures in the contrail ice class vanish, but relatively small values for  $r_e$  are still found throughout the domain.

In the northern part of domain, the cirrus ice class is again undisturbed by aviation. Here, no remarkable differences to the reference simulation can be seen. Obviously, including contrails in our model is not able to change the properties of natural cloud ice in an extensively temporal manner.

### 4.3 Comparison with Satellite Observation

a) Cloud types (CM SAF) at 12 UTC 3 December 2013 with low (l), medium (m), high opaque (h,op) and high transparent (h,tr) clouds (for details see section 4.3):

With the exception of a In the following, satellite images (created with Global Imagery Browse Services (GIBS) NASA/GSFC/ESDIS, 2018) are shown in Fig. 10 for a qualitative assessment of the simulations. The panels a and b show the "MODIS Terra Corrected Reflectance True Color" at 10 UTC and 12 UTC for the simulated day, respectively, both with a resolution of 250 m. The "True Color" composition consists of MODIS bands 1, 4 and 3 (NASA/GSFC/ESDIS, 2018). Beside a cloud bank over the North and Baltic Seas and fog over Southern and Western Germany, a considerable number of line-shaped contrails and diffuse cirrus clouds are present across the visible satellite image of 3 December 2013 at 12 UTC (Fig. 10a). A main contrail cluster is both satellite images. Main contrail clusters are found over Central Germany for both situations. Contrails can also be identified over the Netherlands and Belgium, over the Czech Republic, and south of the Alps. Figure ?? shows the CM SAF (EUMETSAT's Satellite Application Facility on Climate Monitoring) (Schulz et al., 2009) cloud types product CTY for 3 December 2013. At 12 UTC. For simplification, the original types are grouped into low (l), medium (m), high opaque (h,op) and high transparent (h,tr) clouds. In comparison with, the rather widespread high-level cloud cover seems to have decreased compared to 10 UTC. Comparing Fig. 10a, it seems likely that large parts of the transparent high-level clouds, especially over the center and the east and Fig. 10e, obviously, the reference simulation underestimates the coverage of high clouds in the center of the domain (black box), consist of line shaped, which, in large parts, consists of contrails and contrail cirrus. The pattern of optical depth from the reference run (Fig. 10c) misses parts of the high-level transparent clouds over France and the south-eastern part of the domain in Fig. ?. These gaps are closed when contrails and contrail cirrus are included in the simulation (black box in Fig. 10b). Over these areas. Clearly, the amount of cloud cover seems to be underestimated also in the aviation simulation at 10 UTC. This discrepancy is probably due to the fact that air traffic was switched on at 08 UTC and earlier flight movements are disregarded

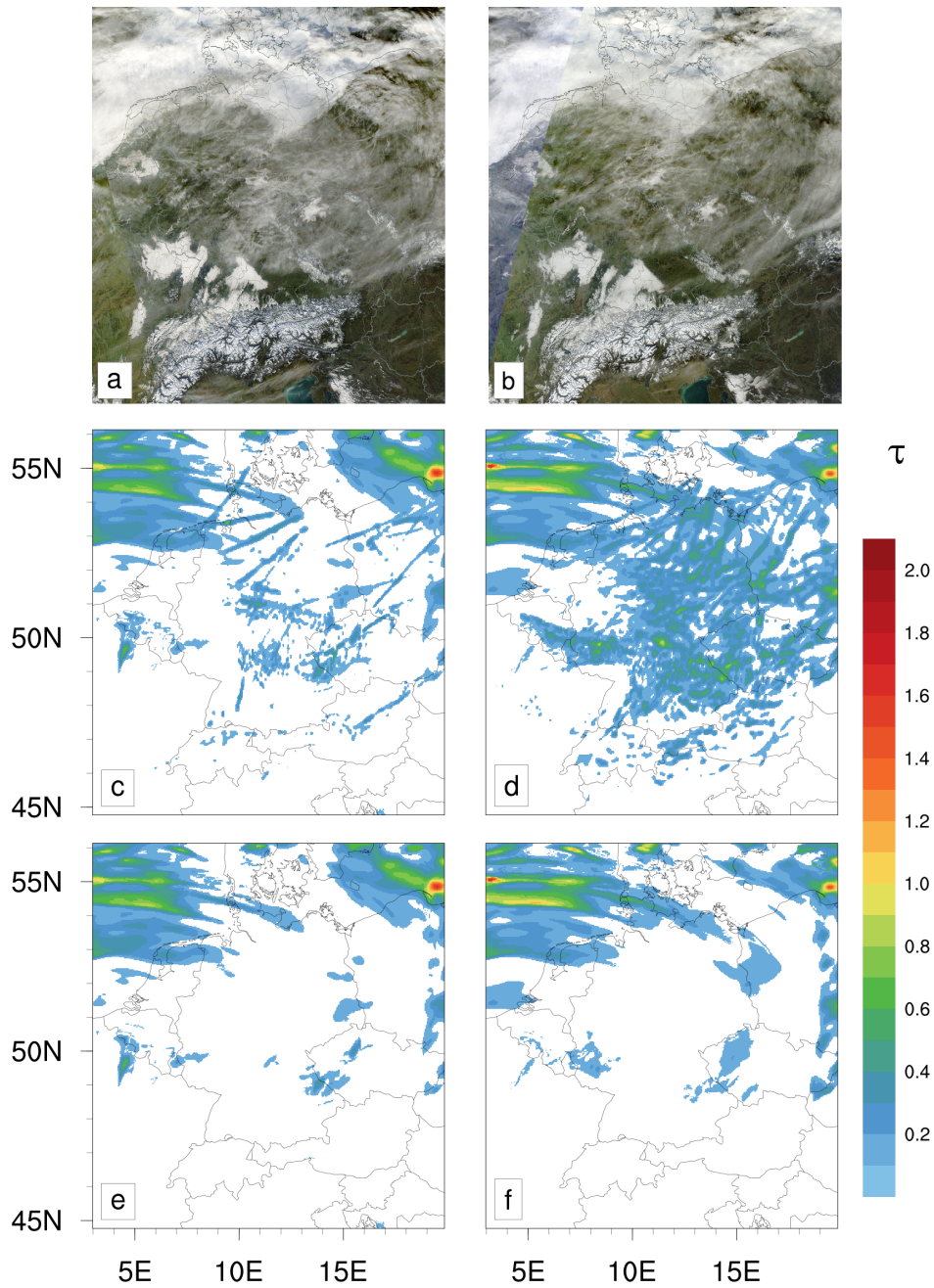


**Figure 10.** Contrails at 12 UTC Top row: a) Satellite satellite image (VISMODIS True Color - Corrected Reflectance) (DLR, 2014) (NASA/GSFC/ESDIS, 2018); b,c) center row: optical depth at  $1.115 \mu\text{m}$  of all ice clouds for the aviation simulation and d; bottom row: optical depth of all ice clouds for the reference simulation; left column: 10 UTC; right column: 12 UTC. The black box is discussed in the text.

in our simulation. Hence, the simulation including aviation produces additional clouds, seen in the patterns of increased values for optical depth at 1.115  $\mu\text{m}$  (Fig. 10b), evaluation at 10 UTC neglects all contrails older than 2 hours. The comparison at 12 UTC is more favorable and observations match much better with the aviation simulation than with the reference simulation.

5 Mostly over the center of the domain, areas with values of  $\tau$  between 0.2 to 0.6 and peaks up to 1.0 are simulated. This is in good agreement with the very high values of the extinction coefficient of contrails compared to those of natural cirrus (Fig. 7j, Fig. 7k, Fig. 7l). The line shaped patterns stem from the contrail ice class ~~and~~ the more patchy structures ~~are due to aged contrails and the contrail cirrus that has been transformed from aged contrails which have been transferred~~ to the cirrus ice class. The case study for this particular day ~~shows~~ demonstrates that the inclusion of aircraft effects in a regional weather forecast model improves the representation of high level clouds.

#### 10 4.4 Contrail Impact on Surface Radiative Fluxes

Figure 11 shows the changes in the incoming shortwave radiation (SW) at two points in time at the surface. Clearly, additional ice crystals caused by air traffic reduce the incoming SW radiation. The line-shaped structure of young contrails at 10 UTC (Fig. 3a) is reflected in similar patterns of reduced SW radiation (Fig. 11a). As ~~disussed~~ discussed earlier, the contrail ice class features numerous very small ice crystals with a high extinction coefficient. In the case investigated, this leads to a reduction in  
15 incoming SW radiation of 1 to 15  $\text{Wm}^{-2}$ . As previously mentioned, our parameterizations are not able to calculate the optical properties of ice crystals with effective radii below the threshold of 5  $\mu\text{m}$ . Rather, crystals with an effective radius of less than 5  $\mu\text{m}$  are assumed to have optical properties of crystals as large as 5  $\mu\text{m}$ . Therefore, the shading effect of the contrail ice crystals might be underestimated in our calculations.

A strong spatial increase in the shading effect is found at 12 UTC (Fig. 11b). Here, the contrail coverage reaches its maximum.  
20 Still partly line shaped contrails are found with a similar reducing impact as two hours before. Additionally, clusters of contrail ice transformed into the cirrus ice class have evolved, particularly over the center of the domain (Fig. 4b). The ice crystals herein are relatively small, but larger than those present in the contrail ice class. Therefore, they inhibit less SW radiation from reaching the ground than the ice crystals in the contrail ice class. Consequently, the reduction on SW radiation here is smaller, but still reaches 1 to 10  $\text{Wm}^{-2}$ .

25 Especially in the north of the domain, small areas with the difference in incoming SW radiation attaining large negative values adjacent to large positive values are found. They occur when subtracting e. g. fields of radiative fluxes of the aviation simulation from those of the reference simulation. The introduction of contrail ice acts as source of disturbance for various processes like convection or turbulence. Those features are to be classified as noise as they do not influence the overall situation.

Non-negligible areas with an increase in SW radiation occur, e. g. at 12 UTC over the south-eastern part of the domain  
30 (Fig. 11b). Besides only reducing the direct incoming SW radiation, contrail ice crystals also enlarge the flux of diffuse SW radiation (see below). On occasion, as the simulated contrails are still rather optically thin, this effect may be larger than the reduction of direct radiation.

The average change of incoming direct and diffuse SW for 3 December 2013 is shown in Fig. 12. Also here, the small scale fluctuating values in the north are most likely noise.

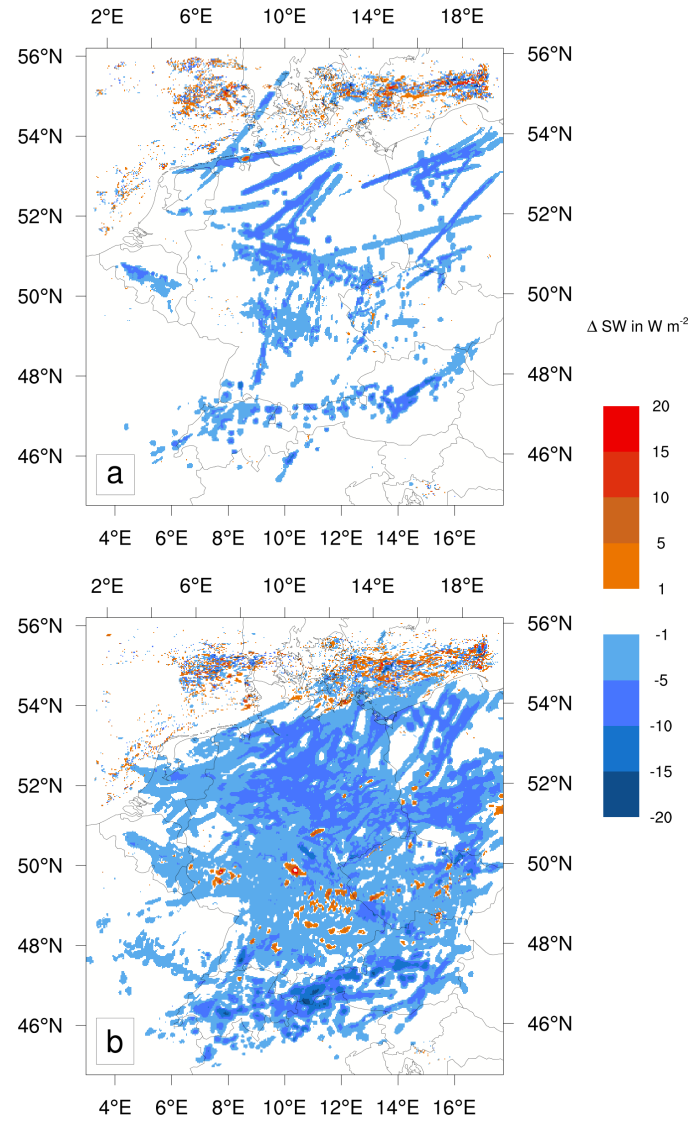


**Figure 11.** Difference in shortwave incoming radiation for aviation simulation and reference simulation for 3 December 2013 at the surface, a) 10 UTC, b) 12 UTC.

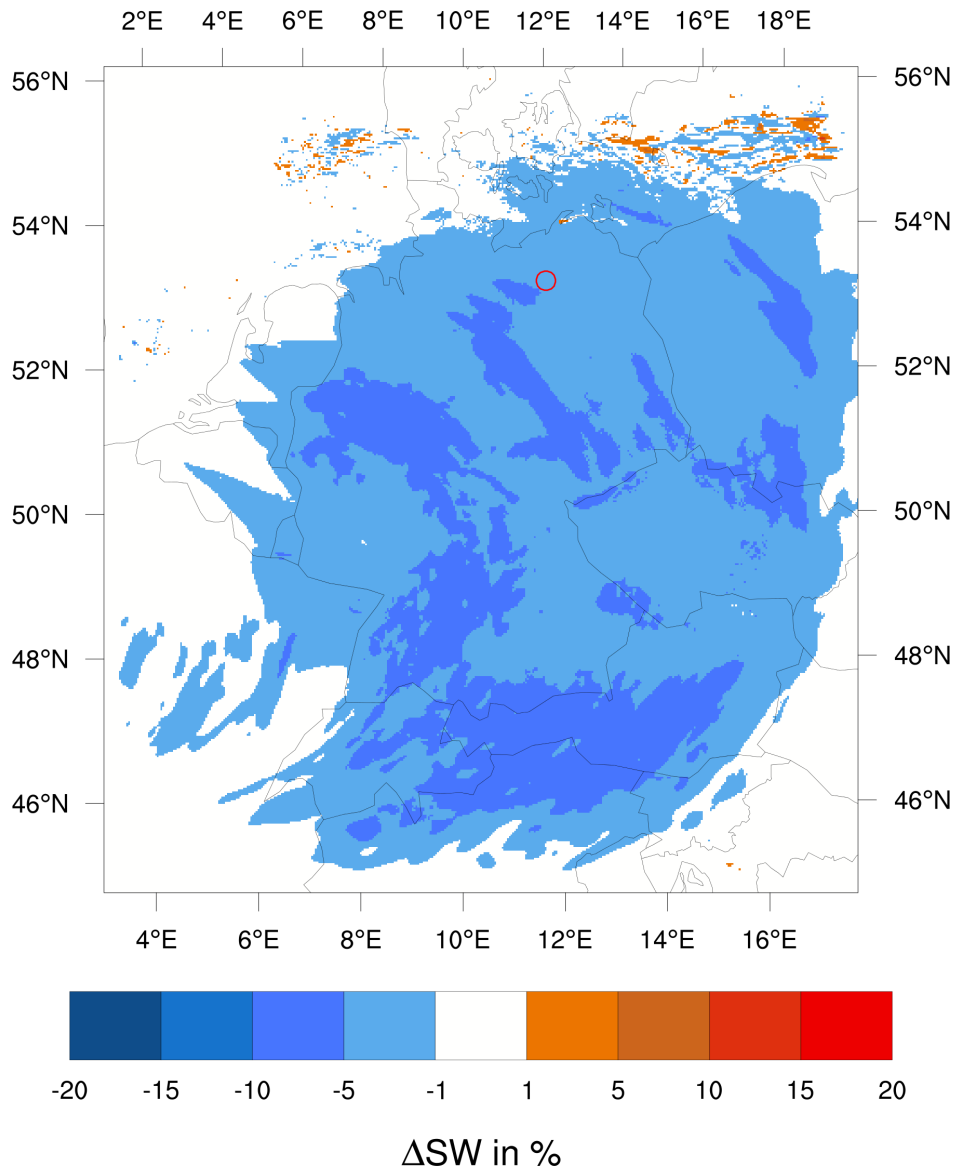


**Figure 12.** Average changes in the amount of incoming diffuse and direct solar radiation during daylight hours of 3 December 2013 at the surface (aviation simulation minus reference simulation). The red circle (53°N, 12°E) marks the location evaluated in Fig. 13.

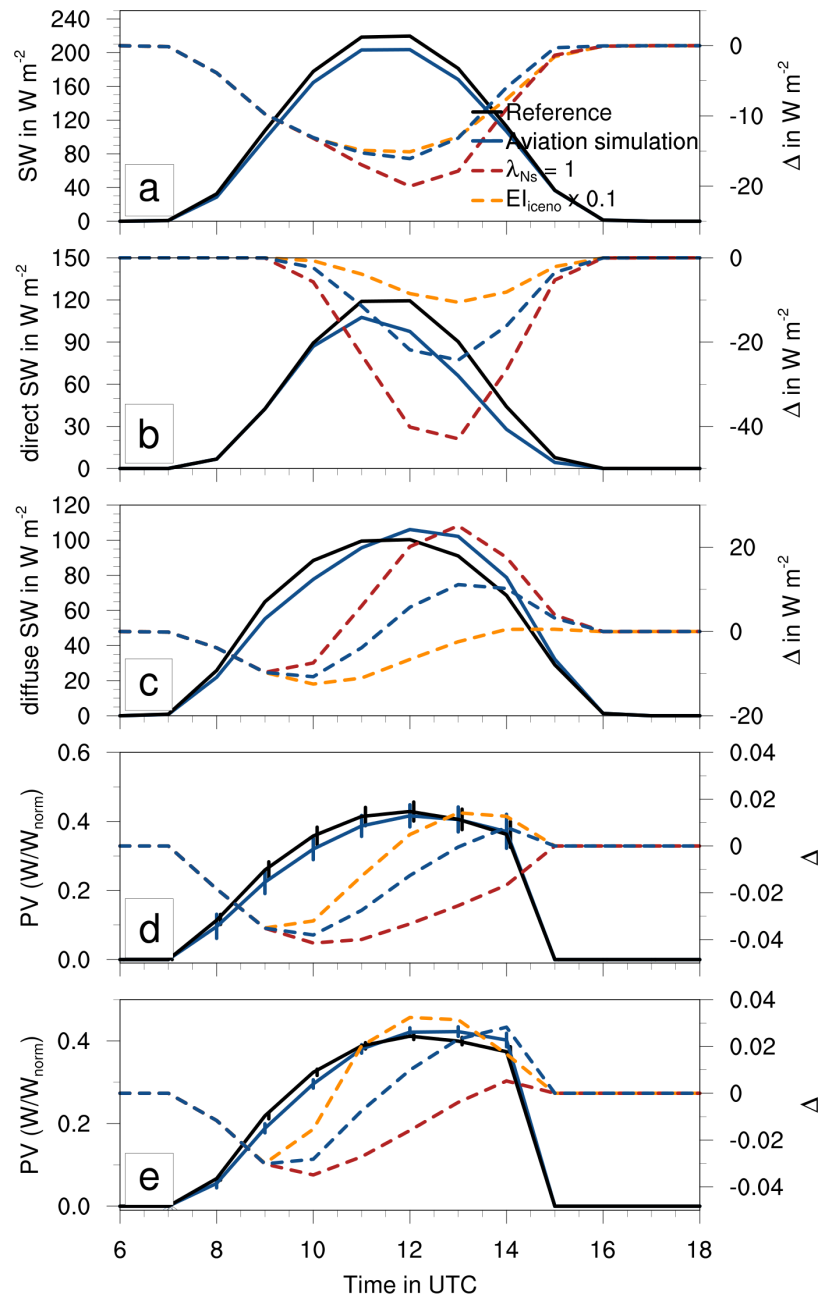


**Figure 13.** Temporal evolution for 3 December 2013 of incoming shortwave radiation: reference (black); aviation simulation as before (blue); "bio-fuel" scenario with  $EI_{iceNO} \times 0.1$  (greenorange), omission of crystal loss during contrail vortex phase with  $\lambda_{Ns} = 1$  (red); Dashed lines (corresponding to right y-Axis) are difference to reference simulation. a) total SW; b) difference in total direct SW between aviation simulation and reference simulation; c) direct diffuse SW; d) diffuse; e) normalized PV-power diffuse. a) - d) over entire domain; all-e) mean for the location marked with the red circle in Fig. 12. Error bars represent mean values +/- standard deviation.

The thin veil of contrail cirrus that spreads over most of the domain causes an average decrease of incoming direct and diffuse SW radiation of 1 to 5 %. The large and persistent contrail cluster over the northern and eastern part of the domain inhibits on average 5 to 10 % of SW radiation from reaching the ground during approximately eight hours of daylight. The reduction is strongest over the south and the west of the domain. Here, contrail ice is present for the longest time, as seen in Fig. 9.

- 5 Fig. 13 ~~a~~ shows the temporal evolution of ~~the total incoming SW radiation in and normalized PV power~~. Panels a to d represent mean values for the entire simulation domain, panel e additionally represents mean values for an area of approximately  $140\text{ km} \times 140\text{ km}$   $50\text{ km} \times 50\text{ km}$  centered at a spot in the north-eastern part of the simulated domain, indicated by the red circle ( $53^\circ\text{N}$ ,  $12^\circ\text{E}$ ) in Fig. 12. Around noon, between 10 UTC and 13 UTC~~This is the location of one of the largest solar parks in Germany (Solarpark Brandenburg-Briest). Also several other major solar parks are located around this area. For~~
- 10 enhanced clearness, values for the sensitivity study (see Sec. 4.5) are depicted only as difference to the reference simulation. The differences between the aviation simulation and the reference simulation are in general more pronounced for the selected location that on average over the entire simulation domain.
- During the whole time of daylight, contrails and contrail cirrus reduce up to  $20\text{ Wm}^{-2}$  of the  $15\text{ Wm}^{-2}$  (about 7 %) of the total incoming SW radiation in the entire domain (Fig. 13a). This is a decrease of about 7 % (Fig. 13b).~~The effect is largest in~~
- 15 the morning during noon and ceases during the day. This corresponds to the size of contrail ice crystals. As in our simulation, contrails start to form at 8-08 UTC, the average contrail ice crystal size grows during the day. Accordingly, contrail ice effective radii also increase with time and lead to ~~a~~ smaller values of the extinction coefficient. At 15 UTC, the incoming SW radiation is larger in the aviation simulation compared to the reference simulation. This is caused by the diffusive share of incoming SW radiation that is enhanced in the aviation simulation. The strongest reduction in the morning as well as the increase in SW
- 20 radiation in the afternoon occur with very small total values of total SW radiation, the effect therefore is negligible here.
- Separating the total SW radiation into its direct (Fig. 13**e**) and diffuse (Fig. 13**d**) fraction, it is clear that especially the direct incoming SW radiation is strongly reduced by up to  $30\text{ Wm}^{-2}$  more than  $20\text{ Wm}^{-2}$  due to the presence of additional ice crystals in the atmosphere. In contrast, the diffuse incoming SW radiation is increased by up to  $20\text{ Wm}^{-2}$   $10\text{ Wm}^{-2}$ . Enhanced scattering of SW radiation caused by the contrail ice crystals increases the diffuse SW radiation at the ground. Between 8-
- 25 Notably, the peak in reduction of diffuse SW radiation occurs in the afternoon, around 13 UTC. Between 08 UTC and about 10-11 UTC, the amount of diffuse SW radiation reaching the ground is larger in the aviation simulation. During this time, as mentioned before, contrail ice crystals are smallest on average and forward scattering is less pronounced than for larger crystals, whereas contrail ice crystals grow on average during the day resulting in enhanced forward scattering.
- The overall picture indicates that~~In the aviation simulation,~~ young and aged contrails generally reduce the incoming SW radiation at the surface. This effect is currently neglected in operational weather forecast models. However, this effect is of relevance for the production of solar energy. The temporal evolution of the normalized PV power is depicted in Fig. 13**e**. ~~This quantity is calculated d) and Fig. 13e. The normalized PV is calculated~~ using the open source PV modeling environment PV\_LIB for python (Andrews et al., 2014). ~~A nominal capacity is assumed, consisting of a specific~~ For a specific combination of a PV module and a PV inverter combination. ~~The tilt and orientation of the PV module as well as the~~, a nominal power and a
- 35 reasonable tilt is assumed. These technical specifications are taken from Rieger et al. (2017). They assume panels consisting

of a south-oriented PV module with a nominal power of 220W and a size of 1.7m<sup>2</sup>. Compared to the reference simulation, the normalized PV power is decreased in the aviation simulation most of the day. The largest losses ~~occur at noon and are of~~ up to 10 % ~~occur in the morning and diminish during the day, even an increase occurs for the selected location in the late afternoon~~ (Fig. 13e). The normalized PV power is somewhat more strongly reduced than the total SW radiation. For production of PV power, the incoming direct radiation is of greater importance than the diffuse; of the two, the direct experiences the larger reduction from contrails and contrail cirrus.

The error bars in Fig. 13d and Fig. 13e represent the mean values +/- the standard deviation with respect to the entire simulation domain and the area of 50 km × 50 km around the selected location, respectively. The standard deviation in Fig. 13d reflects the large-scale variability of the impact of contrails and contrail cirrus on the incoming SW radiation, whereas Fig. 13e illustrates the small-scale variability.

Compared to the selected location, standard deviations are larger for the mean of the domain. Obviously, clouds modify the amount of SW radiation reaching the ground in a non-uniform manner. The magnitudes of the standard deviations for the aviation simulation are about the same magnitude like the ones for the reference simulation. Apparently, the impact of contrails and contrail cirrus on incoming SW radiation is as variable as the impact of natural clouds. E. g., even at 12 UTC, when the impact of contrails and contrail cirrus is largest, confined areas exist, which are unaffected by contrails and contrail cirrus (Fig. 11b).

However, the small-scale variability of the impact of contrails and contrail cirrus on SW radiation is rather small, reflected by much smaller standard deviations in Fig. 13e. One can therefore deduce that the exact location of contrails or contrail cirrus is not crucial for the strength of the impact on SW radiation.

20

#### 4.5 Sensitivity to Initial Ice Crystal Number and Early Contrail Ice Crystal Loss

In this last section, we briefly examine two sensitivities of our model setup.

For the first, we reduce the emission index for ice crystals  $EI_{\text{iceno}}$  by a factor of 10 (~~green-orange~~ lines in Fig. 13). ~~In reality, the usage of biofuels that cause lower soot concentrations when combusted, would have a similar effect~~ This scenario explores lower engine soot emissions caused by either improved engine combustor technologies or fuel composition changes from, e. g., biofuel adoption (Moore et al., 2017). Due to this, the initial number concentration of contrail ice crystals is reduced, thus fewer but larger ice crystals are formed (Unterstrasser, 2014). In the simulation with reduced  $EI_{\text{iceno}}$ , the reduction of total incoming SW radiation is only slightly weaker than for the simulation assuming standard fuel (Fig. 13a, ~~Fig. 13b~~). As ice crystals are slightly larger, their extinction coefficient is lower and the reduction of direct SW radiation is smaller than for the standard setup (Fig. 13eb). Also the increase in incoming diffuse SW radiation is less strong compared to the standard setup (Fig. 13dc). Consequently, the reduction in normalized PV power is also less strong than for the standard setup, even an enhancement occurs during afternoon (Fig. 13d, Fig. 13e).

Second, we set the surviving fraction of ice crystals  $\lambda_{\text{Ns}}$  in the parameterization of the initial ice crystal number to 1. This deliberately neglects the effects of crystal loss during the contrail vortex phase, as parametrized by Unterstrasser (2016). The

influence of this parameter is large. During daytime, a reduction in total incoming SW radiation of up to 15 % is simulated (Fig. 13a, ~~Fig. 13b~~). Both the reduction in direct SW radiation as well as the increase in diffuse SW radiation are much more pronounced for this case (Fig. 13**e**, Fig. 13**d**~~c~~). Especially the reduction in direct SW radiation causes a strong reduction in production of PV power. Here, losses of nearly ~~20 % occur at noon~~ 15 % occur at about 10 UTC. Also concerning the temporal  
5 evolution, the reduction lasts much longer compared to the aviation simulation. When no early crystal loss is parametrized in the model, initial ice crystal number concentrations may be much higher than usual. As the initial *IWC* remains the same, the new crystals are smaller and thus, the simulated contrails are optically thicker. The much stronger reduction in incoming SW radiation demonstrates that the early ice crystal number loss is non-negligible and an important aspect of contrail evolution as it has a long-lasting impact on contrail-cirrus radiative properties.

## 10 5 Conclusions

In this study, the regional atmospheric model COSMO-ART coupled with a two-moment microphysical scheme and a diagnostic treatment of radiation was extended by a parameterization describing contrails and the related physical processes.

Methods for a separate but consistent treatment of contrail ice were implemented to satisfy the special requirements describing the microphysics in young contrails and the transition phase to contrail cirrus. ~~It~~ For a single case study, it was shown how

15 microphysical properties such as ice water content, ice crystal number concentration and the mean ice crystal radius of ice crystals in contrails change over time and depend on the meteorological conditions. The ice water content in young contrails is comparable to that in thin cirrus clouds ranging from 0.2 to 5.0 mg m<sup>-3</sup>, but with considerably higher ice crystal number concentrations between 1 cm<sup>-3</sup> and 100 cm<sup>-3</sup> and effective radii below 10 μm. The numerous small ice crystals produce high values for the extinction coefficient and thus also for the optical depth.

20 The transition of contrail ice into the cirrus ice class causes increasing number concentrations. Here, effective radius of the ice crystals from the contrail ice class grows to an extent comparable to that of natural cirrus. Because of the still relatively high number concentrations, contrail cirrus still features high values for both the extinction coefficient and the optical depth.

Qualitative comparison with satellite data shows good agreement and proves advantages of considering contrails and contrail cirrus in a regional weather forecast model.

25 Contrail cirrus tends to cause changes in the microphysical appearance of high-level cloud coverage to a remarkable extent, which in turn influences the radiative effect in these regions.

In addition, the impact of contrails and contrail cirrus on shortwave radiation and the production of PV power ~~was~~ were quantified. Although the case study was performed for 3 December 2013, when solar zenith angles are low and the length of days is short, a strong influence of contrails is still simulated. They inhibit up to 5 to 10 % of shortwave radiation from reaching the  
30 ground at noon. This results in a loss of PV power production of up to 10 %.

Moreover, it was demonstrated that ice crystal loss in young contrails is an important process which can significantly change the contrail-cirrus properties on a regional scale. This study is the first approach to simulate contrails and contrail cirrus using a numerical weather prediction model with high spatial and temporal resolution. Subsequently, the presented method can serve

as a basis for improving the predictability of the solar radiation in regional weather forecasting by taking into account contrails and contrail cirrus.

## Appendix A: Ice microphysical model

This section expands the description of the microphysical model from section 2.1 and presents a collection of underlying equations. All formulae can be found in Seifert and Beheng (2006) as well. Values of constants used in this section are listed in Tab. 1. The generalized  $\Gamma$ -distribution is defined as

$$f(m) = A m^\nu \exp(-\lambda m^\mu) \quad (\text{A1})$$

[Here,  \$m\$  is in units of kg.](#) The parameters  $\nu$  and  $\mu$  are assumed constant, respectively. The parameter  $A$  is related to the total ice crystal number concentration  $n = M^0$  and  $\lambda$  to the ice crystal mean mass  $\bar{m} = q_i/n = M^1/M^0$ . Expressions involving  $\Gamma$ -functions exist for the moments

$$M^k(A, \lambda) = \int_0^\infty m^k f(m; A, \lambda) dm \quad (\text{A2})$$

of order  $k$  (not shown).

The growth equation of a single ice crystal is given by (Pruppacher and Klett, 1997):

$$\frac{dm}{dt} = \frac{4\pi C(m) F_{\text{ven}}(m) S_i}{\frac{R_v T}{p_{\text{sat},i}(T) D_v} + \frac{L_{\text{iv}}}{K_T T} \left( \frac{L_{\text{iv}}}{R_v T} - 1 \right)} = 4L(m) G_{\text{iv}}(T, p) F_{\text{ven}}(m) S_i \quad (\text{A3})$$

Here,  $T$  is the temperature,  $p$  is the pressure, and  $C = D / \pi$  denotes the capacity of hexagonal crystals (Harrington et al., 1995).  $S_i$  is the supersaturation with respect to ice,  $L_{\text{iv}}$  represents the latent heat of sublimation,  $p_{\text{sat},i}$  denotes the saturation vapor pressure over ice,  $R_v$  is the specific gas constant for water vapor,  $K_T$  is the conductivity of heat, and  $D_v$  is the molecular diffusion coefficient of water vapor. The term  $F_{\text{ven}}$  accounts for ventilation effects and  $G_{\text{iv}}$  considers the diffusion of water vapor and the effect of latent heating:

$$G_{\text{iv}}(T, p) = \left[ \frac{R_v T}{p_{\text{sat},i} D_v} + \frac{L_{\text{iv}}}{K_T T} \left( \frac{L_{\text{iv}}}{R_v T} - 1 \right) \right]^{-1} \quad (\text{A4})$$

Integration of Eq. A3 over the ice crystal mass spectrum yields the temporal derivative of the ice mass density  $q_i$ :

$$\frac{\partial q_i}{\partial t} = 4G_{\text{iv}}(T, p) S_i \int_{m_{\text{min}}}^{m_{\text{max}}} D(m) F_{\text{ven}}(m) f(m) dm \quad (\text{A5})$$

Similar to the The mass-size relation (given by Eq. 2 )uses the values  $a_{\text{geo,nat}} = 1.59$  and  $b_{\text{geo,nat}} = 2.56$  for the cirrus ice class. In order to avoid unreasonably small or large mean masses  $\bar{m} = q_i/n$ , a lower limit  $m_{\text{min}} = 10^{-12}$  kg and upper limit  $m_{\text{max}} = 10^{-6}$  kg are introduced. If  $\bar{m}$  lies outside the interval  $[m_{\text{min}}, m_{\text{max}}]$  in a grid box, the ice crystal number concentration is increased to  $q_i/m_{\text{min}}$  or reduced to  $q_i/m_{\text{max}}$ , respectively. The limits correspond to sizes  $L_{\text{min}} = 17.5 \mu\text{m}$  and  $L_{\text{max}} = 3800 \mu\text{m}$ .

5 For the contrail ice class, a piecewise definition of  $a_{\text{geo}}$  and  $b_{\text{geo}}$  is employed following (Spichtinger and Gierens, 2009; Heymsfield and Iaqu... For masses above  $m_{\text{split}} = 2.15 \times 10^{-13}$  kg (corresponds to  $L_{\text{split}} = 7.42 \mu\text{m}$ ),  $a_{\text{geo,con}} = 0.04142$  and  $b_{\text{geo,con}} = 2.2$  are used. For masses below  $m_{\text{split}}$ , the  $a_{\text{geo,con}} = 526.1$  and  $b_{\text{geo,con}} = 3.0$  is prescribed which defines quasi-spherical hexagonal columns with aspect ratio 1 (see derivation in Spichtinger and Gierens, 2009). The latter constants are valid down to the prescribed lower limit  $m_{\text{min}} = 10^{-15}$  kg. For grid boxes with lower mean masses, the same bounding technique is used as in the cirrus ice

10 class. The upper limit is set to a relatively small value of  $m_{\text{max}} = 2 \times 10^{-11}$  kg and the treatment of grid boxes with too large mean masses is different compared to the cirrus ice class. Instead of bounding  $n$ , the total ice crystal mass and number from such a grid box are transferred from the contrail ice class to the cirrus ice class. The prescribed mass limits of contrail ice class correspond to the size limits  $L_{\text{min}} = 1.24 \mu\text{m}$  and  $L_{\text{max}} = 58 \mu\text{m}$ .

Similar to the mass-size relation, the terminal settling velocity  $v$  is approximated by a power law (Eq. A6) with coefficients

15  $a_{\text{vel}}$  and  $b_{\text{vel}}$ .

$$v(m) = a_{\text{vel}} m^{b_{\text{vel}}} \quad (\text{A6})$$

Integrating  $v(m)$  and  $m v(m)$  over the ice crystal mass spectrum yields mean fall velocities  $\bar{v}_k$  for the ice crystal number ( $k = 0$ ) and mass ( $k=1$ ), respectively:

$$\bar{v}_k = a_{\text{vel}} \frac{\Gamma\left(\frac{k+\nu+b_{\text{vel}}+1}{\mu}\right)}{\Gamma\left(\frac{k+\nu+1}{\mu}\right)} \left[ \frac{\Gamma\left(\frac{\nu+1}{\mu}\right)}{\Gamma\left(\frac{\nu+2}{\mu}\right)} \right]^{b_{\text{vel}}} \bar{m}^{b_{\text{vel}}} \quad (\text{A7})$$

20 In Eqs. A6 and A7,  $m$  and  $\bar{m}$  are in kg and  $v$  and  $\bar{v}_k$  are in in  $\text{m s}^{-1}$ . Using relations relying on potential-power law functions like Eqs. A6 and 2 is beneficial. Then integrals over the mass distribution can often be expressed in terms of moments which avoids employing more expensive numerical quadrature techniques. The contrail ice class uses a piecewise definition of the mass size relation. In this case, truncated moments have to be evaluated.

In the model, both self-collection and collection between the individual classes of frozen hydrometeors are considered. Sink terms (not shown) are included in the prognostic equations of  $n$ . In case that two different hydrometeor classes are present, where class A has a larger mean mass than class B, the ice crystals of class B are collected by those of class A. In addition to

25 the number loss in class B, mass is transferred from class B to class A.

The nucleation process for natural cirrus is not repeated here as ice crystal generation in the contrail [ice](#) class is quite different (see section 3.1)

## Appendix B: Radiation related derivations

For hexagonal columns, the mass of a single ice crystal is given by

$$5 \quad m = \rho_{\text{ice}} \frac{3\sqrt{3}}{8} D^2 L. \quad (\text{B1})$$

Combining the latter equation with Eq. 2 yields

$$D = \sqrt{\frac{8a}{3\sqrt{3}\rho_{\text{ice}}}} L^{\frac{b-1}{2}} \quad (\text{B2})$$

For distributions, the transformation property  $f_L(L) = f(m(L)) \frac{dm}{dL}$  holds. Using the mass-size relation and the definition of a general  $\Gamma$ -distribution, it follows [with  \$L\$  in units of  \$m\$](#) :

$$10 \quad f_L(L) = A (a L^b)^\nu \exp(-\lambda (a L^b)^\mu) a b L^{b-1} \quad (\text{B3})$$

$f_L(L)$  also represents a generalized  $\Gamma$ -distribution with parameters:

$$A_L = A a^{\nu+1} b; \quad \nu_L = b(\nu + 1) - 1; \quad \lambda_L = \lambda a^\mu; \quad \mu_L = b\mu \quad (\text{B4})$$

Plugging Eq. B2 into Eq. 3 and using the latter relations, the integrals in the effective radius definition can be re-formulated in terms of moments.

- 15 *Acknowledgements.* [We appreciate the constructive comments of all reviewers which helped to improve the manuscript. We acknowledge the use of imagery from the Land Atmosphere Near real-time Capability for EOS \(LANCE\) system and services from the Global Imagery Browse Services \(GIBS\), both operated by the NASA/GSFC/Earth Science Data and Information System \(ESDIS, <http://earthdata.nasa.gov>\) with funding provided by NASA/HQ.](#)  
[We acknowledge the use of the radio sounding data provided by the University of Wyoming, Department of Atmospheric Science.](#)

## References

- Andrews, R., Stein, J., Hansen, C., and Riley, D.: Introduction to the Open Source PV\_LIB for Python Photovoltaic System Modelling Package, 40th IEEE Photovoltaic Specialist Conference, 2014.
- Appleman, H.: The Formation of Exhaust Condensation Trails by Jet Aircraft., *Bull. Am. Meteorol. Soc.*, 34, 14 – 20, 1953.
- 5 Baldauf, M., Seifert, A., Forstner, J., Majewski, D., Raschendorfer, M., and Reinhardt, T.: Operational convective-scale numerical weather prediction with the COSMO model: description and sensitivities, *Mon. Wea. Rev.*, 139, 3887 – 3905, doi:10.1175/MWR-D-10-05013.1, 2011.
- Bi, L. and Yang, P.: Improved ice particle optical property simulations in the ultraviolet to far-infrared regime, *J. Quant. Spectrosc. Radiat. Transf.*, 189, 228 – 237, doi:10.1016/j.jqsrt.2016.12.007, 2017.
- 10 Bock, L. and Burkhardt, U.: The temporal evolution of a long-lived contrail cirrus cluster: Simulations with a global climate model, *J. Geophys. Res. Atmos.*, 121, doi:10.1002/2015JD024475, 2016a.
- Bock, L. and Burkhardt, U.: Reassessing properties and radiative forcing of contrail cirrus using a climate model, *J. Geophys. Res.*, 121, 9717 – 9736, doi:10.1002/2016JD025112, 2016b.
- Boucher, O., Randall, D., Artaxo, P., Bretherton, C., Feingold, G., Forster, P., Kerminen, V.-M., Kondo, Y., Liao, H., Lohmann, U., Rasch,  
15 P., Satheesh, S., Sherwood, S., Stevens, B., and Zhang, X.: Clouds and Aerosols. In: T.F. Stocker, D. Qin, G.-K. Plattner, M. Tignor, S.K. Allen, J. Boschung, A. Nauels, Y. Xia, V. Bex, P.M. Midgley (eds.), *Climate Change 2013: The Physical Science Basis (Contribution of Working Group I to the Fifth Assessment Report of the Intergovernmental Panel on Climate Change)*, Cambridge University Press, Cambridge, United Kingdom and New York, NY, USA, 2013.
- Burkhardt, U. and Kärcher, B.: Process-based simulation of contrail cirrus in a global climate model, *J. Geophys. Res.*, 114, D16 201,  
20 doi:10.1029/2008JD011491, 2009.
- Burkhardt, U. and Kärcher, B.: Global radiative forcing from contrail cirrus, *Nat. Clim. Change*, 1, 54 – 58, doi:10.1038/NCLIMATE1068, 2011.
- Caiazzo, F., Agarwal, A., Speth, R. L., and Barrett, S. R. H.: Impact of biofuels on contrail warming, *Environ. Res. Lett.*, 12, 114 013, doi:10.1088/1748-9326/aa893b, 2017.
- 25 DLR: <ftp://taurus.caf.dlr.de/put/wetterbilder/>, 01.01.2014, <ftp://taurus.caf.dlr.de/put/wetterbilder/>, 2014.
- Duda, D. P., Minnis, P., Nyuyen, L., and Palikonda, R.: A case study of the development of contrail clusters over the Great Lakes, *J. Atmos. Sci.*, 61, 1132 – 1146, 2004.
- Eleftheratos, K., Zerefos, C., Zanis, P., Balis, D., Tselioudis, G., Gierens, K., and Sausen, R.: A study on natural and manmade global interannual fluctuations of cirrus cloud cover for the period 1984-2004, *Atmos. Chem. Phys.*, 7, 2631 – 2642, doi:10.5194/acp-7-2631-  
30 2007, 2007.
- Febvre, G., Gayet, J. F., Minikin, A., Schlager, H., Shcherbakov, V., Jourdan, O., Busen, R., Fiebig, M., Kärcher, B., and Schumann, U.: On optical and microphysical characteristics of contrails and cirrus, *J. Geophys. Res.*, 114, D02 204, doi:10.1029/2008JD01018, 2009.
- flightradar24.com: <http://www.flightradar24.com>, 16.08.2015, <http://www.flightradar24.com>, 2015.
- Freudenthaler, V., Homburg, F., and Jäger, H.: Contrail observations by ground-based scanning lidar: Cross-sectional growth, *Geophys. Res. Lett.*, 22, 3501–3504, 1995.
- 35 Fu, Q., Yang, P., and Sun, W.: An Accurate Parameterization of the Infrared Radiative Properties of Cirrus Clouds for Climate Models, *J. Clim.*, 11, 2223 – 2237, 1998.

- Harrington, J., Meyers, M., Walko, R., and Cotton, W.: Parameterization of ice crystal conversion processes due to vapor deposition for mesoscale models using doublemoment basis functions. Part I: Basic formulation and parcel model results, *J. Atmos. Sci.*, 52, 4344 – 4366, 1995.
- Heymsfield, A. and Iaquinta, J.: Cirrus crystal terminal velocities, *J. Atmos. Sci.*, 57, 916–938, 2000.
- 5 Heymsfield, A., Baumgardner, D., DeMott, P., Forster, P., Gierens, K., and Kärcher, B.: Contrail Microphysics, *Bull. Am. Meteorol. Soc.*, 91, 465 – 472, doi:10.1175/2009BAMS2839.1., 2010.
- Heymsfield, A. J., Lawson, R. P., and Sachse, G. W.: Growth of ice crystals in a precipitating contrail, *Geophys. Res. Lett.*, 25, 114 013, doi:10.1029/98GL00189, 1998.
- Inman, R. H., Pedro, H. T., and Coimbra, C. F.: Solar forecasting methods for renewable energy integration, *Prog. Energy Combust. Sci.*, 39, 535 – 576, doi:10.1016/j.pecs.2013.06.002, 2013.
- 10 Kärcher, B., Burkhardt, U., Ponater, M., and Frömming, C.: Importance of representing optical depth variability for estimates of global line-shaped contrail radiative forcing, *Proc. Nat. Acad. Sci. USA*, 107, 19 181–19 184, 2010.
- Kärcher, B., Burkhardt, U., Bier, A., Bock, L., and Ford, I.: The microphysical pathway to contrail formation, *J. Geophys. Res. Atmos.*, 120, 7893–7927, doi:10.1002/2015JD023491, 2015.
- 15 Key, J. R., Yang, P., Baum, B. A., and Nasiri, S. L.: Parameterization of shortwave ice cloud optical properties for various particle habits, *J. Geophys. Res. Atmos.*, 107, AAC 7–1–AAC 7–10, doi:10.1029/2001JD000742, 2002.
- Khou, J.-C., Ghedhaïfi, W., Vancassel, X., and Garnier, F.: Spatial Simulation of Contrail Formation in Near-Field of Commercial Aircraft, *J. Aircraft*, 52, 1927–1938, doi:10.2514/1.C033101, <http://dx.doi.org/10.2514/1.C033101>, 2015.
- Köhler, C., Steiner, A., Saint-Drenan, Y.-M., Ernst, D., Bergmann-Dick, A., Zirkelbach, M., Bouallègue, Z. B., Metzinger, I., and Ritter, B.: Critical weather situations for renewable energies - Part B: Low stratus risk for solar power, *Renew. Energ.*, 101, 535 – 576, doi:10.1016/j.renene.2016.09.002, 2017.
- 20 Lew, D. and Richard, P.: Western wind and solar integration study, Tech. rep., National Renewable Energy Laboratories, 2010.
- Lewellen, D. and Lewellen, W.: The effects of aircraft wake dynamics on contrail development, *J. Atmos. Sci.*, 58, 390 – 406, 2001.
- Lewellen, D., Meza, O., and Huebsch, W.: Persistent Contrails and Contrail Cirrus. Part I: Large-Eddy Simulations from Inception to Demise, *J. Atmos. Sci.*, 71, 4399 – 4419, doi:10.1175/JAS-D-13-0316.1., 2014.
- 25 Lewellen, D. C.: Persistent contrails and contrail cirrus. Part 2: Full Lifetime Behavior, *J. Atmos. Sci.*, pp. 4420–4438, doi:10.1175/JAS-D-13-0317.1, 2014.
- Marquart, S., Ponater, M., Mager, F., and Sausen, R.: Future development of contrail cover, optical depth and radiative forcing: Impacts of increasing air traffic and climate change, *J. Clim.*, 16, 2890 – 2904, 2003.
- 30 Minnis, P., Ponater, M., Young, D. F., Garber, D. P., Nguyen, L., Jr, W. L. S., and Palikonda, R.: Transformation of Contrails into Cirrus during SUCCESS, *Geophys. Res. Lett.*, 25, 1157 – 1160, 1998.
- Moore, R. H., Thornhill, K. L., Weinzierl, B., Sauer, D., D’Ascoli, E., Kim, J., Lichtenstern, M., Scheibe, M., Beaton, B., Beyersdorf, A. J., Barrick, J., Bulzan, D., Corr, C. A., Crosbie, E., Jurkat, T., Martin, R., Riddick, D., Shook, M., Slover, G., Voigt, C., White, R., Winstead, E., Yasky, R., Ziemba, L. D., Brown, A., Schlager, H., and Anderson, B. E.: Biofuel blending reduces particle emissions from aircraft engines at cruise conditions, *Nature*, 543, 411–415, <http://dx.doi.org/10.1038/nature21420>, 2017.
- 35 NASA/GSFC/ESDIS: <https://earthdata.nasa.gov>, 01.02.2018, <https://earthdata.nasa.gov>, 2018.
- Paoli, R., Nybelen, L., Picot, J., and Cariolle, D.: Effects of jet/vortex interaction on contrail formation in supersaturated conditions, *Phys. Fluids*, 25, 1–28, doi:10.1063/1.4807063, 2013.

- Petzold, A., Busen, R., Schröder, F. P., Baumann, R., Kuhn, M., Ström, J., Hagen, D. E., Whitefield, P. D., Baumgardner, D., Arnold, F., Borrmann, S., and Schumann, U.: Near-field measurements on contrail properties from fuels with different sulfur content, *J. Geophys. Res.*, 102, 114 013, doi:10.1029/97JD02209, 1997.
- Poellot, M. R., Arnott, W. P., and Hallett, J.: In situ observations of contrail microphysics and implications for their radiative impact, *J. Geophys. Res.*, 104, 12 077–12 084, doi:10.1029/1999JD900109, <http://dx.doi.org/10.1029/1999JD900109>, 1999.
- Ponater, M., Marquart, S., and Sausen, R.: Contrails in a comprehensive global climate model: Parameterization and radiative forcing results, *J. Geophys. Res. Atmos.*, 107, 941 – 960, doi:10.1029/2001JD000429, 2002.
- Pruppacher, H. R. and Klett, J. D.: *Microphysics of clouds and precipitation*, Dordrecht: Kluwer Academic Publishers, 1997.
- Rieger, D., Steiner, A., Bachmann, V., Gasch, P., Förstner, J., Deetz, K., Vogel, B., and Vogel, H.: Impact of the 4 April 2014 Saharan dust outbreak on the photovoltaic power generation in Germany, *Atmos. Chem. Phys. Discuss.*, <https://doi.org/10.5194/acp-2017-441>, 2017.
- Ritter, B. and Geleyn, J.-F.: A comprehensive radiation scheme for numerical weather prediction models with potential applications in climate simulations, *Mon. Wea. Rev.*, 120, 303 – 325, 1992.
- Sausen, R., Isaksen, I., Grewe, V., Hauglustaine, D., Lee, D. S., Myhre, G., Köhler, M. O., Pitari, G., Schumann, U., Stordal, F., and Zerefos, C.: Aviation radiative forcing in 2000: An update on IPCC (1999), *Meteorol. Z.*, 14, 555 – 561, doi:10.1127/0941-2948/2005/0049, 2005.
- Schmidt, E.: Die Entstehung von Eisnebel aus den Auspuffgasen von Flugmotoren, *Schriften der Deutschen Akademie der Luftfahrtforschung*, 44, 1 – 15, 1941.
- Schröder, F., Kärcher, B., Duroure, C., Ström, J., Petzold, A., Gayet, J.-F., Strauss, B., Wendling, P., and Borrmann, S.: On the Transition of Contrails into Cirrus Clouds, *J. Atmos. Sci.*, 57, 464 – 480, 2000.
- Schulz, J., Albert, P., Behr, H.-D., Caprion, D., Deneke, H., Dewitte, S., Dürr, B., Fuchs, P., Gratzki, A., Hechler, P., Hollmann, R., Johnston, S., Karlsson, K.-G., Manninen, T., Nüller, R., Reuter, M., Riihelä, A., Roebeling, R., Selbach, N., Tetzlaff, A., Thomas, W., Werscheck, M., Wolters, E., and Zelenka, A.: Operational climate monitoring from space: the EUMETSAT Satellite Application Facility on Climate Monitoring (CM-SAF), *Atmos. Chem. Phys.*, 9, 1687 – 1709, doi:10.5194/acp-9-1687-2009, 2009.
- Schumann, U.: On conditions for contrail formation from aircraft exhausts, *Meteorol. Z.*, 5, 4 – 23, 1996.
- Schumann, U.: A contrail cirrus prediction model, *Geosci. Model Dev.*, 5, 543–580, doi:10.5194/gmd-5-543-2012, 2012.
- Schumann, U. and Graf, K.: Aviation-induced cirrus and radiation changes at diurnal timescales, *J. Geophys. Res. Atmos.*, 118, 2404–2421, doi:10.1002/jgrd.50184, 2013.
- Schumann, U. and Heymsfield, A.: On the lifecycle of individual contrails and contrail cirrus, *Meteor. Monogr.*, 58, 3.1 – 3.24, doi:10.1175/AMSMONOGRAPHS-D-16-0005.1, 2017.
- Schumann, U., Penner, J. E., Chen, Y., Zhou, C., and Graf, K.: Dehydration effects from contrails in a coupled contrail-climate model, *Atmos. Chem. Phys.*, 15, 11 179–11 199, doi:10.5194/acp-15-11179-2015, 2015.
- Seifert, A. and Beheng, K. D.: A two-moment cloud microphysics parameterization for mixed-phase clouds. Part 1: Model description, *Meteorol. Atmos. Phys.*, 92, 45 – 66, doi:10.1007/s00703-005-0112-4, 2006.
- Spangenberg, D. A., Minnis, P., Bedka, S. T., Palikonda, R., Duda, D. P., and Rose, F. G.: Contrail radiative forcing over the Northern Hemisphere from 2006 Aqua MODIS data, *Geophys. Res. Lett.*, 40, 595–600, doi:10.1002/grl.50168, <http://dx.doi.org/10.1002/grl.50168>, 2013.
- Spichtinger, P. and Gierens, K. M.: Modelling of cirrus clouds - Part 1a: Model description and validation, *Atmos. Chem. Phys.*, 9, 685–706, 2009.
- Stubenrauch, C. and Schumann, U.: Impact of air traffic on cirrus coverage, *Geophys. Res. Lett.*, 32, doi:10.1029/2005GL022707, 2005.

- Stuber, N. and Forster, P.: The impact of diurnal variations of air traffic on contrail radiative forcing, *Atmos. Chem. Phys.*, 7, 3153 – 3162, 2007.
- Unterstrasser, S.: Large-eddy simulation study of contrail microphysics and geometry during the vortex phase and consequences on contrail-to-cirrus transition, *J. Geophys. Res. Atmos.*, 119, 7537–7555, doi:10.1002/2013JD021418, 2014.
- 5 Unterstrasser, S.: Properties of young contrails - a parametrisation based on large - eddy simulations, *Atmos. Chem. Phys.*, 16, 2059 – 2082, doi:10.5194/acp-16-2059-2016, 2016.
- Unterstrasser, S. and Gierens, K.: Numerical simulations of contrail-to-cirrus transition - Part 1: An extensive parametric study, *Atmos. Chem. Phys.*, 10, 2017–2036, 2010a.
- Unterstrasser, S. and Gierens, K.: Numerical simulations of contrail-to-cirrus transition - Part 2: Impact of initial ice crystal number, radiation, stratification, secondary nucleation and layer depth, *Atmos. Chem. Phys.*, 10, 2037–2051, 2010b.
- 10 Unterstrasser, S. and Görsch, N.: Aircraft-type dependency of contrail evolution, *J. Geophys. Res. Atmos.*, 119, 14,015–14,027, doi:10.1002/2014JD022642, 2014JD022642, 2014.
- Unterstrasser, S., Gierens, K., Sölch, I., and Lainer, M.: Numerical simulations of homogeneously nucleated natural cirrus and contrail-cirrus. Part 1: How different are they?, *Meteor. Z.*, doi:10.1127/metz/2016/0777, <http://dx.doi.org/10.1127/metz/2016/0777>, 2016a.
- 15 Unterstrasser, S., Gierens, K., Sölch, I., and Wirth, M.: Numerical simulations of homogeneously nucleated natural cirrus and contrail-cirrus. Part 2: Interaction on local scale, *Meteor. Z.*, doi:10.1127/metz/2016/0780, <http://dx.doi.org/10.1127/metz/2016/0780>, 2016b.
- Unterstrasser, S., Gierens, K., Sölch, I., and Lainer, M.: Numerical simulations of homogeneously nucleated natural cirrus and contrail-cirrus. Part 1: How different are they?, *Meteorol. Z.*, 26, 621 – 642, doi:10.1127/metz/2016/0777, <http://dx.doi.org/10.1127/metz/2016/0777>, 2017a.
- 20 Unterstrasser, S., Gierens, K., Sölch, I., and Wirth, M.: Numerical simulations of homogeneously nucleated natural cirrus and contrail-cirrus. Part 2: Interaction on local scale, *Meteorol. Z.*, 26, 643 – 661, doi:10.1127/metz/2016/0780, <http://dx.doi.org/10.1127/metz/2016/0780>, 2017b.
- UWYO: <http://weather.uwyo.edu/upperair/sounding.html>, 01.02.2018, <http://weather.uwyo.edu/upperair/sounding.html>, 2018.
- Vogel, B., Vogel, H., Bäumer, D., Bangert, M., Lundgren, K., Rinke, R., and Stanelle, T.: The comprehensive model system COSMO-ART - Radiative impact of aerosol on the state of the atmosphere on the regional scale, *Atmos. Chem. Phys.*, 9, 8661 – 8680, doi:10.5194/acpd-9-14483-2009, 2009.
- 25 Voigt, C., Schumann, U., Jurkat, T., Schäuble, D., Schlager, H., Petzold, A., Gayet, J.-F., Krämer, M., Schneider, J., Borrmann, S., Schmale, J., Jessberger, P., Hamburger, T., Lichtenstern, M., Scheibe, M., Gourbeyre, C., Meyer, J., Kübbeler, M., Frey, W., Kalesse, H., Butler, T., Lawrence, M. G., Holzäpfel, F., Arnold, F., Wendisch, M., Döpelheuer, A., Gottschaldt, K., Baumann, R., Zöger, M., Sölch, I., Rautenhaus, M., and Dörnbrack, A.: In-situ observations of young contrails – overview and selected results from the CONCERT campaign, *Atmos. Chem. Phys.*, 10, 9039–9056, doi:10.5194/acp-10-9039-2010, 2010.
- 30 Voigt, C., Schumann, U., Minikin, A., Abdelmonem, A., Afchine, A., Borrmann, S., Boettcher, M., Buchholz, B., Bugliaro, L., Costa, A., Curtius, J., Dollner, M., Dörnbrack, A., Dreiling, V., Ebert, V., Ehrlich, A., Fix, A., Forster, L., Frank, F., Fütterer, D., Giez, A., Graf, K., Groß, J., Groß, S., Heimerl, K., Heinold, B., Hüneke, T., Järvinen, E., Jurkat, T., Kaufmann, S., Kenntner, M., Klingebiel, M., Klimach, T., Kohl, R., Krämer, M., Krisna, T., Luebke, A., Mayer, B., Mertes, S., Molleker, S., Petzold, A., Pfeilsticker, K., Port, M., Rapp, M., Reutter, P., Rolf, C., Rose, D., Sauer, D., Schäfler, A., Schlage, R., Schnaiter, M., Schneider, J., Spelten, N., Spichtinger, P., Stock, P., Walser, A., Weigel, R., Weinzierl, B., Wendisch, M., Werner, F., Wernli, H., Wirth, M., Zahn, A., Ziereis, H., and Zöger, M.:

ML-CIRRUS: The Airborne Experiment on Natural Cirrus and Contrail Cirrus with the High-Altitude Long-Range Research Aircraft HALO, Bull. Amer. Meteor. Soc., 98, 271 – 288, doi:10.1175/BAMS-D-15-00213.1, 2017.

**Table 1.** Microphysical constants of microphysical model. If different values are used for Constants characterizing the natural and the contrail ice class, the subscripts con and nat are added.

Symbol	Definition	Value	Unit	Reference
$m_{\min, \text{con}}$	minimum $\bar{m}$	$10^{-15}$	kg	$m_{\max, \text{con}}$ this study
$m_{\min, \text{nat}}$	minimum $\bar{m}$	$10^{-12}$	kg	Value Seifert and Beheng (2006)
$a_{\text{geo, con}}$	parameter in mass-size relation	526.1 and 0.04142	-	$\mu$ parameter of size distribution Spichtinger and Gierens (2009); Heymsfield and Platt (2009)
$a_{\text{geo, nat}}$	parameter in mass-size relation	1.59	-	2.56 A. Seifert, personal communication, June, 01, 2006
$b_{\text{geo, nat}}$	exponent in mass-size relation	2.56	-	Seifert and Beheng (2006)
$\alpha_{\text{vel}}$	parameter in fallspeed relation	317.0	$\text{m s}^{-1} \text{g}^{\text{bal}} \text{kg}^{-1}$	10-12 Seifert and Beheng (2006)
$\beta_{\text{vel}}$	parameter in fallspeed relation	0.363	kg	10-6 Seifert and Beheng (2006)
$L_{\max, \text{con}}$	crystal size corresponding to $m_{\max, \text{con}}$	$\mu\text{m}$	$\mu\text{m}$	17.5
$L_{\min, \text{con}}$	crystal size corresponding to $m_{\min, \text{con}}$	58	$\mu\text{m}$	3800
$L_{\max, \text{nat}}$	crystal size corresponding to $m_{\max, \text{nat}}$	2.4	$\mu\text{m}$	-
$L_{\min, \text{nat}}$	crystal size corresponding to $m_{\min, \text{nat}}$	3800	$\mu\text{m}$	-
$\nu$	parameter of size distribution	-	-	-
$a_{\text{vel}}$	parameter of fallspeed relation	-	-	-
$b_{\text{vel}}$	parameter of fallspeed relation	-	-	-

Symbol	Definition	Unit
$\Gamma$	gamma function	-
$\lambda, \lambda_L$	slope parameter of generalized $\Gamma$ -distribution	<del><math>\text{kg}^{-\mu}, \text{m}^{-\mu}</math></del>
$\lambda_{\text{Ns}}$	surviving fraction of ice crystals	-
$\mu$	parameter of generalized $\Gamma$ -distribution	-
$\nu$	parameter of generalized $\Gamma$ -distribution	-
$\rho, \rho_{\text{ice}}$	air density, density of ice	$\text{kg m}^{-3}$
$A, A_L$	scaling parameter of generalized $\Gamma$ -distribution	$\text{m}^{-3} \text{kg}^{-1}, \text{m}^{-4}$
$a_{\text{geo}}, a_{\text{nat}}$	parameter in mass-size relation	-
$a_{\text{vel}}$	parameter in fallspeed relation	<del><math>\text{m s}^{-1} \text{kg}^{-b_{\text{vel}}}</math></del>
$b_{\text{con}}, b_{\text{nat}}$	exponent in mass-size relation	-
$b_{\text{vel}}$	exponent in fallspeed relation	-
$c_p$	specific heat capacity of air	$\text{J kg}^{-1} \text{K}^{-1}$
$C$	capacity	-
$CTY$	cloud type	-
$d$	flight distance	m
$D_v$	molecular diffusion coefficient	m
$E$	extinction coefficient	$\text{m}^{-1}$
$E_{\text{AB}}$	collision efficiency for classes A and B	-
$EI_{\text{iceno}}$	emission index for ice crystals	$\text{kg}^{-1}$
$f, f_L$	number concentration size distribution	$\text{m}^{-3} \text{kg}^{-1}, \text{m}^{-3} \text{m}^{-1}$
$F_{\text{ven}}$	ventilation coefficient	-
$I$	ice mass mixing ratio	$\text{kg kg}^{-1}$
$q_{\text{init}}$	"emitted" ice crystal mass concentration	$\text{kg m}^{-3}$
$I_0$	water vapor emission per flight distance	$\text{kg m}^{-1}$
$q_i$	ice crystal mass concentration	$\text{kg m}^{-3}$
$K_T$	conductivity of heat	$\text{J m}^{-1} \text{s}^{-1} \text{K}^{-1}$
$L$	ice crystal size	m
$L_{\text{iv}}$	latent heat for sublimation	$\text{J kg}^{-1}$
$L_{\text{max}}$	maximum particle length	m
$L_{\text{min}}$	minimum particle length	m
$M^k$	$k^{\text{th}}$ power moment of $f(x)$	$\text{kg}^k \text{m}^{-3}$
$n$	ice crystal number concentration	$\text{m}^{-3}$
$N$	number concentration	$\text{kg}^{-1}$
$N_{\text{BV}}$	Brunt-Väisälä frequency	$\text{s}^{-1}$

$n_{\text{init}}$	"emitted" ice crystal number concentration	$\text{m}^{-3}$
$N_s$	number of surviving ice crystals per flight distance	$\text{m}^{-1}$
$N_0$	number of produced ice crystals per flight distance	$\text{m}^{-1}$
$p$	pressure	hPa
$p_{\text{sat}}$	saturation pressure	hPa
$r$	radius	$\mu\text{m}$
$r_e$	effective radius	$\mu\text{m}$
$R_d$	specific gas constant for dry air	$\text{J kg}^{-1} \text{K}^{-1}$
$R_v$	specific gas constant for water vapor	$\text{J kg}^{-1} \text{K}^{-1}$
$RH_i$	relative humidity with respect to ice	-
$S_i$	supersaturation with respect to ice	-
$t$	time	s
$T$	temperature	kg
$v$	velocity	$\text{m s}^{-1}$
$V$	volume	$\text{m}^3$
$b_{\text{span}}$	wing span	m